RCA REVIEW

a technical journal

RADIO AND ELECTRONICS
RESEARCH • ENGINEERING

VOLUME XIV SEPTEMBER 1953 NO. 3

PRINTED IN U.S.A.

RCA REVIEW, published quarterly in March, June, September and December by RCA Laboratories Division, Radio Corporation of America, Princeton, New Jersey. Entered as second class matter July 3, 1950 at the Post Office at Princeton, New Jersey, under the act of March 3, 1879. Subscription price in the United States, Canada and Postal Union; one year $2.00, two years $3.50, three years $4.50: in other countries; one year $2.40, two years $4.30, three years $5.70. Single copies in the United States, $.75; in other countries, $.85.

RCA REVIEW

a technical journal

RADIO AND ELECTRONICS
RESEARCH • ENGINEERING

Published quarterly by

RCA Laboratories Division
Radio Corporation of America

in cooperation with

RCA Victor Division
Radiomarine Corporation of America
RCA International Division
RCA Communications, Inc.
National Broadcasting Company, Inc.
RCA Institutes, Inc.

VOLUME XIV SEPTEMBER, 1953 NUMBER 3

CONTENTS

RCA REVIEW is regularly abstracted and indexed by *Industrial Arts Index, Science Abstracts* (I.E.E.-Brit.), *Electronic Engineering Master Index, Chemical Abstracts, Proc. I.R.E., and Wireless Engineer.*

RCA REVIEW

BOARD OF EDITORS

RECENT MARITIME RADIO AND RADAR DEVELOPMENTS*

By

Irving F. Byrnes

Engineering Department, Radiomarine Corporation of America, New York, N. Y.

Summary—*Several types of shipboard radiotelegraph and radiotelephone equipment are described. Included are telegraph sets which meet the requirements of the Safety of Life at Sea Convention and the Atlantic City Radio Regulations. New multi-channel telephone apparatus for the various maritime radio-frequency bands are covered. A surface-search ship radar using a sixteen-inch display tube is described.*

ELECTRONIC equipment is essential in the maritime industry in both communications and navigation. Ocean going vessels of any nation must be able to exchange messages with one another and with coastal stations throughout the world. The radio direction finder is a familiar, internationally used instrument for medium ranges, while loran has become a valuable long- and medium-distance position fixing system. Merchant marine radar, an important microwave navigational aid, may now be found in the pilot houses of small harbor tugboats as well as on passenger liners, tankers, and freighters.

Various portions of the radio spectrum are allocated to the marine services. Equipment installed aboard ship may use a frequency as low as 110 kilocycles for telegraphy, or as high as 9500 megacycles for surface-search radar. This span of about 16 octaves indicates the diversified nature of development and design techniques that are necessary to produce the required apparatus. The major applications of shipboard installations and the frequency bands in which they operate are as follows:

Long Range Telegraphy	110-160 kilocycles
Direction Finding	285-525 kilocycles
Medium Range Telegraphy	410-525 kilocycles
Medium Range Telephony	2-3 megacycles
Loran	1.9-2.0 megacycles
Long Range Telegraphy	2, 4, 6, 8, 12, 16, and 22 megacycles
Long Range Telephony	4, 8, 12, 16, and 22 megacycles

* Decimal Classification: R537.1 × R510.

Short Range Telephony	156-162 megacycles
Radar	3000-3246, 5460-5650 and 9320-9500 megacycles

A new radiotelegraph console designed for tankers, general cargo ships, and the smaller passenger liners is shown in Figure 1. This "single package" radio station contains, in the upper section, three transmitters, two receivers, an automatic alarm, and a keying device for transmitting the alarm signal. The lower section houses the high-voltage rectifier, a modulator (for A2 emission), battery-charging facilities, and a dynamotor for the emergency transmitter.

Fig. 1—Radiotelegraph console.

Two of the transmitters cover the 410-515 kilocycle band. One is designated as the main transmitter and delivers 250 watts to a 4-ohm 750-micromicrofarad antenna. The other is a storage-battery-operated emergency transmitter with 40 watts output. Since 500 kilocycles is the important marine calling and distress frequency, there are international and Federal Communications Commission (FCC) requirements with respect to the ranges of ship transmitters using this frequency. The Safety of Life at Sea Convention (London 1948) specifies, for ships over 1600 gross tons, a minimum field strength of 50 microvolts per meter at 150 miles for main transmitters, and at 100 miles for emergency transmitters. FCC regulations are based upon a mini-

mum antenna power of 200 watts for a 200-mile range with a main transmitter, and 25 watts for 100 miles with an emergency transmitter. Such transmitters on an average antenna will give about 80 microvolts per meter at the specified ranges.

It is evident that antenna efficiency as well as power must be considered in determining range. There is little published information on ship antennas; perhaps the most extensive measurements were those made in 1938 by the FCC in connection with hearings to establish required powers for ship transmitters. The results of measurements at 500 kilocycles on approximately 100 different vessels are summarized below.

	Percentage of antennas whose parameters exceed values given below						
Antenna Parameter	5	10	20	30	50	75	95
Efficiency (per cent)	50	43	33	24	16	11	5.5
Effective height (meters).	19	18	16	15	13	11	8
Resistance at 500 kilocycles (ohms)	8	7	6	5	4	3	2.4
Equivalent capacitance (micromicrofarads)	1500	1250	1100	1000	900	700	600
Natural frequency (kilocycles)	1250	1225	1180	1100	1000	900	800
Resistance at natural frequency (ohms)	16	13	11	10	9	7	6

The values under the 50 per cent column may be used as a median for designing 500 kilocycle transmitters and receivers. On this basis the average antenna will have an efficiency better than 16 per cent and an effective height exceeding 13 meters.

The field strength at 1 nautical mile is given by the expression

$$F = 5.12\sqrt{PE}$$

where F is in millivolts per meter, P is antenna power in watts, and E is antenna efficiency in per cent. In the case of the 250-watt main and 40-watt emergency transmitters of the console unit, the 500-kilocycle field strength at various ranges is shown in Figure 2. These curves are based on an antenna efficiency of 16 per cent. The main transmitter field at 200 nautical miles is approximately 90 microvolts per meter, and the emergency transmitter field at 100 nautical miles is 100 microvolts per meter.

For long distance communication, the console has a 300-watt radio-

telegraph crystal controlled transmitter which can be tuned in a matter of seconds to frequencies in the band 2 to 24 megacycles. During the year 1953, ships are scheduled to begin using the new calling and working high frequencies under the 1947 Atlantic City Radio Regulations. The changeover from the old to new frequencies will be on a

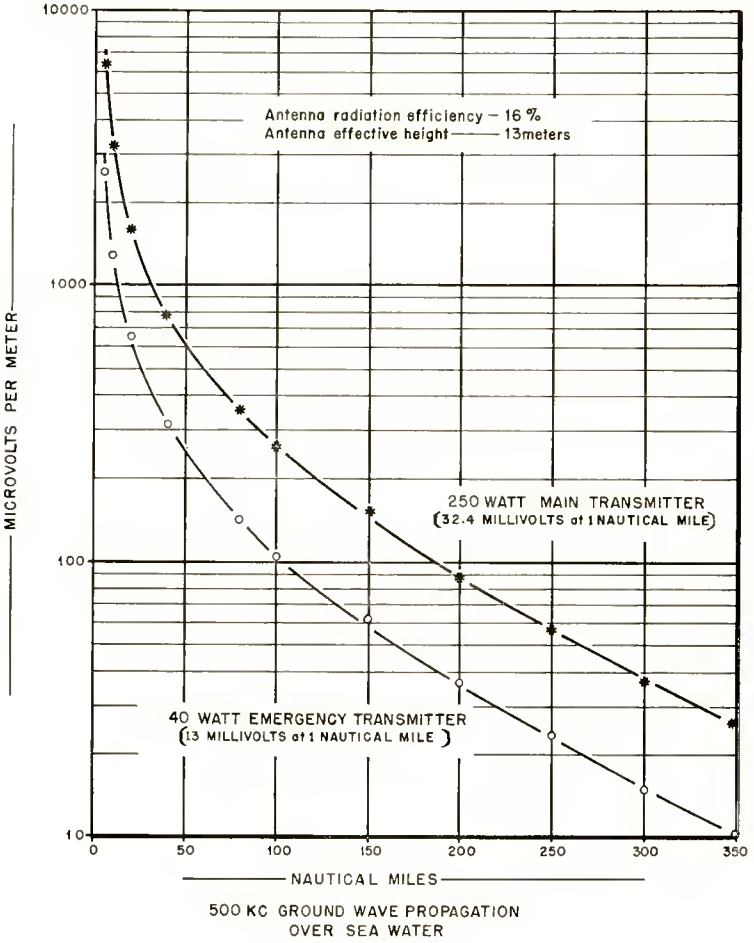

Fig. 2—500-kilocycle ground-wave propagation over water.

world-wide basis, affecting an estimated 8000 ships.

The new allocation system is planned to allow a large number of ship stations to share narrow, long-distance frequency bands. Cargo vessels are required to have one calling and two working frequencies in each high-frequency band that is used. Five of the bands—4, 6, 8,

12 and 16 megacycles—have a harmonic relationship such that the same three crystals will provide three output frequencies in each of these five bands in the 300-watt transmitter. Three more crystals are used for the nonharmonic 22-megacycle band. Therefore, six crystals will give a total of 18 output frequencies, or one calling and two working frequencies in each of the six bands. Passenger vessels, because of their heavier traffic load, are assigned several working frequencies in each band. Ships in Region 2 (North and South American waters) also may use one calling and one working frequency in the 2-megacycle band. The assignable radiotelegraph frequencies in each international band, with their spacing and bandwidth, are tabulated below.

	15 Frequencies Passenger Working		9 Frequencies Calling		98 Frequencies Cargo Working	
Band mc	Spacing* kc	Width kc	Spacing kc	Width kc	Spacing kc	Width kc
4	2.5	40	1.0	8	0.5	48.5
6	3.75	60	1.5	12	0.75	72.75
8	5.0	80	2.0	16	1.0	96.
12	7.5	120	3.0	24	1.5	145.5
16	10	160	4.0	32	2.0	192.
22**	10	140	5.0	40	2.5	122.5

The very close spacing in the cargo working bands accounts for the comparatively large number of assignable frequencies. The required new ship frequency tolerance of 0.02 per cent is greater than this spacing. For example, at 8 megacycles the tolerance is 1.6 kilocycles, as compared with a separation between frequencies of 1 kilocycle. However, it is believed that improved communications will result from the new allocation system by assigning the frequencies in rotation among the thousands of ships involved. Interference will be reduced as more and more ships use crystal control for minimum frequency drift during any one transmission, thereby permitting the coast stations to employ highly selective receivers.

Turning now to passenger ships, the new superliner *United States* has an elaborate radiotelegraph and radiotelephone system. The control panel for radiotelephone service is illustrated in Figure 3. There are

* Passenger ships have two of the working frequencies in each band with twice the spacing shown.

** In the 22-megacycle band there are only 13 passenger and 50 cargo working frequencies.

telegraph transmitters which cover all commercial frequencies. Special long-distance telephone equipment is provided for use by the passengers for ship to shore communication. There is also an emergency telegraph transmitter.

An outstanding feature of the radio installation on the *United States* is the remote receiving system. In the after part of the ship there are remotely controlled receivers for various telephone frequencies. These receivers deliver signals to the radio room, where they may be patched, through the telephone control panel, to staterooms throughout the ship. The remote receiving antennas are located as far aft as possible to minimize their exposure to the strong field from the transmitting antennas. Simultaneous use of telephone and telegraph in the same frequency bands imposes severe selectivity require-

Fig. 3—Radiotelephone control panel, *S.S. United States.*

ments on the receiving systems.

The transmitting antennas are supported by outriggers attached to either side of the vessel's stacks. The arrangement on the forward stack is shown in Figure 4.

Other equipment on the *United States* includes two loran receivers, a direction finder, a 75-watt radiotelephone set in the chartroom, and radio equipped motor lifeboats.

Medium-range telephone communications have, for many years, been carried out in the 2-megacycle band. Pleasure craft, fishing boats and coastwise shipping have ship-to-shore and ship-to-ship frequencies allocated for this service. Public coast stations provide the link between the ships and the land-line telephone system. At present, ships transmit

to shore in the 2110-2206 kilocycle band and receive in the 2506-2598 kilocycle band. Intership frequencies are 2638 and 2738 kilocycles. A calling and distress frequency, 2182 kilocycles, now has international status and will be valuable as a common "contact" frequency for telephone equipped vessels throughout the world.

A new design of 2-megacycle (and higher) shipboard radiotelephone set is shown in Figure 5. This has eleven channels, with crystal control for both the transmitter and receiver. Plate power input to the radio-frequency amplifier of the transmitter is 150 watts, the maximum

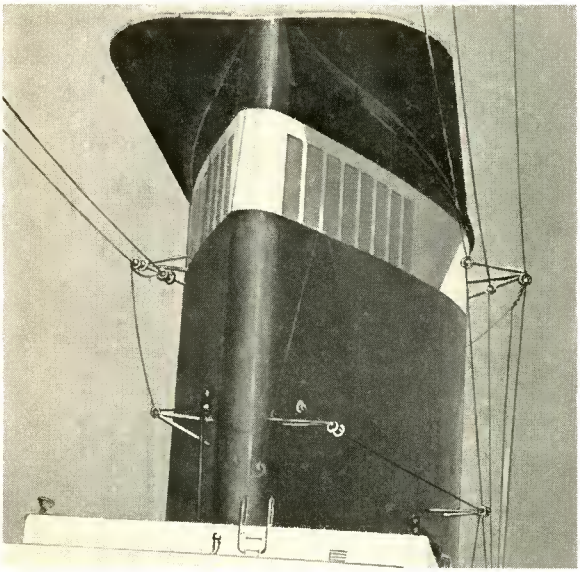

Fig. 4—Antennas on forward stack of *S.S. United States.*

permitted by FCC for ship-to-ship communications. The power delivered to a typical 20-ohm 200-micromicrofarad antenna is 85 watts. The transmitter audio circuits include a limiter to suppress overmodulation. A squelch circuit in the receiver silences the loudspeaker in the absence of incoming signals. Selective calling from the coast station may also be used in lieu of a loudspeaker watch.

For many vessels which operate in salt water coastal areas, frequencies in the 2-megacycle band are well suited to provide ranges up to a few hundred miles. Where propagation conditions are less favorable and long ranges are needed, such as in the Great Lakes and Mississippi River regions, frequencies in the 4, 6, and 8 megacycle bands can be provided by the telephone set shown in Figure 5. Still

higher frequencies, up to the 18-megacycle band, are sometimes used for long distance "high seas" service by fishing craft and other ships which must communicate with public coast stations when far off shore.

There are many vessels on which it is advantageous to use short-range telephony in the 156-megacycle very-high-frequency (VHF) band. For this service the FCC has assigned nine "simplex" and two "duplex" channels between 156.3 and 162.0 megacycles. The simplex channels use the same frequency for transmission and reception. The duplex channels are for public correspondence with coast stations, the ship transmitting on 157.3 and receiving on 162 megacycles, or transmitting on 157.4 and receiving on 161.9 megacycles. These duplex

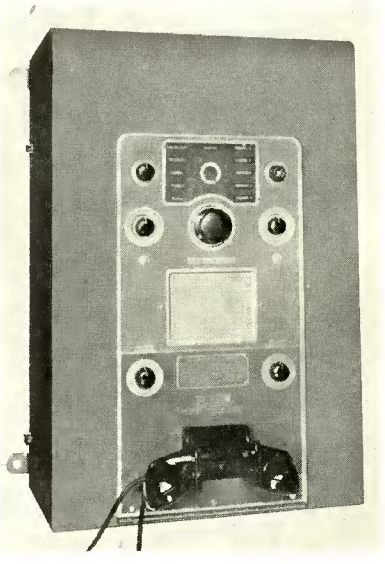

Fig. 5—Medium- and high-frequency radiotelephone equipment.

channels enable the coast stations to patch the ship signals to the land-line telephone circuits on a "constant carrier" basis. (Coast station transmitter and receiver are simultaneously energized.) Aboard ship the transmitter is energized only while talking, either by a press-to-talk switch or by voice operated relays.

Beginning in 1954, ships licensed by FCC in the 156-megacycle band must have provisions for at least three channels. Two of these are 156.3 megacycles for ship-to-ship communication and 156.8 megacycles for calling and safety purposes. The third channel may be used for business and operational needs such as dispatching from a limited coast station operated by a tugboat company. Other channels are assigned

for port operations, pilot vessels, harbor radar communication, ferries, fishing craft, shipyards, etc.

It may be noted that the assigned VHF frequencies occupy a total band width of 1.1 megacycles (156.3-157.4) with the exception of the 161.9 and 162 megacycle shore-to-ship channels. The tuned circuits in a multi-channel transmitter, used aboard ship, will pass a 1.1-megacycle band with negligible attenuation. Crystal switching will, therefore, permit the desired frequency to be selected. Similar considerations apply to the receiver circuits if they are designed so that the intermediate frequencies are maintained close to their center values when crystals are switched. However, to receive 161.9 or 162 megacycles from the public correspondence coast stations, a separate receiver appears to be the best solution.

An eight-channel frequency-modulation transmitter–receiver unit

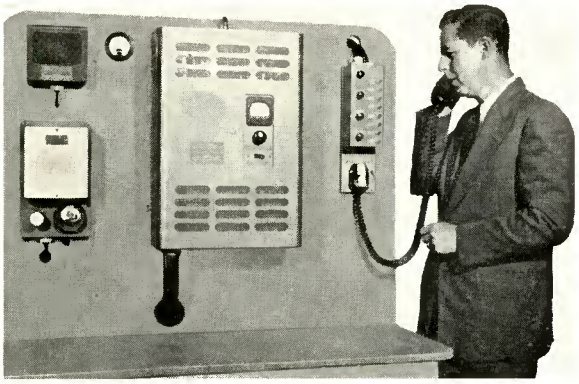

Fig. 6—Eight-channel VHF transmitter-receiver.

for the VHF band is shown in Figure 6. This equipment is designed primarily for service on the Great Lakes and other areas where the ships require several channels. The transmitter delivers 12 watts to a vertical quarter-wave antenna. There are two receivers, one for six channels between 156.3 and 157.4 megacycles, and the other for two channels (161.9 and 162 megacycles). Complete remote control operation is provided, using push button selection of frequency. Solenoid operated rotary switches connect the appropriate crystals to the transmitter and receivers. Voice operated relay circuits perform the send–receive function automatically or, if desired, a press-to-talk type of handset may be used. A small rotary converter delivers 115-volt, 400-cycle, single-phase power to the equipment.

For harbor craft which communicate with their own limited coast stations and with each other, a four-channel VHF telephone set is

illustrated in Figure 7. This set has a transmitter–receiver unit for the band 156.3-157.4 megacycles. If service is also required with the public correspondence coast stations, a separate external receiver is added for the 161.9 or 162 megacycle channel.

One of the newer requirements of the Safety Convention is a portable radiotelegraph transmitter and receiver for use in lifeboats. The equipment shown in Figure 8 is a watertight self-contained radio station, including power supply and antenna system. The transmitter is crystal controlled, with an output of 2 watts on 500 kilocycles and 5 watts on 8364 kilocycles. The receiver is pretuned for 492-508 kilocycles and is also tunable from 8240 to 8800 kilocycles. A hand-driven generator furnishes filament and plate power, so that no batteries are required.

Since a lifeboat set may be operated by unskilled personnel, sev-

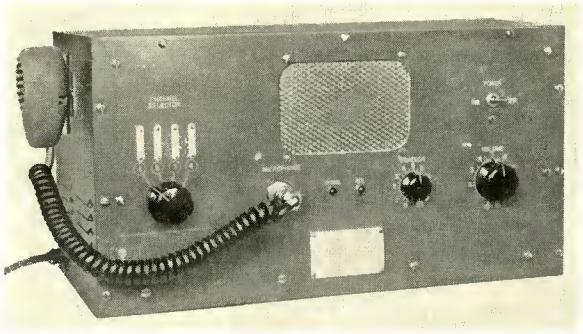

Fig. 7—Four-channel VHF transmitter-receiver.

eral automatic features are included. The international alarm signal (4-second dashes and 1-second spaces) and SOS signals are automatically transmitted on 500 kilocycles. The keying device then switches the transmitter circuits to 8364 kilocycles for a group of SOS signals and a 30-second dash which can be received by high-frequency direction finders. The cycle then repeats, and continues as long as the generator is cranked. If a trained radio operator is present, he can switch from automatic to manual, and both send and receive CW on either frequency.

A collapsible aluminum rod antenna is stowed inside the set. When assembled, this antenna is 15 feet high, and plugs into an insulated socket at the top of the cabinet. It has a capacitance of about 75 micromicrofarads and requires considerable inductance loading at 500 kilocycles. On the basis of an effective height of 2.3 meters (one-half physical height) and an antenna current of 0.5 ampere, the 500-kilocycle field strength at one mile is only about 400 microvolts per

meter, resulting in a relatively short useful range. Longer ranges are provided by the 8364-kilocycle frequency. This frequency is in the center of the 8-megacycle calling band monitored by stations in the maritime services.

In the marine radar field, the latest developments show progress in the continuing effort to improve performance and reduce complexity. A shipboard surface search radar for the larger vessels with six range

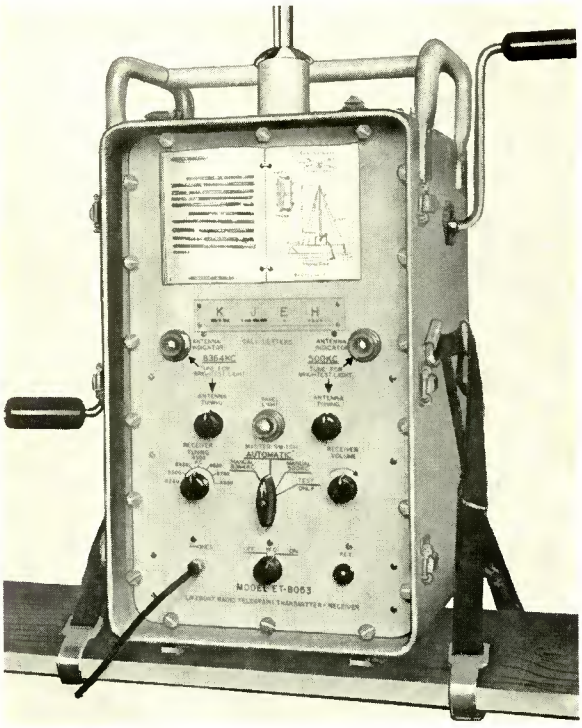

Fig. 8—Lifeboat radiotelegraph transmitter–receiver.

scales between 1 and 40 miles uses an indicator unit as shown in Figure 9. The plan-position indicator (PPI) tube is a 16-inch metal-shell type with a P-7 long-persistence phosphor. A display of this size provides good accuracy of bearings and ranges.

For true bearings, there is a movable azimuth scale, driven by a gyro compass repeater motor. Earlier designs used gyro information to control the PPI deflection system so that North was "up" on the scope. While this gave a desirable stabilized presentation for true bearings, it displaced the relative picture from its "natural" position. On a 180-degree course, for example, the relative picture would be

upside down. With the newer design, simultaneous bearings may be taken, true bearings being read from the movable scale, and relative bearings from the fixed scale. Thus the relative picture is properly oriented.

Radar tracking or plotting of the relative courses of vessels seen on the scope has usually been done by transferring the PPI information to maneuvering boards or charts. A more direct method, involving a "position tracker" mounted over the scope, has been developed. This

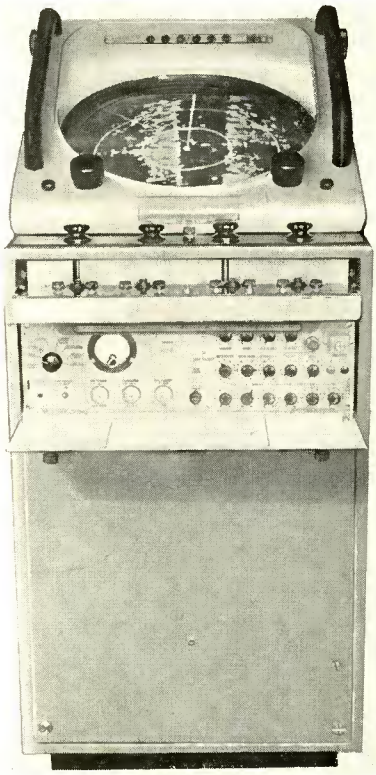

Fig. 9—Radar indicator with 16-inch tube.

device, shown in Figure 10, uses a dichroic mirror midway between the scope face and an upper edge-lighted concave writing glass. Wax crayon markings on the upper glass are projected downward, without parallax, and appear as clear red lines on the scope. The navigator may thus keep track of the relative course and speed of other ships, predict passing distances and, in general, keep more direct control of a particular situation.

Optimum radar performance is closely related to fundamental factors such as pulse length, pulse repetition rate and receiver band width. A short pulse, a high repetition rate, and a wide-band receiver are needed for good short-range performance, while the converse is true for longer ranges. In the radar under discussion, the three lower ranges (1, 2, and 4 miles) use a 0.25-microsecond pulse, a 2000-cycle repetition rate and an 8-megacycle pass band for the receiver. For the longer ranges (8, 20, and 40 miles) the pulse is 0.65 microsecond, the rate 800 cycles and the receiver pass band is 2.5 megacycles. Peak power from the magnetron is 40 kilowatts in the 9375-megacycle (3.2-centimeter)

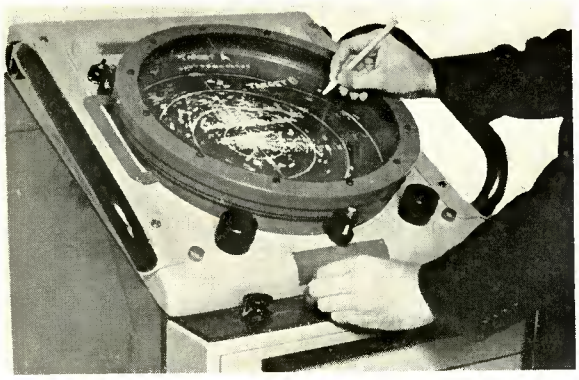

Fig. 10—Radar position tracker.

band. The magnetron duty cycle is maintained substantially constant (.0005 to .00052) by using the two repetition rates. This keeps the average power uniform on each range. The antenna half-power beam pattern is 1.9 degrees horizontal and 20 degrees vertical. Side lobes are attenuated 32 decibels.

Besides the usual fixed range rings, the indicator has a variable range marker which can be read in tenths of a mile from one-half to twenty miles. Main operating controls are kept to a minimum (range, gain and suppressor), while secondary controls are on a hinged panel which opens to a horizontal position for heading flash, focus, fast time constant, ring intensity, and the like.

A VHF-UHF TELEVISION TURRET TUNER*

By

T. Murakami

Home Instruments Department, RCA Victor Division,
Camden, N. J.

Summary—*A sixteen-position turret type of tuner covering both the very-high-frequency (VHF) and ultra-high-frequency (UHF) television channels has been designed and tested. The measured electrical performance data and field tests of the tuner indicate that it gives excellent performance.*

Introduction

With the advent of ultra-high-frequency television and the subsequent allocation of specific UHF channels, the need for a VHF-UHF television tuner becomes apparent. This tuner should ideally make the maximum use of the same components on VHF and UHF, so that there would be a minimum duplication of parts. This design should be one which would give optimum performance and still be easy to fabricate and align. The tuner should also use a 41-megacycle intermediate frequency to take full advantage of the protection from interference which the Federal Communications Commission provided in its channel allocation plan. A sixteen-position turret type of tuner which has been developed accomplishes some of the objectives of the ideal tuner. A careful study of the television channel allocations showed that sixteen positions on the turret would cover channel requirements of almost any receiver location in the United States. This report describes the technical aspects of the television tuner.

General Description

The tuner covers both the VHF and UHF television channels. Figure 1 is a photograph of the tuner showing the drive assembly and channel indicating system. A 2:1 step down ratio is used for the turret drive system for ease of tuning. Figure 2 shows the turret with its divided shielding compartments, inside the main housing.

The tube complement for this tuner consists of a 6BQ7A for the VHF radio-frequency (r-f) amplifier, a 6AF4 for the VHF-UHF oscillator, a 6BQ7A for the intermediate-frequency (i-f) amplifier, and

* Decimal Classification: R583.5.

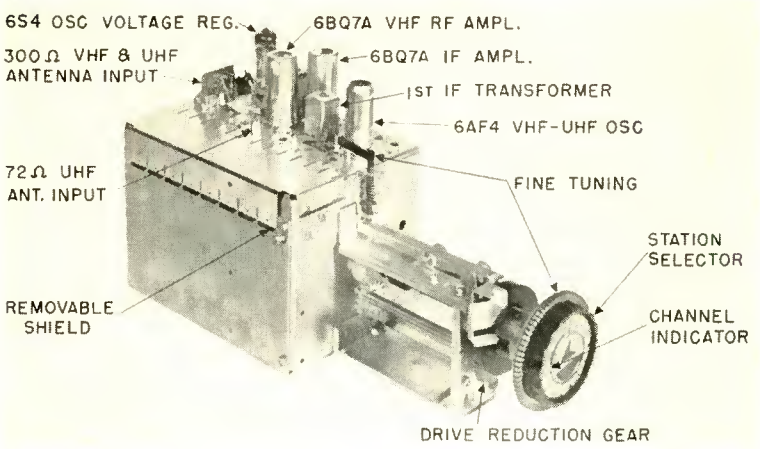

Fig. 1—VHF-UHF tuner.

a 6S4 for the oscillator plate voltage regulator. A 1N82 silicon crystal is used in the mixer circuit for both VHF and UHF. In the VHF range a low-noise r-f amplifier is used before the crystal mixer which, in turn, is followed by another low-noise stage operating on the 41-megacycle intermediate frequency. For the UHF, the arrangement is similar except there is no r-f amplifier ahead of the crystal mixer. Figures 3a and 3b show block diagrams of the tuner operating at VHF and UHF. Figure 4 is a bottom view of the r-f shield showing some of the circuits described.

The antenna input circuit for the VHF portion of the tuner consists essentially of a single-tuned circuit with the 300-ohm balanced antenna input tapped down on this circuit for impedance match. A double-tuned circuit is used between the r-f amplifier and the crystal mixer,

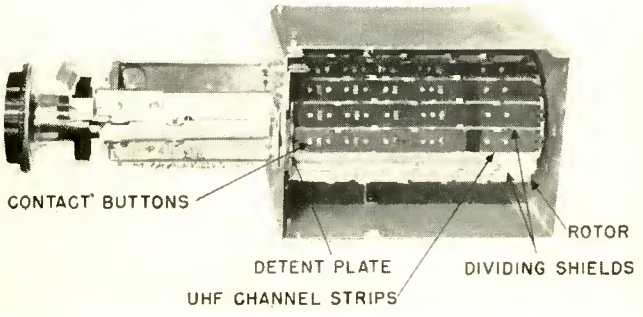

Fig. 2—Turret and housing of VHF-UHF tuner.

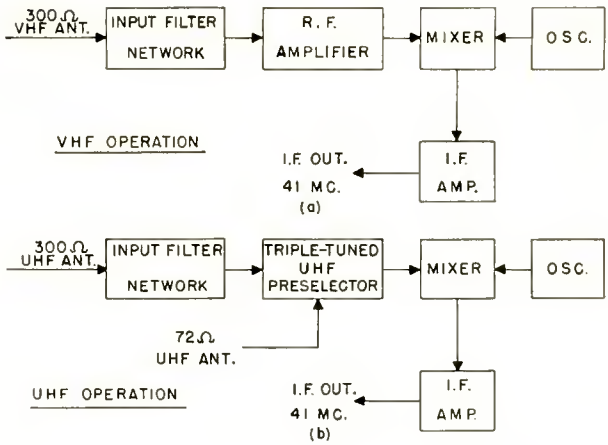

Fig. 3—Block diagram of VHF-UHF tuner.

with the crystal tapped down on the secondary circuit to obtain the proper circuit loading. Four different channel strips, shown in Figure 5, are used for the VHF range. On UHF, a triple-tuned preselector is used between the antenna input and the crystal mixer. Both 72-ohm unbalanced and 300-ohm balanced antenna input impedances are available on UHF. Two different channel strips are used to cover the frequency range from 470 to 890 megacycles; these are shown in Figure 6.

The only portion of the oscillator circuit which is switched when changing channels on the tuner is the circuit between the grid and plate of the 6AF4 oscillator tube. An incremental change in impedance

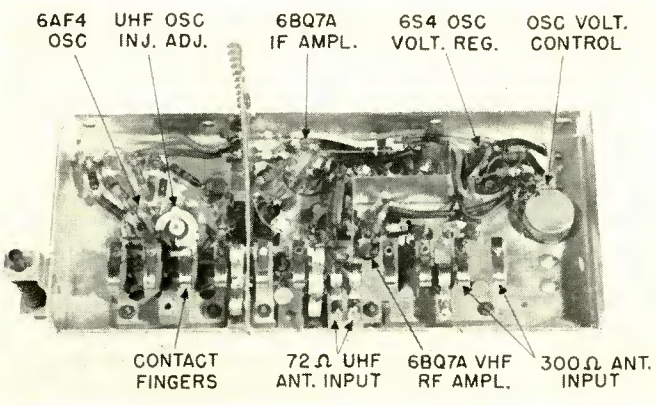

Fig. 4—Bottom view of r-f shelf.

in the plate side of the oscillator circuit provides fine tuning for both VHF and UHF. The oscillator and intermediate-frequency on this tuner have been designed for a picture i-f of 45.75 megacycles and a sound i-f of 41.25 megacycles. The i-f output system of the tuner consists of a link-coupled transformer, with a coaxial cable in the link

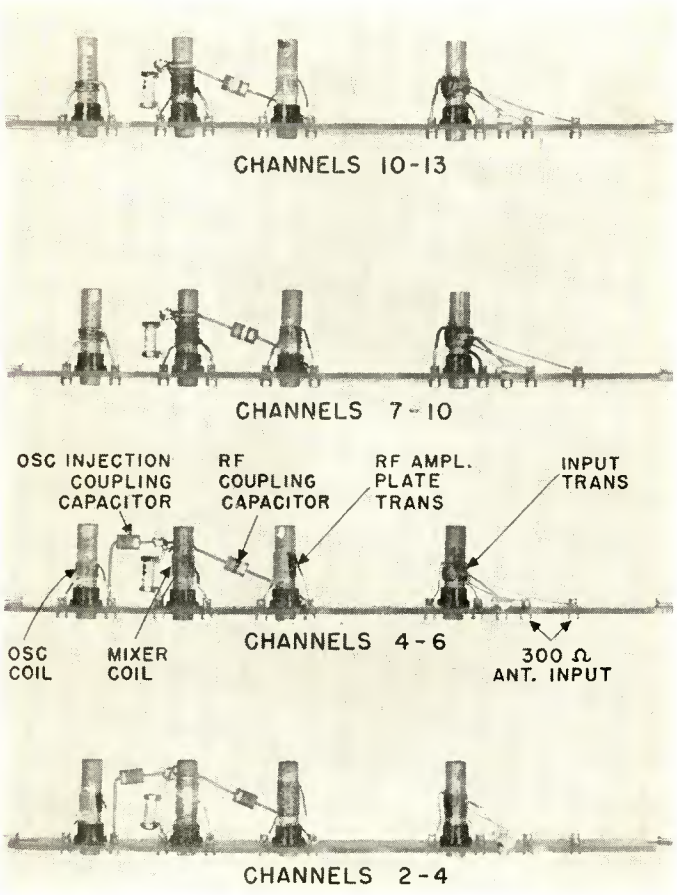

Fig. 5—VHF channel strips.

circuit. The primary of the link-coupled transformer is on the tuner chassis, the secondary being located in the i-f amplifier section on the main chassis. All switching on the tuner is done by means of the silver plate type of contact, which is used on VHF tuners. The contact springs are made of phosphor bronze with a silver overlay.

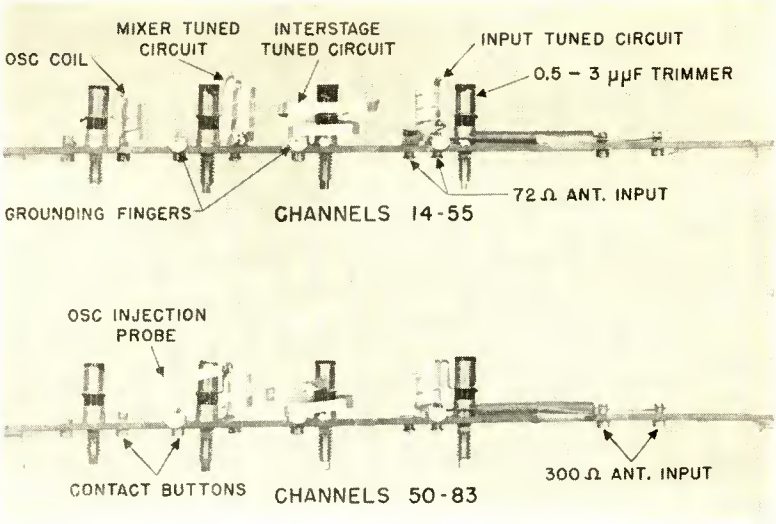

Fig. 6—UHF channel strips.

VHF Circuit Description

Antenna Input Circuit

Figure 7 shows the basic input circuit used in the VHF channel strip. An antenna impedance of 300 ohms is used, since in most receiver locations balanced 300 ohms is most convenient. To obtain a 72-ohm unbalanced input impedance, a 4:1 wide-band-impedance trans-

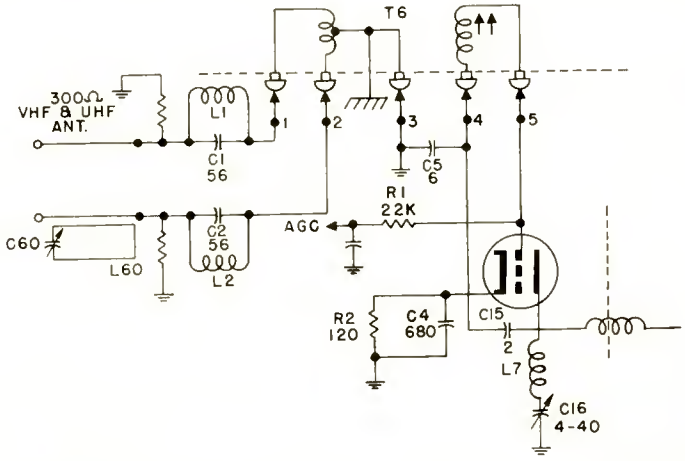

Fig. 7—VHF amplifier circuit.

former may be used. Referring to Figure 7, C60 and L60 form a variable trap which is made of a section of 300-ohm transmission line and a trimmer capacitor. This trap is mutually coupled to the input line to attenuate undesired signals between 88 and 108 megacycles (frequency modulation broadcast band). Since the 300-ohm antenna is common to both VHF and UHF, the length of transmission line is so chosen that the UHF resonances fall below 470 megacycles and above 890 megacycles. Two i-f traps tuned to 43.5 megacycles, shown by L1, C1 and L2, C2 in Figure 7, are used to improve the i-f rejection of the tuner. These traps have very low impedance to the signals in the VHF and UHF range.

The antenna input transformer, shown as T6 in Figure 7, is of the single-tuned variety with very tight coupling between the primary and secondary circuits. The primary coil is wound directly over the secondary with a center tap provided as shown. The secondary is inductively tuned with the input capacitance of the amplifier by means of a brass core inside the coil. Since the input impedance of the 6BQ7A r-f amplifier tube decreases with an increase in frequency, the impedance step-up from the antenna to the r-f grid must be varied accordingly for the various channels in order to obtain the best performance. The impedance step-up ratios used are the ratios which give the r-f amplifier a reasonably good noise figure, but not the best possible input standing-wave ratio; however, the impedance match to 300 ohms is quite reasonable.

R-F Amplifier Circuit

The VHF r-f amplifier is a low-noise driven-grounded-grid stage using a 6BQ7A twin triode. The circuit which is used is shown in Figure 8.

The relatively high transconductance of this tube, 6400 micromhos per section, permits high gain and reduced equivalent noise resistance. The 6BQ7A also provides low input loading minimizing induced grid noise and aids in obtaining high input circuit gain over all of the VHF channels. The low plate-to-cathode capacitance minimizes direct feed-through of the local oscillator.

A capacity bridge type of neutralization is used to prevent detuning of the input circuit with change in grid bias because of Miller effect and to improve the noise figure of the amplifier. The arms of the capacity bridge are C_{15}, C_5, C_{gp} and C_{gk}, where C_{gp} and C_{gk} are the grid-to-plate and grid-to-cathode capacitances respectively. The requirement for neutralization is

$$\frac{C_{15}}{C_5} = \frac{C_{gp}}{C_{gk}}.$$

The circuit used provides a wide-band type of neutralization which is fairly effective over all the VHF channels.

The gain of the r-f amplifier is improved on the upper VHF channels by use of a series inductance between the plate of the first triode section and the cathode of the second section of the 6BQ7A. This inductance is series resonated with the total capacitance from the cathode of the second triode to ground, the inductance being adjusted so that the resonance occurs near the upper end of the high VHF channels. This series circuit further improves the neutralization of the r-f stage on the upper VHF channels by keeping the plate of the

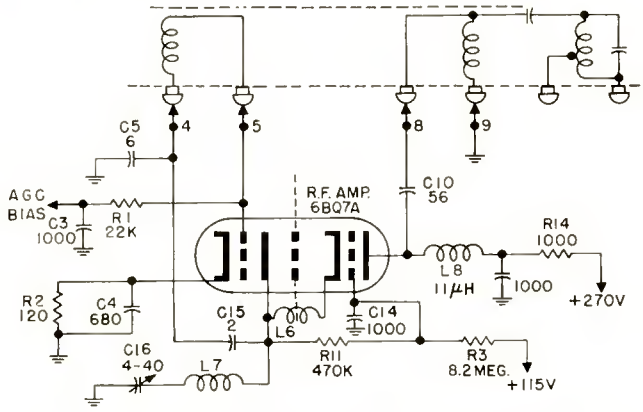

Fig. 8—Radio-frequency amplifier circuit (VHF only).

first triode section at low impedance so that little r-f voltage is fed back from the plate to the input grid. For the lower VHF channels, the effect of the series resonant circuit is negligible since the inductive reactance is small.

Direct coupling extends the cutoff characteristics, resulting in less cross modulation when automatic-gain-control bias is applied to the first grid. However, for most effective gain control over the wide range of input levels encountered in the field, it is desirable to allow the bias of the second half of the driven-grounded-grid amplifier to vary somewhat with signal level. This is accomplished by tapping the second grid on a d-c voltage divider between the second cathode and a fixed voltage source having a potential slightly less than the cathode potential under minimum bias conditions. In Figure 8, this voltage divider

is formed by resistors R3 and R11. Under strong signal conditions, automatic-gain-control bias applied to the first grid increases the plate resistance, resulting in a higher positive potential on the direct-coupled second cathode. The second grid, however, is prevented from following the cathode potential completely, because of the voltage divider connection to the fixed potential source. Therefore, the grid bias developed in the second triode is a function of the ratio of the voltage on the divider and the potential of the fixed source, which have been chosen to maintain a desirable characteristic over a wide range of input levels. For the best noise figure under weak signal conditions, the bias on the first triode should not drop below 1.25 volts. The cathode resistor R2 has been chosen to maintain this condition.

In order to make the VHF and UHF channel strips similar as to the grounding contacts, shunt feeding of the plate-supply voltage to the r-f amplifier stage was necessary. The amplifier plate choke, L8, is so designed that high impedance is maintained over both the lower and upper VHF channels. It was found that in nearly all of the chokes designed, resonances caused the choke impedance to fall off near channel 7 and near channel 13. By using a fluted bakelite coil form to reduce the distributed capacitance of the coil, a choke was made with resonances sufficiently removed in frequency from channels 7 and 13 to give satisfactory performance.

An adjustable i-f trap is provided to increase the i-f rejection of the amplifier, since there is insufficient i-f rejection provided by the r-f circuits alone on channel 2 when 41-megacycle i-f is used. This trap is of the series resonant type, placed between the plate of the first triode of the driven-grounded-grid stage and ground, and is composed of the elements C16 and L7 in Figure 8.

The plate circuit of the r-f amplifier shown in Figure 9 consists of a capacity-coupled double-tuned circuit. The primary on the transformer is tuned with the output capacitance of the plate of the grounded-grid section of the r-f amplifier. The secondary of the transformer is tuned with a 5-micromicrofarad capacitor for all the channel strips. The bandwidth of the coupled circuit is determined by the coupling capacitance and the crystal loading. The amount of loading provided by the crystal depends upon the effective crystal tap point on the secondary of the transformer, and the oscillator injection current to the crystal. The nominal over-all operating bandwidth has been designed such that approximately 4.5 megacycles exist between peaks of the selectivity curves for the over-coupled double-tuned circuits. The tuning of the circuits is accomplished by means of threaded brass cores instead of the powdered iron type since the latter have a tendency

to bind or be too abrasive when used with paper base coil forms. Four sets of strips are used to cover the VHF range, with at least a one-channel overlap between strips covering adjacent groups of channels.

Crystal Mixer Circuit

The crystal mixer circuit used for the VHF range is shown in Figure 9. The 1N82 mixer feeds into a 41-megacycle i-f system with an approximate input bandwidth of 8 megacycles, under operating conditions. For the lower VHF channels, the oscillator injection for the crystal is obtained by capacity coupling with a 1 micromicrofarad capacitor from the grid side of the oscillator circuit to the high side of the mixer tuned circuit. On the upper VHF channels, the oscillator injection is obtained by mutual inductance coupling of the mixer circuit to the oscillator tuned circuit.

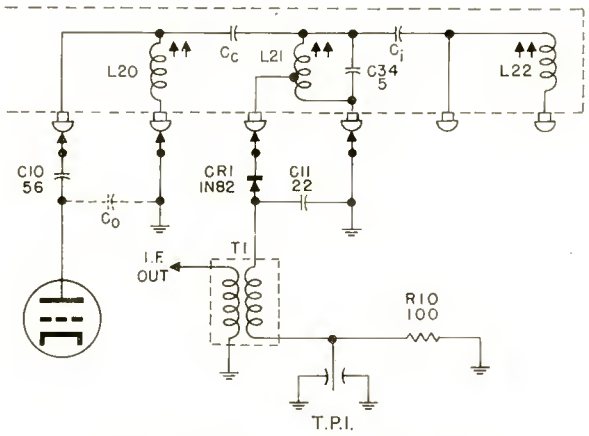

Fig. 9—VHF crystal mixer circuit.

The d-c crystal return is through a 100-ohm resistor, R10, which puts a little self bias on the crystal. This generally improves the noise figure of the crystal circuit. This resistance provides a test point TP 1, where a millivoltmeter may be used to measure the amount of oscillator injection. This point is also used to look at the over-all r-f circuit response with a cathode-ray oscilloscope.

Since the low-noise r-f amplifier is used ahead of the crystal mixer circuit, the noise figure of the mixer stage is not so important on VHF as on UHF where no r-f amplifier is used.

VHF Oscillator Circuit

The oscillator circuit used in the tuner is of the Colpitts type, with

the tuning between the various channel strips accomplished by switching in various amounts of grid to plate inductance. The schematic diagram of the circuit is shown in Figure 10.

Fine tuning for the VHF range is accomplished by changing the effective capacitance from plate to ground by means of a brass core inserted into a low inductance sleeve in series with the plate circuit of the oscillator. The inductive reactance used in the plate-to-grid circuit on VHF causes the plate of the oscillator tube to assume very nearly an r-f voltage maximum. The fine-tuning element is therefore quite sensitive to capacitative changes. The ratio of the inductance change of the fine-tuning element to the total circuit inductance is quite small, so that the capacitative change masks any change in frequency which is due to the change in inductance.

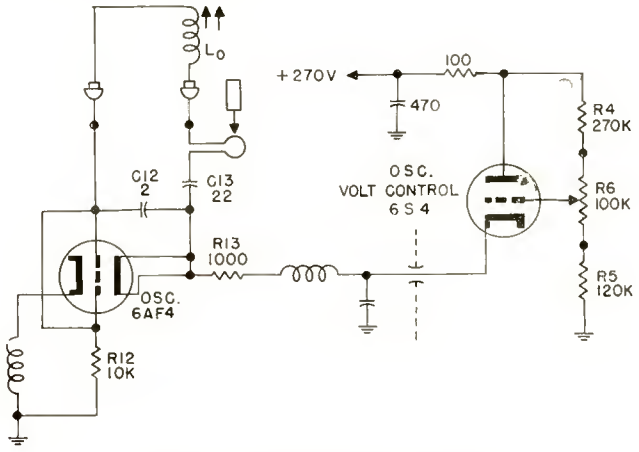

Fig. 10—VHF oscillator circuit.

To decrease the strength of oscillation on the VHF channels, a resistor, R13, is used in series with the plate choke L11. The inductance of L11 is made low enough to further decrease the strength of oscillation, particularly on the upper VHF channels. To allow for the variation in electrical characteristics of different 6AF4 tubes, a voltage-control tube has been used. The 6S4 tube shown in series with the plate-supply system of the 6AF4 in Figure 10 controls the voltage at the plate of the oscillator tube, the voltage being set by means of the grid potential chosen. The plate voltage of the 6AF4 is set so that a maximum cathode current of 28 milliamperes is obtained when the tube is not oscillating. The variation in 6AF4's is such that the voltage required at the plate of the tube to set this condition is between 85 and 115 volts. Since the cathode of the 6S4 stays near grid potential

and is a low impedance, the cathode voltage, and therefore the oscillator plate voltage, stays constant with changes in the current drawn by the oscillator tube.

UHF Circuit Description

Antenna Input Circuit

On UHF, an input circuit impedance of 300 or 72 ohms may be used. The 300-ohm input is the same as that used for VHF, but the 72-ohm input is made separate so that a separate UHF antenna may be used. The circuit diagram of the basic input circuit used for the UHF strips is shown in Figure 11.

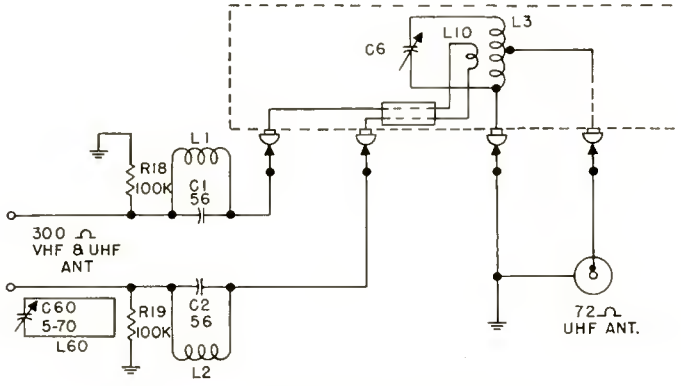

Fig. 11—UHF antenna input circuit.

The 88-108 megacycle trap composed of elements C60 and L60 has resonances outside the UHF range, and therefore does not deteriorate the UHF performance. Similarly, the 43.5 megacycle i-f traps are designed so that the first resonance after 43.5 megacycles occurs above 950 megacycles. Since the 300-ohm antenna-coupling coil does not have a grounded center tap, two static drain resistors, R18 and R19, have been used. The 300-ohm input coupling loops consist of one- or two-turn self-supporting coils made small enough to fit inside the input coil L3. All of the UHF circuits on the strips are capacity tuned using Erie type 535 0.5-3.0 micromicrofarad trimmer capacitors. The 72-ohm UHF input consists of a tap on the input coil, the tap point being set to give the proper input loading under operating conditions.

UHF Preselector Circuit

The UHF preselector consists of a triple-tuned circuit using high-Q tuning coils as shown in Figure 6. The coils are self-supporting and

are wound with silver-plated strap stock 0.093 inch wide and .010 inch thick. The input and output coils are the ordinary cylindrical type with an inside coil diameter of 0.203 inch. The interstage coupling coil is shaped in the form of a racetrack to obtain the required coupling to the input and output coils. The circuit diagram of the UHF strip with the associated crystal mixer circuit is shown in Figure 12.

The three tuned circuits on the strip are predominately inductively coupled by proximity and by the coupling loop formed by grounding contacts and the shielding trough in which the strip rests. By proper adjustment of the center-to-center distance between the input and mixer coils and the length of the race-track shaped coupling coil, the bandwidth of the preselector circuit across the UHF range can be made substantially constant. The tap on the crystal mixer circuit is made high enough to give the over-all r-f response a reasonably flat amplitude

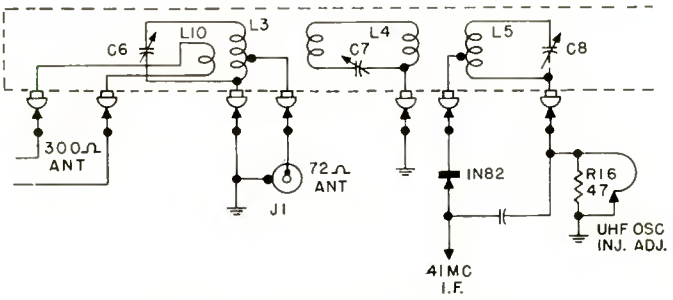

Fig. 12—UHF preselector circuit.

characteristic over a 4.5-megacycle frequency range when local oscillator injection is applied to the crystal.

The r-f selectivity curve varies with frequency. It is triple-peaked at the low end of the UHF range, double-peaked at midband, and flat-top to round nosed at the upper end of the frequency range. The efficiency of the triple-tuned preselector is quite high, due to the high Q of the tuned circuits. The insertion loss of the preselector is in the order of 1 decibel over the UHF range. Additional grounding fingers have been used between the rotor and the r-f shelf to decrease the direct coupling between the antenna and the mixer circuit of the preselector. This improves the rejection for the image frequency and also reduces the spurious responses due to the resonance of the rotor and the main housing.

The 1N82 crystal diode which is used for the UHF mixer had the most satisfactory oscillator current injection and noise figure charac-

teristics at the high end of the UHF range among all the crystal mixers tested. The oscillator injection to the crystal mixer circuit on the UHF range of the tuner is obtained by means of an adjustable inductance from the ground side of the mixer circuit on the strip to a ground point on the r-f shelf. A 47-ohm resistor, R16, shown in Figure 12, is used to decrease the oscillator injection between 470 and 600 megacycles. A coupling probe on the high side of the mixer circuit on the 50-83 channel strip is used to increase oscillator injection at the upper end of the range.

UHF Oscillator Circuit

The UHF oscillator circuit is the same as that used for the VHF range except that the tuning between channels is accomplished by switching in a variable capacitance in series with an inductance.

An oscillator frequency range of 480 to 970 megacycles is covered in the two UHF strips using different oscillator tank circuit inductances in series with the 0.5 to 3.0 micromicrofarad trimmer capacitor. The fine tuning for the UHF range is accomplished by changing the effective inductance in the grid-to-plate circuit of the oscillator. The fine tuning element consists of a low inductance, one-turn coil in the shape of a slit cylinder into which is inserted a brass core which changes the effective inductance of the one-turn coil. In this case, the plate of the oscillator tube is very nearly a voltage node, and the ratio of the fine tuning inductance change to the total circuit inductance is much higher than on VHF. The inductive change, therefore, predominates over any shift in frequency due to the capacitative change. To compensate for the oscillator frequency drift at the low end of the UHF range, a negative temperature coefficient capacitor is used for the plate blocking capacitor C12. At the high end of the UHF range, a small piece of bimetallic strip is used near the oscillator trimmer capacitor to compensate for oscillator frequency drift caused by the circuit components and the oscillator tube.

Low Noise I-F Amplifier

The noise figure of the tuner at UHF depends primarily on the noise contributed by the crystal mixer and by the first i-f amplifier following the mixer circuit. Therefore, a low-noise, driven-grounded-grid stage is used for the first i-f amplifier. A schematic diagram of the circuit used is shown by Figure 13.

The input transformer T1 is designed so that enough loading is provided by the crystal diode to give a 3-decibel bandwidth of approximately 8 megacycles. The 22 micromicrofarad capacitor C11, which is used for the crystal r-f bypass and the input capacitance of the tube,

provides the capacitance required to tune this circuit to 43.5 megacycles.

The neutralization of the grid-to-plate capacitance is accomplished by means of a shunt inductance, L12, from grid to plate which resonates with this capacitance. The output transformer of the amplifier is of the link-coupled type so that a low-impedance circuit can be used between the tuner and the i-f amplifier on the main chassis.

The complete circuit diagram of the VHF-UHF tuner, with the various channel strips, is shown in Figure 14.

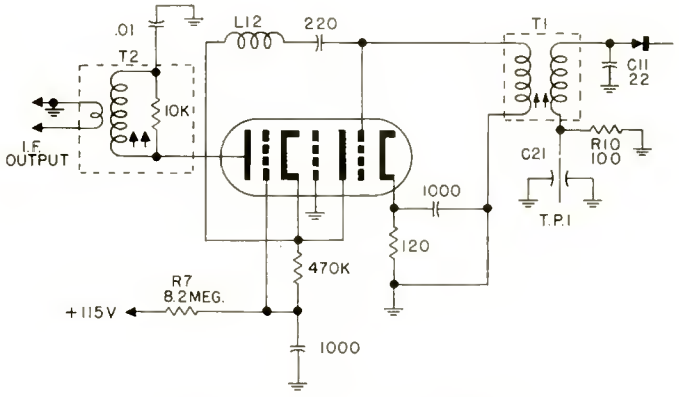

Fig. 13—Low-noise i-f amplifier.

VHF Performance

Noise Figure

The noise figure of the tuner on VHF depends primarily on the driven-grounded-grid r-f amplifier, although some noise is contributed by the crystal mixer and the low-noise i-f amplifier following the crystal mixer. The antenna input circuit has been designed with the signal to noise ratio as the criterion; therefore, the coupling of the antenna transformer has been increased beyond the value which would give maximum gain.[1] The neutralization of the grid-to-plate capacitance of the first triode section of the driven-grounded-grid r-f amplifier also improves the noise figure. The measured noise figures for the VHF channels are given in Table I along with other performance characteristics of the tuner. These measurements were taken using a balanced type of noise diode with a source impedance of 300 ohms.

[1] Wm. A. Harris, "Some Notes on Noise Theory and Its Application to Input Circuit Design," *RCA Review*, Vol. IX, No. 3, pp. 406-418, September, 1948.

Gain

The VHF voltage gain of the tuner from the antenna terminals to the grid of the first i-f tube on the main chassis is shown in Table I.

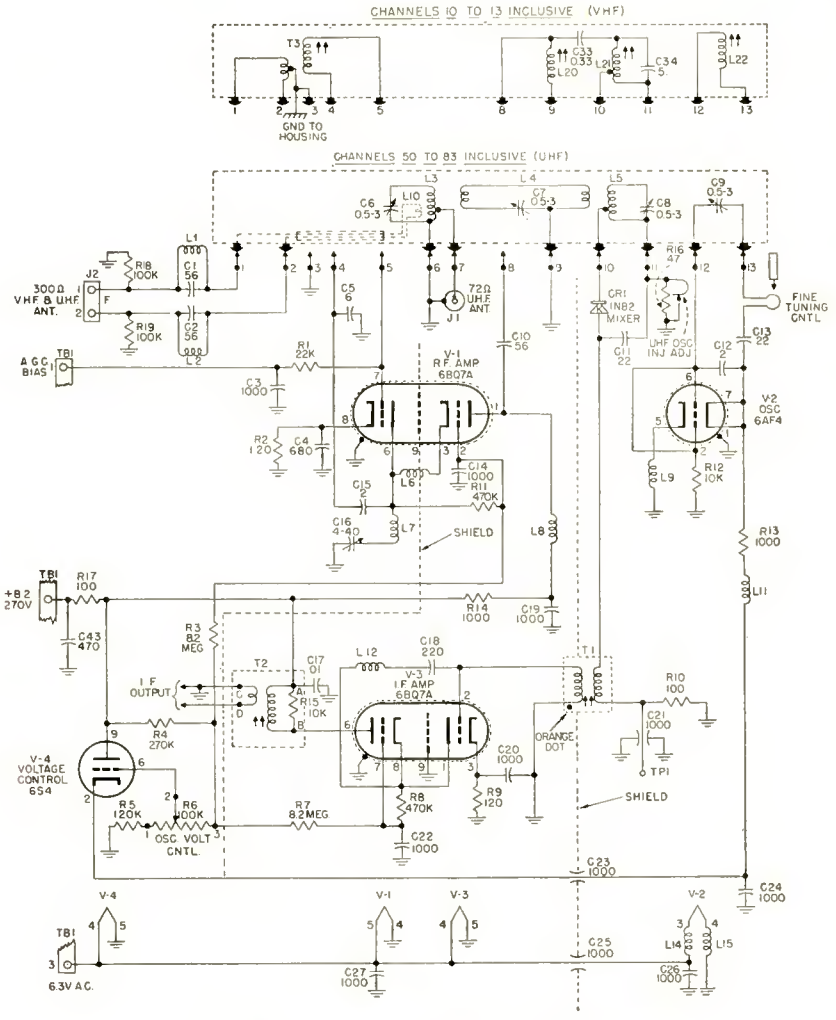

Fig. 14—Schematic diagram of tuner.

The gain on channel 13 is somewhat higher than that on the other upper VHF channels; this is due to the peaking caused by the inductance L61, in Figure 8, resonating with the total input capacitance of the cathode of the second triode section of the r-f amplifier tube.

Input Standing-Wave Ratio

The voltage-standing-wave ratio of the VHF antenna input circuit was measured by the long-line method. The ratio could be improved by decreasing the coupling between the primary and secondary windings of the input transformer, but the input circuit bandwidth would then be too narrow on some of the lower VHF channels. On the upper VHF channels, a decrease in coupling would result in a poorer over-all noise figure for the r-f amplifier, even though the input circuit gain and bandwidth would be improved.

Undesired Responses

The image and i-f rejections for the VHF channels shown in Table I were measured with zero automatic-gain-control bias. The other undesired responses are more than 80 decibels below the desired signal. For cross-modulation to exist under weak signal (50-microvolt desired signal) conditions, the undesired signal must be at least 80 decibels greater than the desired signal to produce perceptable interference. This is under the conditions where the most cross-modulation exists, e.g., the undesired signal is within the r-f pass-band but outside the i-f pass-band. Under strong signal conditions (50-millivolt desired signal), the undesired signal must be at least 40 decibels greater than the desired signal to produce appreciable cross-modulation. For other frequencies, this ratio of strength of the undesired to desired signals would have to be greater to produce interference.

The use of a 41-megacycle intermediate-frequency gives the possibility of self-generated interference on channel 6 (82-88 megacycles) due to the second harmonic of the i-f generated in the first detector, or generated in the second detector and fed back overall through the i-f amplifier. The over-all feedback can be reduced by proper shielding and filtering in the i-f amplifier. Both the first detector and the feedback harmonic interferences increase as the detectors are operated at higher signal levels; therefore, these types of interference can be reduced somewhat by operating the r-f and i-f amplifiers at lower signal levels by use of higher automatic-gain-control bias under strong signal conditions. Also, they can be reduced by tuning the 88-108 megacycle trap in the VHF antenna circuit to the sound carrier of channel 6 (87.75 megacycles).

Oscillator Radiation

The VHF oscillator radiation data is also shown in Table I. These measurements were taken with a Stoddart NMA-5 field intensity meter at a standard Institute of Radio Engineers radiation test site. The data shown is given for two cases: first, without an auxiliary shield

Table I—Typical VHF Tuner Operating Characteristics

Channel No.	Noise Figure (Decibels)	Voltage Gain	Image Rejection (Decibels)	I.F. Rejection 43.5 Mc. (Decibels)	I.F. Rejection 45.75 Mc. (Decibels)	Input V.S.W.R.	Oscillator Radiation Without Shield Max μv/m at 100′	Oscillator Radiation With Shield Max μv/m at 100′
2	3.7	80	59.1	80	66	2.36	30.0	< 5
3	4.0	83	60.0	90	72	2.48		
4	4.5	77	59.5	90	79	2.06	32.1	< 5
5	4.6	95	57.3	90	88	2.82		
6	5.1	95	57.4	90	90	2.25	48.1	< 5
7	6.7	67	75.2	90	90	1.83	165.0	25.0
8	6.9	55	78.0	90	90	1.59		
9	6.6	55	75.9	90	90	1.66		
10	6.7	54	78.5	90	90	1.85	101.5	23.7
11	6.6	50	70.7	90	90	2.62		
12	6.6	51	78.8	90	90	2.73		
13	6.4	83	72.5	90	90	2.11	123.2	30.5

Table II—Typical UHF Tuner Operating Characteristics

Channel No.	Center Freq. (Mc.)	Noise Figure (Decibels)	Voltage Gain	Input 300Ω	V.S.W.R. 72Ω	R.F. Band-width (Mc.)	Image Rejection (Decibels)	I.F. Rejection (Decibels) 300-ohm Input	I.F. Rejection (Decibels) 72-ohm Input	Oscillator Radiation Without Shield Max μv/m at 100′	Oscillator Radiation With Shield Max μv/m at 100′
14	473	12.5		1.41	1.18	9	47.2	90	59.8		
19	503	13.0	10.0	1.34	1.22	9	46.0	90	60.6	1530	161
27	551	12.2		1.33	1.16	11	47.6	90	60.6		
35	599	13.6		1.34	1.27	11	36.5	90	60.1	1495	414
44	653	13.1		1.63	1.22	11	38.7	90	60.2		
52	701	15.6	7.8	1.70	1.25	9	50.9	90	62.2	2008	559
60	749	15.6		1.83	1.31	6	42.8	90	62.4		
69	803	16.2	8.7	1.74	1.17	8	42.9	90	63.0	1092	218
77	851	15.4		1.71	1.36	9	58.4	90	65.0		
83	887	16.4	5.3	1.20	1.22	8	50.3	90	62.1	2880	212

covering the oscillator tube and the fine tuning plunger; and second, with the shield. With the shield, the oscillator radiation is well within the Radio and Television Manufacturers Association's recommended limits for oscillator radiation of 50 microvolts per meter on the lower VHF channels and 150 microvolts per meter for the upper VHF channels. Without the shield, the oscillator radiation on channel 7 is just above the recommended limit.

Oscillator Stability

The oscillator frequency drift for a lower and an upper VHF channel is shown in Figure 15. The warm-up drift of the oscillator on other VHF channels is similar. The initial reading in all cases was taken one half minute after the power for the tuner was turned on.

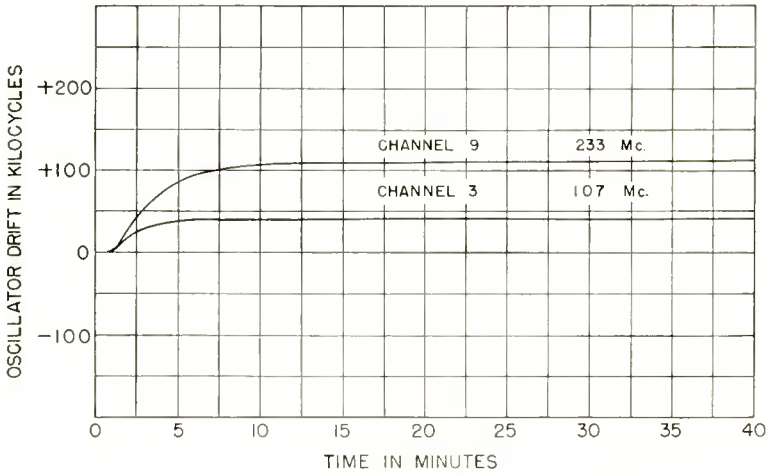

Fig. 15—VHF oscillator frequency drift.

UHF Performance

Noise Figure

When operating on UHF, the noise figure of the tuner depends primarily upon the crystal mixer and the low-noise i-f amplifier following the mixer. With the 1N82 silicon crystal used as the mixer, the maximum noise figure variation among crystals is approximately ±2.5 decibels, with an average noise figure of 13.2 decibels at 500 megacycles. The noise figure of the tuner for various frequencies in the UHF range is shown in Table II. These measurements were made using a "Mega-Node Sr." noise diode, a 50 to 72 ohm coaxial line transformer, and a 75 to 300 ohm UHF balun. The noise figure measurements were essentially the same when 72 or 300 ohm antenna inputs were used.

Gain

The over-all voltage gain between the antenna terminals and the grid of the first i-f tube, when operating on UHF, is considerably less than that obtained on VHF due to the absence of the r-f amplifier.

Input Standing-Wave Ratio

The voltage standing wave ratios of the UHF antenna input circuit for both 300 and 72 ohm input impedances are given in Table II. The values shown are the average values over a 4.5-megacycle frequency

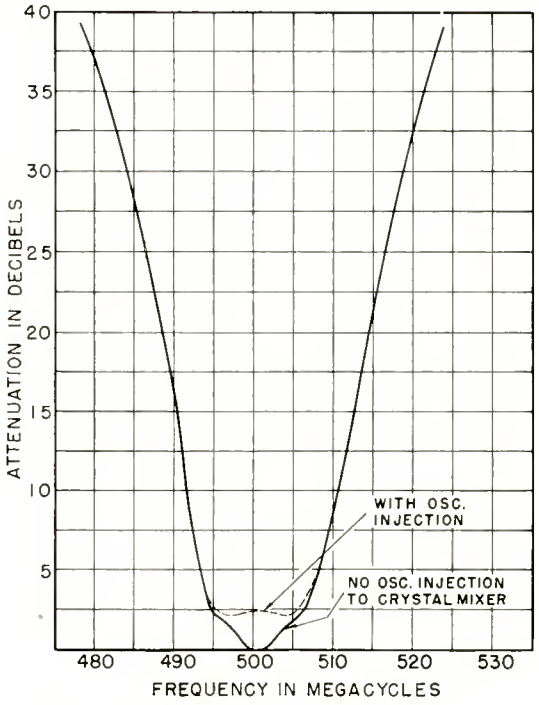

Fig. 16—UHF preselector selectivity at 500 megacycles.

range. The long-line method of measuring standing-wave ratio was employed for these measurements, using approximately 130 feet of low-loss 75-ohm coaxial cable.

Preselector Bandwidth and Selectivity

The approximate r-f bandwidth of the triple-tuned UHF preselector is shown in Table II. The bandwidth has been measured with oscillator injection to the crystal mixer. The over-all r-f selectivity curve is shown in Figure 16 for a center frequency of 500 megacycles. For

other frequencies in the UHF range, the response curves are similar to that shown.

Undesired Responses

The image and i-f rejections of the tuner when operating in UHF range are given in Table II. The decrease in image rejection for channels 35 and 44 is due to a 700-megacycle resonance in the crystal mixer circuit. The 300-ohm input gives more i-f rejection than the 72-ohm input due to the extra trap circuit in the antenna. Other undesired responses below 980 megacycles are more than 60 decibels below the

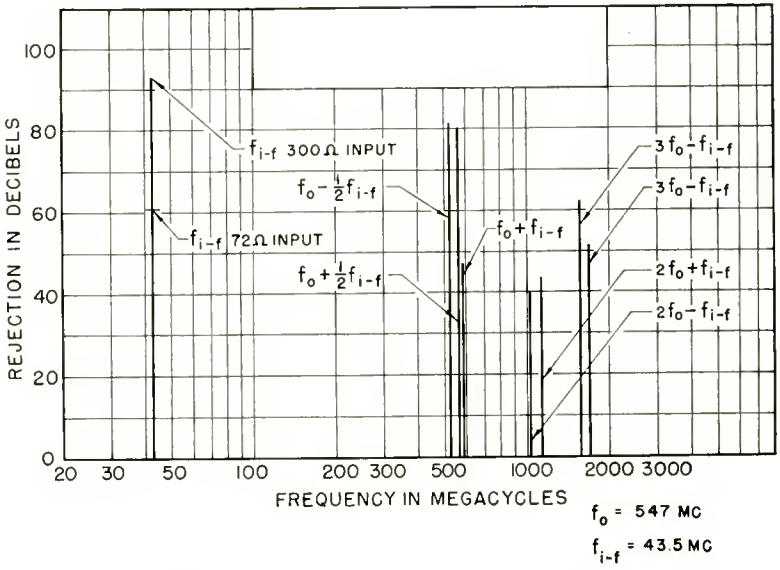

Fig. 17—Rejection of undesired signals for a desired signal of 500 megacycles.

desired signal level. Figure 17 shows the various responses when the tuner is tuned to 500 megacycles.

Oscillator Radiation

The UHF oscillator radiation data is shown in Table II. The measurements were taken with a Stoddart NM-50A field intensity meter at a standard Institute of Radio Engineers radiation test site. In order to reduce the antenna radiation, the oscillator compartment was isolated from the antenna by use of several small grounding fingers which contact the rotor at various points on its periphery. The data shown is given for two cases: first, without an auxiliary shield covering the

oscillator tube and the fine tuning plunger; and second, with the shield in place. The shield is seen to reduce the chassis radiation from 3 to 13 times.

Oscillator Stability

The oscillator frequency drift for various frequencies in the UHF range is shown in Figure 18. The initial reading in all cases was taken one half minute after the power for the tuner was turned on. For the strip covering channels 50-83, the compensation is not sufficient for frequencies above 800 megacycles. To add compensation above 830 megacycles, a $\frac{1}{8} \times \frac{1}{2} \times 0.005$-inch piece of bimetal was used near the oscillator trimmer capacitor on the strip.

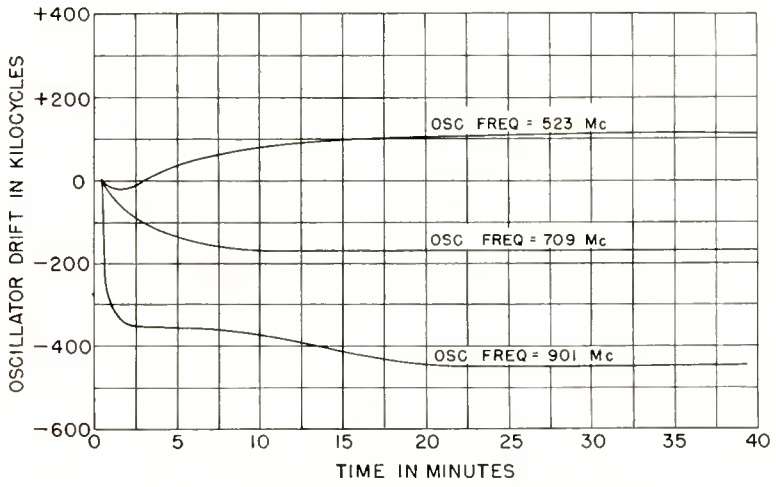

Fig. 18—UHF oscillator frequency drift.

Field Tests

Field tests of the tuner on the VHF channels indicate that it performs as well or better than most current tuners under normal operating conditions. The low noise figure on the VHF channels results in a better picture in weak signal locations. The tuner was extensively field tested for UHF operation in various locations such as Portland, Oregon (channel 27), Harrisburg (channel 55), Reading (channels 33 and 61), and York (channel 43). These tests indicated that this tuner on a "B" line chassis (3 i-f stage set) performed very well. The low noise figure on UHF results in a picture with less snow than other receivers tested in moderately weak signal areas. The resetability on

UHF is very good, the tuning on UHF being very similar to that on the VHF channels.

Acknowledgments

The author wishes to acknowledge the work contributed by J. C. Achenbach and G. C. Hermeling, and particularly the guidance of J. C. Achenbach in the development of the tuner. The mechanical design of the tuner is credited to W. T. Prock.

A COMPARISON OF MONOCHROME AND COLOR TELEVISION WITH REFERENCE TO SUSCEPTIBILITY TO VARIOUS TYPES OF INTERFERENCE*

By

Gordon L. Fredendall

Research Department, RCA Laboratories Division, Princeton, N. J.

Summary—*A subjective study has been made of the relative susceptibilities of color and monochrome television to various types of interference. The types of interference considered include cochannel and adjacent-channel television transmissions, random noise, sine wave, multipath, and impulse noise. The results of this study are set forth.*

Introduction

THE purpose of the study covered by this paper was the accumulation of data which would measure the relative susceptibility of standard monochrome television and color television[1] to cochannel and adjacent-channel interference, random and impulse noise, multipath, and sine-wave interference.

Observers differ appreciably in their reactions to interference. A certain ratio of desired to interfering signal may cause intolerable degradation of the picture for a sensitive observer and entirely tolerable imperfections for a less susceptible observer. The measurement of such subjective reactions calls for viewing tests with a sufficiently large number of observers. The "average observer" is then the hypothetical person who finds that the arithmetic average of the ratios of all observers in a particular test marks the limit of tolerability or threshold perception as the case may be. In these tests the term tolerable ratio is the ratio of desired signal to interfering signal which corresponds to interference that is just at the point of becoming annoying in the test picture. Signals are measured at the peak of sync. The threshold ratio denotes the point at which interference is just about to disappear from view.

Test runs were made with 15 to 25 observers drawn from the nontechnical staff of the David Sarnoff Research Center of the RCA Laboratories, approximately half of whom were men and half were women.

All tests were performed in the laboratory under conditions that

---

* Decimal Classification: R583.5.

[1] According to the NTSC color field test specifications dated February 2, 1953.

simulated an actual transmitter–receiver relationship, as illustrated in the block diagram of Figure 1. The picture transmitters were television signal generators complete with vestigial sideband filters. The transmission amplitude characteristics are shown in Figures 2a and 2b. Synchronizing waveforms for the desired and interfering signals were generated by completely independent synchronizing and burst generators. Other test information is summarized below:

Color receiver: RCA color field test receiver operating according to the NTSC (National Television System Committee) color field test specifications dated February 2, 1953.

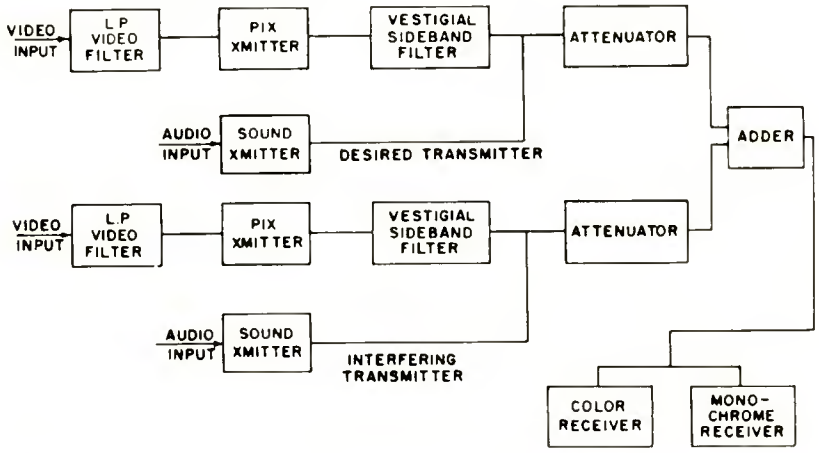

Fig. 1—Arrangement of apparatus for cochannel and adjacent-channel interference observations.

Monochrome receiver: (a) RCA color field test receiver with chroma channels turned off; (b) standard RCA monochrome receiver, type T120.

Picture size: $8\frac{1}{2} \times 11$ inches.

Picture highlight brightness: 12 foot-lamberts.

Viewing distance: 6 feet.

Desired picture: Color slide (Figure 3) scanned by flying spot scanner. Figure 3 is a black and white reproduction of a Kodachrome slide used by RCA, NTSC and others for test purposes; the same is the case with respect to Figures 4 and 5.

Interfering picture for cochannel and lower-adjacent-channel interference tests: Color test pattern (Figure 4) by color camera.

Interfering picture for upper-adjacent-channel interference: Scene by color camera (Figure 6).

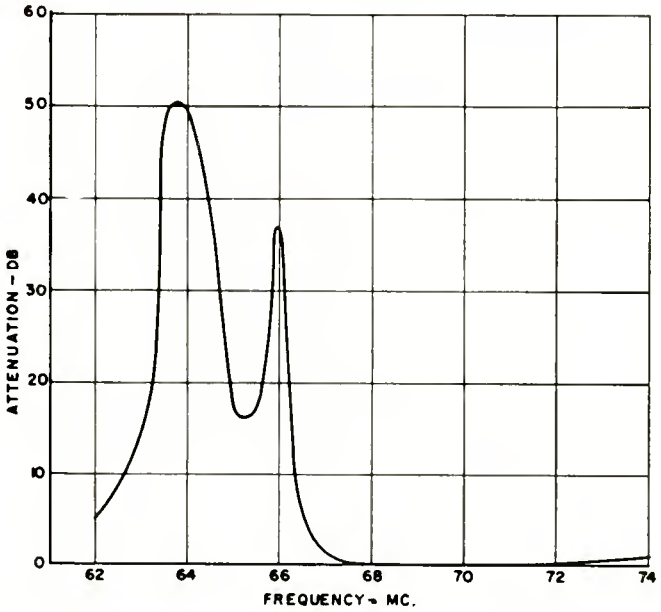

Fig. 2a—Transmission characteristic channel 4 (undesired).

Sound: Frequency-modulated sound according to current monochrome standards. Ratio of picture signal to sound signal, 1.4. Frequency relation of cochannel picture carriers: 10.5 kilocycles offset.

Test channels: Channel 4 for cochannel interference. Channels 3 and 4 for adjacent-channel interference.

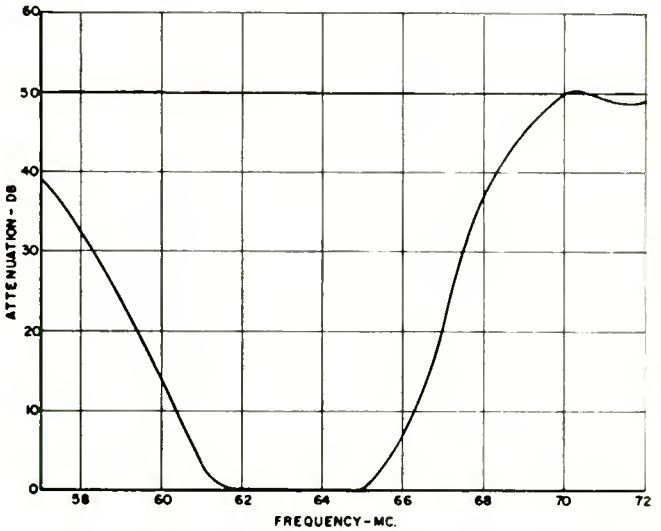

Fig. 2b—Transmission characteristic channel 3.

Fig. 3—Desired picture (black and white reproduction of Kodachrome slide).

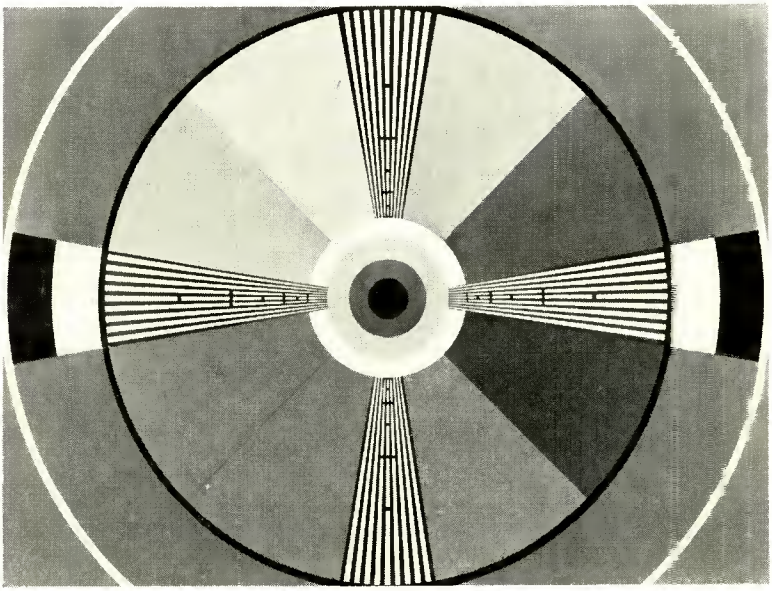

Fig. 4—Interfering test pattern (black and white reproduction of Kodachrome slide).

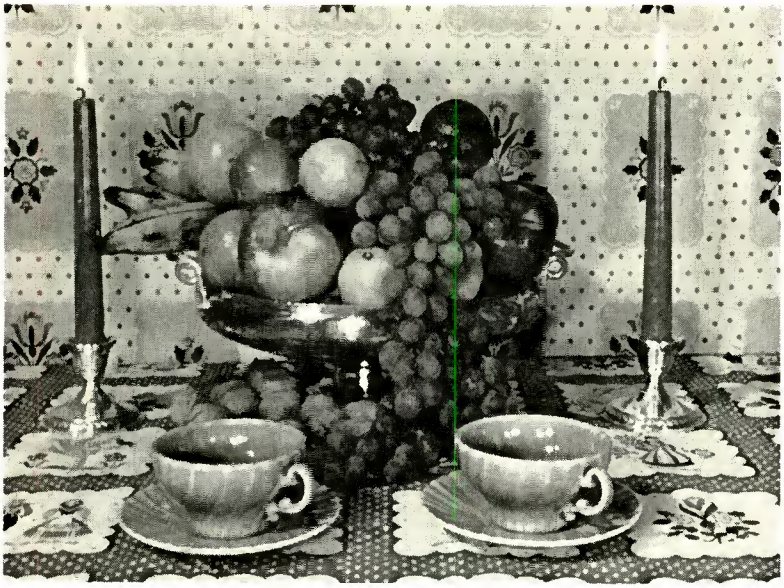

Fig. 5—Fruit bowl scene for multipath reception (black and white reproduction of Kodachrome slide).

Fig. 6—Interfering picture (black and white reproduction of Kodachrome slide).

Cochannel Interference

An observer of cochannel interference views the desired picture through a superimposed pattern of regularly spaced horizontal bars of light and shade. The frequency of the bars corresponds to the difference frequency of the two picture carriers. The visibility of the bars, considered as a function of the beat frequency, varies in a cyclical manner, with alternating minima and maxima having a separation of 30 cycles, as illustrated in Figure 7. Points of minimum visibility also exhibit a cyclic variation with least minima occurring at odd multiples

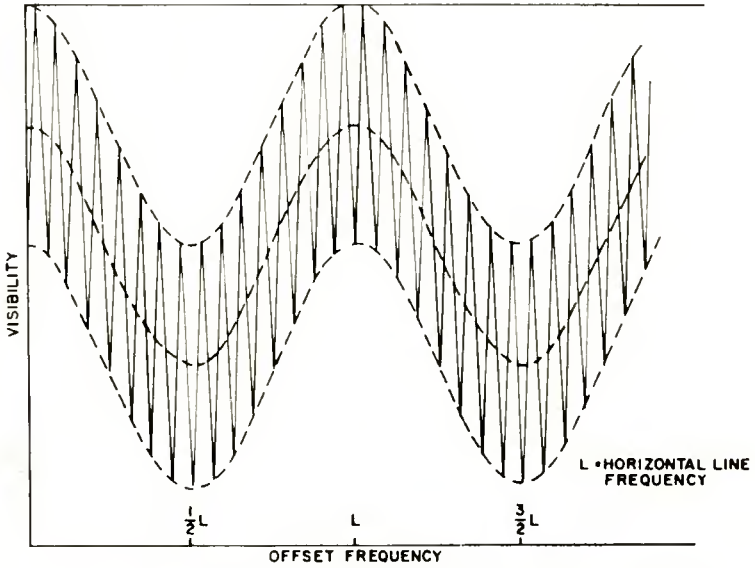

Fig. 7—Illustrative sketch of visibility of cochannel interference as a function of offset frequency.

of half line frequency. It will be recognized that the frequency components of the desired and interfering signals are interleaved for offset frequencies corresponding to the minima points and that they coincide at the maxima points.

An allocation plan for television stations cannot utilize the optimum offsets corresponding to the least minima, since two stations in a group of three stations in the same channel would be offset by a multiple of line frequency which results in maximum interference. However, stations may be offset by approximately 10.5 kilocycles with equal, though somewhat reduced, benefit to each. The offset which is standard was not specified with the view of taking advantage of the fine structure illustrated in Figure 7, since the present broadcast crystals do

not have the required stability for holding the frequency offset within a few cycles of the optimum. However, the stability is sufficiently good to bring about prolonged periods of maximum visibility.[2] In all of the present observations of cochannel interference, the offset frequency was adjusted about the nominal frequency of 10.5 kilocycles for maximum visibility.

Signal Combinations Used

Four signal combinations are possible:

	Abbreviation
1. Desired signal, color; interfering signal, color.	C/C
2. Desired signal, monochrome; interfering signal, color.	M/C
3. Desired signal, monochrome; interfering signal monochrome.	M/M
4. Desired signal, color; interfering signal monochrome.	C/M

The monochrome signal was the brightness component of the color signal.

Three conditions of reception are possible:

1. Color receiver with chroma channels switched off (simulated monochrome receiver).	(CM)
2. Color receiver.	(C)
3. Standard monochrome receiver.	(M)

A comparison of the interference properties of the standard monochrome system and the color system is more straightforward if the same color receiver is adjusted for monochrome operation by switching off the chroma circuits. This comparison is favored here although a full set of observations was made on a standard monochrome receiver.

Test Results

A summary of the average ratios of desired carrier to interfering carrier amplitudes for threshold and tolerable interference appears in Table I. On the basis of the data it must be concluded that no substantial difference exists between color and standard monochrome[3] with regard to cochannel interference. In general, the average observer does not detect the change in the visual interference level corresponding to a change in the ratio of less than about 2 decibels.

---

[2] Figure 7 is to be regarded only as illustrative and not quantitatively accurate.

[3] Color receiver used as monochrome receiver.

Table I—Cochannel Interference Ratios

Signal Condition		Receiver					
desired	interfering	Standard Monochrome		Color		Color used as Monochrome	
		threshold	tolerable	threshold	tolerable	threshold	tolerable
		(decibels)		(decibels)		(decibels)	
C	C	42.0	31.8	39.8	28.9	38.9	30.2
M	C	42.2	32.4	39.7	29.5	37.2	28.3
M	M	42.3	32.7	39.3	30.0	37.4	28.9
C	M	42.0	32.0	39.5	30.1	38.3	30.7

Ratios taken with the monochrome receiver are higher by about 3 decibels than the corresponding ratios recorded with the color receiver with chroma channels switched off. Differences in spot size and methods of d-c restoration and kinescope characteristics could account for this small discrepancy.

The average ratios for the monochrome receiver for the four signal combinations differed by 0.9 decibel. A similar picture is revealed for the less important threshold perception. It is noted that on the average, the tolerable ratio is about 9 decibels lower than the threshold ratio.

The spreads of twenty-five observers' ratios are shown in Figure 8. If the normal law is followed in observations of this kind, the data points should be along a straight line when plotted on arithmetic probability paper.

Upper–Adjacent–Channel Interference

Upper adjacent sound is 10.5 megacycles removed from the desired picture carrier and is not a source of interference. The concern is only with the upper adjacent picture carrier and sidebands. The appearance and visibility of the interference are controlled by the following factors:

(1) Attenuation of the receiver for the upper adjacent picture carrier.

(2) Attenuation characteristic of the vestigial sideband filter at the interfering transmitter for the lower sidebands of the picture carrier.

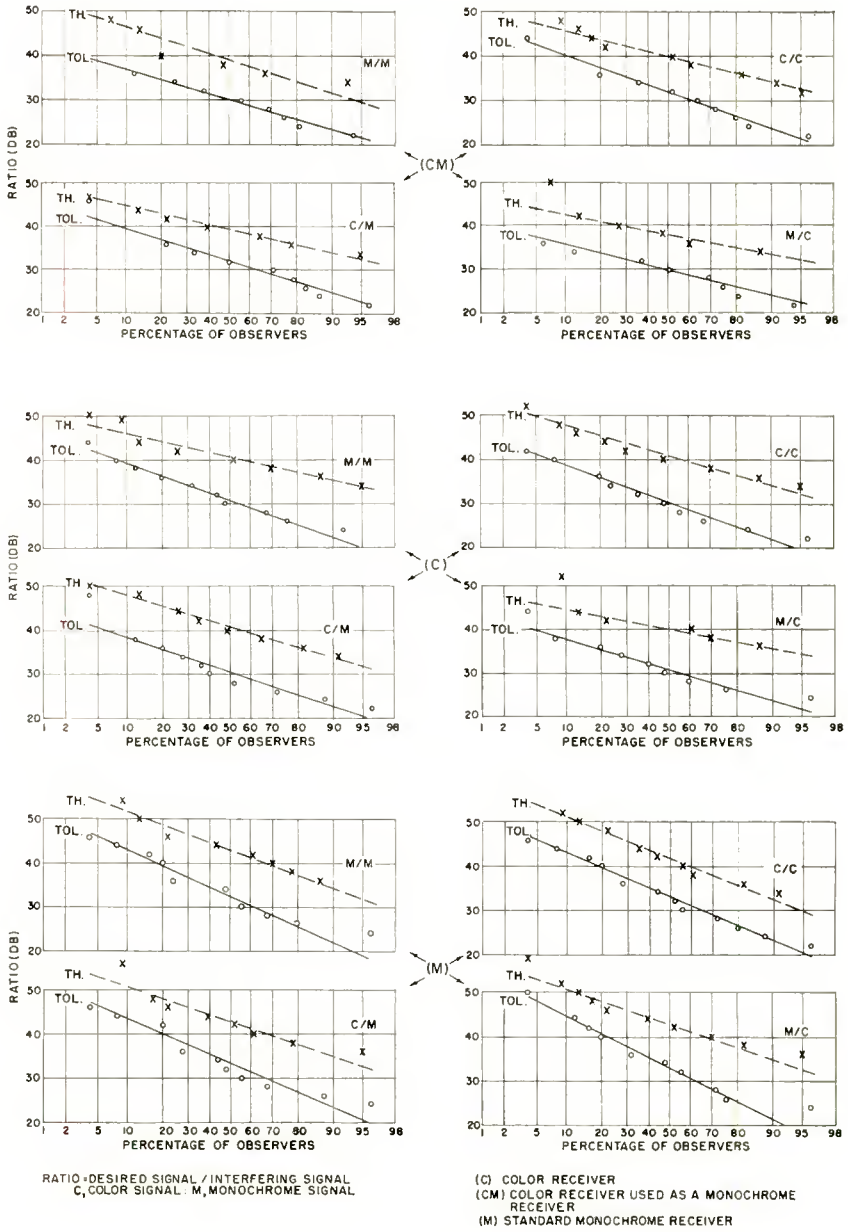

Fig. 8—Tolerable (Tol.) and Threshold (Th.) values of cochannel interfering television signals as a function of the percentage of observers requiring ratios greater than the ordinate values.

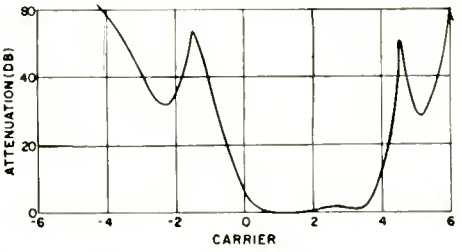

Fig. 9—Selectivity of monochrome receiver.

(3) Nearness of the two synchronizing generators to an in-step condition.

(4) Amplitudes of the lower sidebands of the interfering carrier.

Item (1) is under the control of the receiver design, item (3) is controlled by standardization, and items (2) and (4) are transmitter considerations.

Insufficient attenuation of the upper adjacent carrier permits the interfering picture to appear either as a meaningless fleeting interference, or, if the desired and interfering synchronizing signals are almost in step, as a recognizable picture. Since the NTSC color specifications for synchronizing signals call for crystal control, the interference from a color transmission will be a clearly defined picture in slow motion across the desired picture when adjacent picture carrier attenuation is inadequate. This type of interference was not observed in the present study since both receivers offered ample adjacent picture carrier attenuation (see Figures 9 and 10).

Items (2) and (4) were found to be controlling. The net effect of (2) and (4) is proportional to the product of the amplitude of the lower-sideband spectrum of the interfering signal and the attenuation offered by the vestigial sideband filter (Figure 2a).

The data in Table II indicates that, under the present test conditions for upper-adjacent-channel interference, the susceptibility of

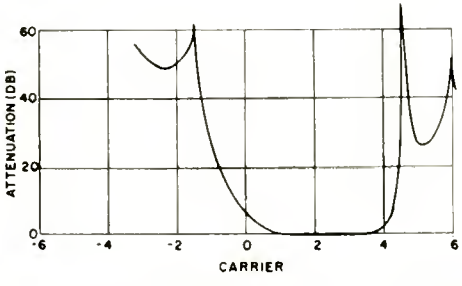

Fig. 10—Selectivity characteristic of color receiver.

color reception to color interference is 6-8 decibels greater than the susceptibility of monochrome reception to monochrome interference. This is caused by the interaction of the desired color subcarrier signal and the lower sidebands of the interfering carrier that lie in the vicinity of the color subcarrier. In monochrome reception, beats must occur with the picture carrier, in which case lower sidebands of the interfering carrier in the vicinity of 3.58 megacycles produce a fine beat pattern which is less visible.

The 6-decibel margin in standard monochrome reception is of no special consequence since the average ratios of tolerable interference for all signal combinations of color and monochrome in Table II are at least as favorable as —16 decibels. The present allocation plan of the Federal Communications Commission indicates that the tolerable ratio of 0 decibels is satisfactory. The margin of safety is therefore adequate in the present tests. Figure 11 shows the spread of the ratios for the group of 15 observers.

Table II—Upper-Adjacent-Channel Interference Ratios*

Signal Condition		Receiver					
desired	interfering	Standard Monochrome		Color		Color used as Monochrome	
		threshold	tolerable	threshold	tolerable	threshold	tolerable
		(decibels)		(decibels)		(decibels)	
C	C	—16.1	—20.9	—11.5	—16.3	—16.8	—22.0
M	C	—16.3	—20.4	—13.1	—16.1	—17.4	—22.1
M	M	—16.9	—22.5	—15.3	—20.0	—19.0	—24.5
C	M	—16.9	—22.4	—13.7	—20.0	—19.5	—24.7

* The negative signs indicate that the interfering signal was stronger than the desired signal.

Lower-Adjacent-Channel Interference

Interference from the picture and sound transmitters on the lower adjacent channel is determined by the attenuation of the receiver in this region. In the present series of tests, the average observer found that interference due to the sound signal became intolerable before interference from the picture signal was noticeable, irrespective of the nature of the picture signal, whether color or monochrome.

Table III lists the ratios for the various signal combinations and receiver conditions. Figure 11 shows the spread in values for the 25

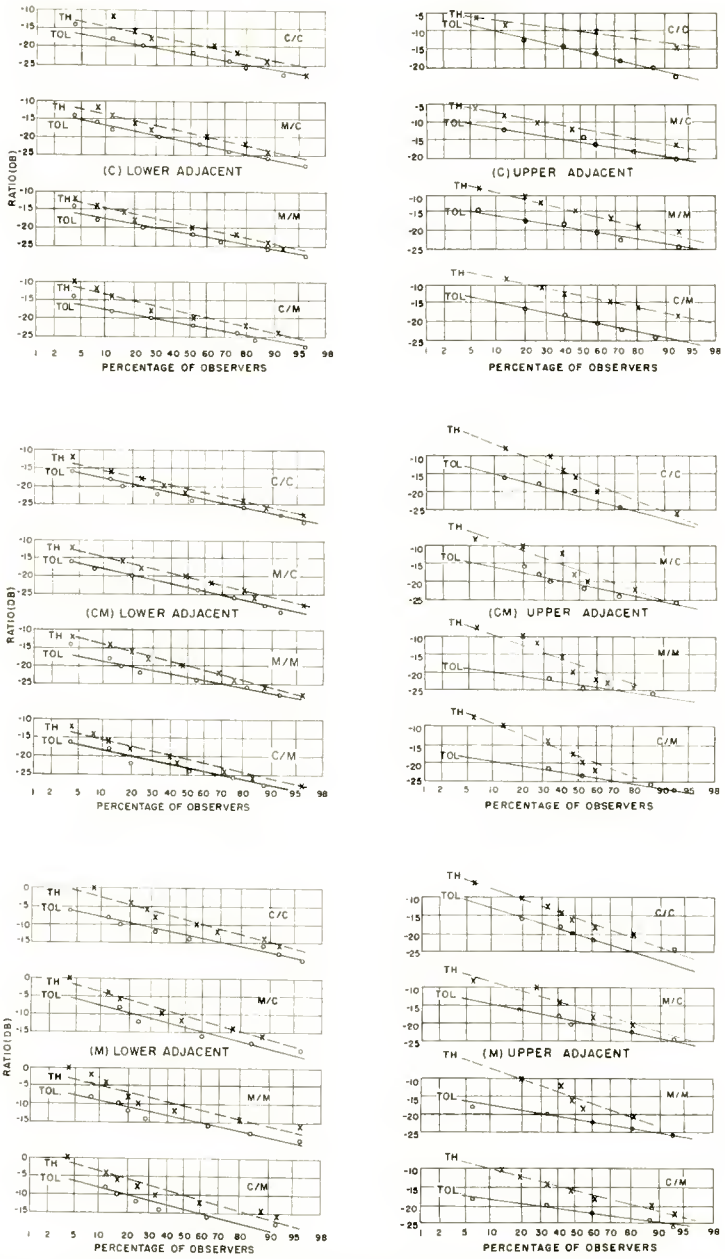

Fig. 11—Tolerable (Tol.) and Threshold (Th.) values of adjacent channel interfering television signals as a function of the percentage of observers requiring ratios greater than the ordinate values.

observers. Ratios for the color receiver are approximately —23 ±1 decibels, and for the monochrome receiver —15 ±1 decibels. The difference between the ratios is accounted for by the increased attenuation of 8 decibels which the color receivers offered to the lower adjacent sound signal (see Figures 9 and 10).

The present allocation plan of the Federal Communications Commission indicates that the tolerable ratio of 0 decibels is satisfactory. The margin of safety is therefore adequate in the present tests.

Table III—Lower-Adjacent-Channel Interference Ratios*

Signal Condition		Receiver					
desired	interfering	Standard Monochrome		Color		Color used as Monochrome	
		threshold	tolerable	threshold	tolerable	threshold	tolerable
		(decibels)		(decibels)		(decibels)	
C	C	—10.0	—14.0	—20.3	—23.2	—22.0	—24.3
M	C	—12.0	—15.7	—20.3	—22.6	—21.5	—24.7
M	M	—12.0	—15.7	—20.9	—23.2	—21.2	—24.2
C	M	—11.3	—15.3	—20.5	—22.9	—22.4	—24.3

* The negative signs indicate that the interfering signal was stronger than the desired signal.

Random Noise

The relative susceptibilities of color and monochrome pictures to random noise were measured for a group of 25 observers. Random noise of uniform spectral distribution was added in controllable amounts to a high-level radio-frequency signal and each observer was requested to compare a monochrome picture and a color picture. As in previous tests, the monochrome signal was derived from the color signal by elimination of burst and color components at the encoder. All chroma circuits were turned off in the color receiver when a monochrome rendition was desired. Noise was introduced into the signal in three steps which could be described as:

(1) Moderate noise.

(2) Noise somewhat greater than could be tolerated by most observers.

(3) Heavy, intolerable noise.

For each of the three steps, the average observer found that color was only slightly more susceptible to random noise—to the extent of about 1 decibel. The results of individual observations are listed in Table IV.

Table IV—Relative Susceptibilities of Monochrome and Color Signals to Random Noise*

Type	Number of observers reporting reading	Relative susceptibility* (decibels)
1	2	—2
	2	—1
	9	0
	2	1
	3	2
	7	3
		average 1
2	1	—3
	1	—1
	11	0
	5	1
	3	2
	4	3
	1	4
		average 1
3	13	0
	1	1
	5	2
	6	3
		average 1.2

* Positive values indicate that color is more susceptible than monochome, negative values the opposite.

Sine-Wave Interference

The relative susceptibility of monochrome and color reception to radio-frequency sine-wave interference was measured by one expert observer for the test picture shown in Figure 3. Since a relative measure is of principal interest, the difference in tolerable ratios for monochrome and color were plotted as a function of sine-wave frequency in Figure 12. The monochrome signal was derived from the color signal by omitting burst and the chroma component. Variations in the characteristics not related to color of a standard monochrome

and a color receiver were eliminated by switching off the chroma circuits of the color receiver when monochrome reception was desired.

Observations indicate that monochrome and color reception are about equally susceptible to sine-wave interference in the range of frequencies 1.7 megacycles on both sides of the picture carrier in which the interference appears as a brightness beat. Above this range the beat frequency continues to increase in frequency and become more tolerable. In color reception, a second beat with the color subcarrier appears as a rainbow bar pattern that increases in visibility as the subcarrier frequency is approached.

Over a narrow band about the associated sound carrier there is less divergence between color and monochrome susceptibility due to the trapping action around the position of the associated sound carrier.

In reality, Figure 12 is the locus of the maxima of interference which occur in the color picture at intervals separated by line frequency (15,750 cycles per second).

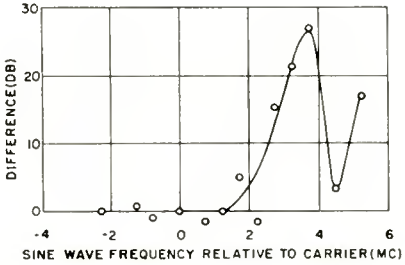

Fig. 12—Difference between tolerable ratios for sine-wave interference for monochrome and color reception as a function of the sine-wave frequency. Positive ratio indicates less susceptibility in monochrome.

Multipath Interference

Reflections were introduced in the radio-frequency signal by the addition of controllable amounts of the same signal delayed by transmission through a coaxial cable. Delays of approximately 0.5, 2, and 4 microseconds, corresponding to 2, 7, and 14 cycles at the subcarrier frequency, were viewed by 15 observers. The delays corresponded to spacings on the receiving screen of approximately 0.1, 0.4, and 0.9 inch respectively. Through the use of additional short delay lines, each multipath signal could be phased relative to the phase of the main radio-frequency signal.

Observers were shown the color and monochrome pictures reproduced by the same color receiver and requested to indicate when the multipath effects were equally objectionable in the two pictures. For

this test, the amplitude of the reflection was fixed at 8 decibels below the desired signal for color. In all trials, the radio-frequency phasing of the main and reflected signals was adjusted for the greatest degradation of the picture.

Since it was anticipated that the nature of the scene would influence the observer's judgment of the amount of degradation, three widely different stationary scenes were used—the boat scene reproduced in Figure 3, a garden scene including distant scenery reproduced in Figure 13, and a close-up of an assorted fruit bowl reproduced in Figure 5.

Fig. 13—Flower garden scene for multipath reception (black and white reproduction of Kodachrome slide).

A somewhat increased susceptibility of color to degradation by multipath reception is indicated in Table V for the average observer. Generalization of the test results probably justify an average estimate of 1-2 decibels. In any event, the factor is small. In attempting to correlate the results to field experience the following comments have a bearing:

(1) A reflection only 8 decibels down relative to the desired signal is strong and probably may be regarded as not tolerable by the average observer whether in monochrome or color.

(2) Reflections from fixed objects do not arrive in the most unfavorable phase relation on the average.

(3) The radio-frequency phase relations and the delay of a reflec-

tion from a moving object vary continuously. In color reception this means that the hue of the reflection changes in rainbow fashion.

Table V—Relative Susceptibility of Color and Monochrome to Multipath Interference*

Multipath delay (microseconds)	Relative susceptibility (decibels) 0.5	2	4
Scene			
Boat	0	3	1.9
Flower garden	1.4	1.5	0.3
Fruit bowl	1.3	2.5	2.7

* Positive values indicate that color is more susceptible than monochrome.

Impulse Noise

Information was sought on the relative susceptibility of the monochrome and the color systems to impulse noise. Special or different handling of impulse noise in one test receiver and not in another would confuse the comparison. Hence in these tests the color receiver served as a monochrome receiver when the chroma circuits were turned off. Random impulse noise generated by an electric pencil eraser was mixed with the radio-frequency signals giving definitely noisy reproductions of the boat scene (Figure 3). Observers were shown color and monochrome renditions and then requested to classify their comparison under one of the following headings:

(1) Monochrome deteriorated considerably more than color.
(2) Monochrome deteriorated just noticeably more than color.
(3) Sumstantially no difference.
(4) Color deteriorated just noticeably more than monochrome.
(5) Color deteriorated considerably more than monochrome.

Four observers registered opinions that the color picture was deteriorated just noticeably more than the monochrome picture; 4 observers reported that the monochrome picture was deteriorated just noticeably more; and 17 observers saw no noticeable difference. The conclusion is that the average observer placed color and monochrome on an equal basis with reference to impulse interference.

Conclusions

1. Cochannel Interference	Color and monochrome are substantially equally susceptible.
2. Upper-Adjacent-Channel Interference	Color is somewhat more susceptible than monochrome (6-8 decibels) in the present tests. Transmitter attenuation in the adjacent channel is the determining factor provided that receiver attenuation for the adjacent picture carrier is sufficient. However, the ratio desired carrier to interfering carrier of —16 decibels for tolerable interference is well above the ratio of 0 decibels set by the Federal Communications Commission.
3. Lower-Adjacent-Channel Interference	Color and monochrome are substantially equally susceptible. Lower adjacent sound signal is predominant cause of interference. Receiver attenuation in lower adjacent channel is a determining factor.
4. Random Noise	Color is only slightly more susceptible to random noise—about 1 decibel.
5. Sine-Wave Interference	Color is more susceptible to sine-wave interference but only in the vicinity of the color subcarrier (see Figure 12).
6. Multipath	Color is only slightly more susceptible—about 1-2 decibels.
7. Impulse Noise	Color and monochrome are substantially equally susceptible.

TECHNICAL SIGNAL SPECIFICATIONS PROPOSED AS STANDARDS FOR COLOR TELEVISION

ON February 2, 1953, the National Television System Committee approved for publication signal specifications for field testing compatible color television. These specifications were published in this journal.*

As a result of field tests conducted during the first half of 1953, several minor modifications were found to be desirable. Accordingly, a revised set of specifications was adopted by the NTSC on July 21, 1953, and was submitted to the Federal Communications Commission on July 23, 1953, as proposed standards for color television. These specifications are reproduced below.

I. General Specifications

A. Channel

The color television signal and its accompanying sound signal shall be transmitted within a 6-megacycle channel.

B. Picture Signal Frequency

The picture signal carrier, nominally 1.25 Mc above the lower boundary of the channel, shall conform to the frequency assigned by the Federal Communications Commission for the particular station.

C. Polarization

The radiated signals shall be horizontally polarized.

D. Vestigial Sideband Transmission

Vestigial sideband transmission in accordance with Figure 2 shall be employed.

E. Aspect Ratio

The aspect ratio of the scanned image shall be four units horizontally to three units vertically.

F. Scanning and Synchronization

1. The color picture signal shall correspond to the scanning of the image at uniform velocities from left to right and from top to bottom with 525 lines per frame interlaced 2:1.

2. The horizontal scanning frequency shall be 2/455 times the

* *RCA Review*, Vol. XIV, pp. 190-194, June, 1953.

color subcarrier frequency; this corresponds nominally to 15,750 cycles per second (with an actual value of 15,734.264 ± 0.047 cycles per second). The vertical scanning frequency is 2/525 times the horizontal scanning frequency: this corresponds nominally to 60 cycles per second (the actual value is 59.94 cycles per second).

3. The color television signal shall consist of color picture signals and synchronizing signals, transmitted successively and in different amplitude ranges except where the chrominance penetrates the synchronizing region, and the burst penetrates the picture region.

4. The horizontal, vertical, and color synchronizing signals shall be those specified in Figure 1, as modified by vestigial sideband transmission specified in Figure 2 and by the delay characteristic specified in III.B.

G. Out-of-Channel Radiation

The field strength measured at any frequency beyond the limits of the assigned channel shall be at least 60 decibels below the peak picture level.

II. Sound

A. Sound-Signal Frequency

The frequency of the unmodulated sound carrier shall be 4.5 Mc ± 1000 cycles above the frequency actually in use for the picture carrier.

B. Sound-Signal Characteristics

The sound transmission shall be by frequency modulation, with maximum deviation of ± 25 kilocycles, and with pre-emphasis in accordance with a 75-microsecond time constant.

C. Power Ratio

The effective radiated power of the aural-signal transmitter shall be not less than 50 per cent nor more than 70 per cent of the peak power of the visual signal transmitter.

III. The Complete Color Picture Signal

A. General Specifications

The color picture signal shall correspond to a luminance (brightness) component transmitted as amplitude modulation of the picture carrier and a simultaneous pair of chrominance (coloring) components transmitted as the amplitude modulation sidebands of a pair of sup-

pressed subcarriers in quadrature having the common frequency relative to the picture carrier of + 3.579545 Mc ± 0.0003 per cent with a maximum rate of change not to exceed 1/10 cycle per second per second.

B. Delay Specification

A sine wave, introduced at those terminals of the transmitter which are normally fed the color picture signal, shall produce a radiated signal having an envelope delay, relative to the average envelope delay between 0.05 and 0.20 Mc, of zero microseconds up to a frequency of 3.0 Mc; and then linearly decreasing to 4.18 Mc so as to be equal to —0.17 μsec at 3.58 Mc. The tolerance on the envelope delay shall be ± 0.05 μsec at 3.58 Mc. The tolerance shall increase linearly to ± 0.1 μsec, down to 2.1 Mc, and remain at ± 0.1 μsec down to 0.2 Mc.* The tolerance shall also increase linearly to ± 0.1 μsec at 4.18 Mc.

C. The Luminance Component

1. An increase in initial light intensity shall correspond to a decrease in the amplitude of the carrier envelope (negative modulation).

2. The blanking level shall be at (75 ± 2.5) per cent of the peak amplitude of the carrier envelope. The reference white (luminance) level shall be (12.5 ± 2.5) per cent of the peak carrier amplitude. The reference black level shall be separated from the blanking level by the setup interval, which shall be (7.5 ± 2.5) per cent of the video range from the blanking level to the reference white level.

3. The over-all attenuation versus frequency of the luminance signal shall not exceed the value specified by the FCC for black and white transmission.

D. Equation of Complete Color Signal

1. The color picture signal has the following composition:

$$E_M = E'_Y + \{E'_Q \sin(\omega t + 33°) + E'_I \cos(\omega t + 33°)\}$$

where

$$E'_Q = 0.41\,(E'_B - E'_Y) + 0.48\,(E'_R - E'_Y)$$

$$E'_I = -0.27\,(E'_B - E'_Y) + 0.74\,(E'_R - E'_Y)$$

$$E'_Y = 0.30\,E'_R + 0.59\,E'_G + 0.11\,E'_B.$$

The phase reference in the above equation is the phase of the (color

* Tolerances for the interval of 0.0 to 0.2 Mc should not be specified in the present state of the art.

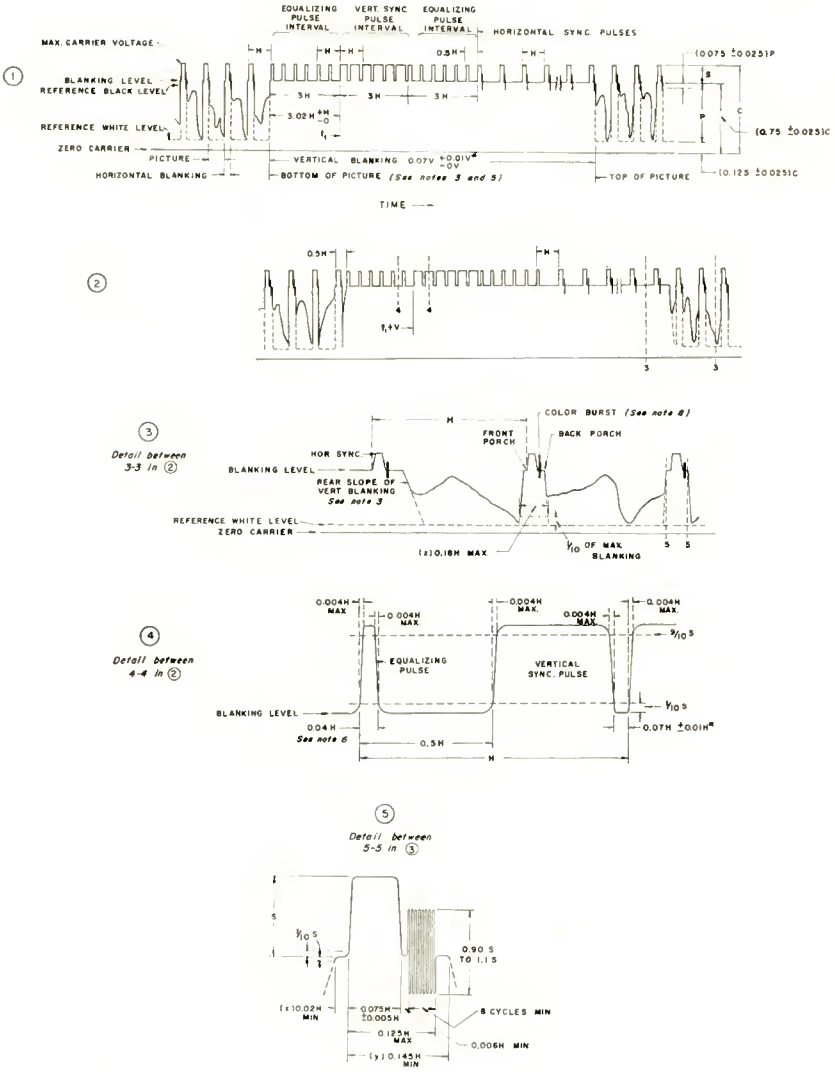

Fig. 1—Television synchronizing waveform. Horizontal dimensions not to scale in 1, 2, and 3.

Notes

1. H = Time from start of one line to start of next line.
2. V = Time from start of one field to start of next field.
3. Leading and trailing edges of vertical blanking should be complete in less than 0.1H.
4. Leading and trailing slopes of horizontal blanking must be steep enough to preserve minimum and maximum values of $(x + y)$ and (z) under all conditions of picture content.

*5. Dimensions marked with asterisk indicate that tolerances given are permitted only for long time variations and not for successive cycles.

6. Equalizing pulse area shall be between 0.45 and 0.5 of area of a horizontal sync pulse.

7. Color burst follows each horizontal pulse, but is omitted following the equalizing pulses and during the broad vertical pulses.

8. Color bursts to be omitted during monochrome transmissions.

9. The burst frequency shall be 3.579545 Mc. The tolerance on the frequency shall be ± 0.0003 per cent with a maximum rate of change of frequency not to exceed 1/10 cycle per second per second.

10. The horizontal scanning frequency shall be 2/455 times the burst frequency.

11. The dimensions specified for the burst determine the times of starting and stopping the burst, but not its phase. The color burst consists of amplitude modulation of a continuous sine wave.

12. Dimension "P" represents the peak excursion of the luminance signal from blanking level, but does not include the chrominance signal. Dimension "S" is the sync amplitude above blanking level. Dimension "C" is the peak carrier amplitude.

13. Refer to text for further explanations and tolerances.

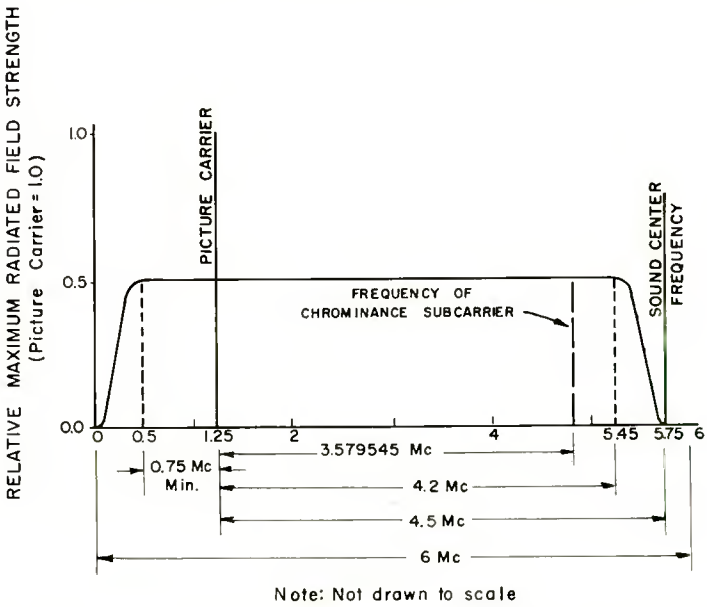

Fig. 2—Idealized picture transmission amplitude characteristic.

burst + 180°), as shown in Figure 3. The burst corresponds to amplitude modulation of a continuous sine wave.

NOTES: For color-difference frequencies below 500 Kc, the signal can be represented by

$$E_M = E'_Y + \left\{ \frac{1}{1.14} \left[\frac{1}{1.78} (E'_B - E'_Y) \sin \omega t + (E'_R - E'_Y) \cos \omega t \right] \right\}$$

In these expressions the symbols have the following significance:

E_M is the total video voltage, corresponding to the scanning of a particular picture element, applied to the modulator of the picture transmitter.

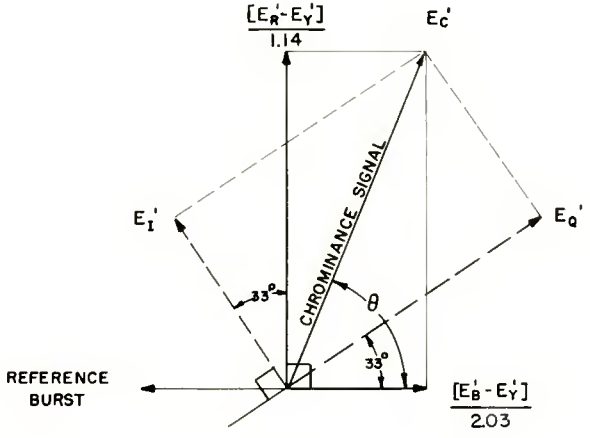

Fig. 3

E'_Y is the gamma-corrected voltage of the monochrome (black-and-white) portion of the color picture signal, corresponding to the given picture element.*

E'_R, E'_G, and E'_B are the gamma-corrected voltages corresponding to red, green, and blue signals during the scanning of the given picture element.

The gamma-corrected voltages E'_G, E'_R, and E'_B are suitable for a color picture tube having primary colors with the following chromaticities in the CIE system of specification:

* Forming of the high-frequency portion of the monochrome signal in a different manner is permissible and may in fact be desirable in order to improve the sharpness on saturated colors.

	x	y
Red (R)	0.67	0.33
Green (G)	0.21	0.71
Blue (B)	0.14	0.08

and having a transfer gradient (gamma exponent) of 2.2** associated with each primary color. The voltages E'_R, E'_G, and E'_B may be respectively of the form $E_R^{1/\gamma}$, $E_G^{1/\gamma}$, and $E_B^{1/\gamma}$ although other forms may be used with advances in the state of the art.

E'_Q and E'_I are the amplitudes of two orthogonal components of the chrominance signal corresponding respectively to narrow-band and wide-band axes, as specified in paragraph D.5.

The angular frequency ω is 2π times the frequency of the chrominance subcarrier.

The portion of each expression between brackets represents the chrominance subcarrier signal which carries the chrominance information.

2. The chrominance signal is so proportioned that it vanishes for the chromaticity of CIE Illuminant C ($x = 0.310$, $y = 0.316$).

3. E'_Y, E'_Q, E'_I and the components of these signals shall match each other in time to 0.05 μsec.

4. A sine wave of 3.58 Mc introduced at those terminals of the transmitter which are normally fed the color picture signal shall produce a radiated signal having an amplitude, (as measured with a diode on the R.F. transmission line supplying power to the antenna) which is down (6 ± 2) decibels with respect to a radiated signal produced by a sine wave of 200 kilocycles. In addition, the amplitude of the radiated signal shall not vary by more than ± 2 decibels between the modulating frequencies of 2.1 and 4.18 Mc.

5. The equivalent bandwidths assigned prior to modulation to the color-difference signals E'_Q and E'_I are given by Table I.

Table I

Q-Channel Bandwidth

at 400 kilocycles less than 2 decibels down
at 500 kilocycles less than 6 decibels down
at 600 kilocycles at least 6 decibels down.

I-Channel Bandwidth

at 1.3 megacycles less than 2 decibels down
at 3.6 megacycles at least 20 decibels down.

** At the present stage of the art it is considered inadvisable to set a tolerance on the value of gamma and correspondingly this portion of the specification will not be enforced.

6. The angles of the subcarrier measured with respect to the burst phase, when reproducing saturated primaries and their complements at 75 per cent of full amplitude, shall be within ± 10° and their amplitudes shall be within ± 20 per cent of the values specified above. The ratios of the measured amplitudes of the subcarrier to the luminance signal for the same saturated primaries and their complements shall fall between the limits of .8 and 1.2 of the values specified for their ratios. Closer tolerances may prove to be practicable and desirable with advance in the art.

WIDE-BAND AMPLIFIERS USING SECONDARY-EMISSION TUBES*

By

C. H. Chandler† and G. D. Linz‡

Summary—*This paper describes three applications of an experimental secondary-emission receiving tube, having a grid–plate transconductance of 15,000 micromhos, in amplifier circuits of general utility. One of these circuits was a band-pass cascade amplifier employing double-tuned, one-side-loaded coupling, centered on approximately 100 megacycles. Each stage of this amplifier provided a voltage gain of 6.4 and a half-power bandwidth of 55 megacycles. A second circuit was a low-pass distributed amplifier, in which output was taken from both plates and dynodes to obtain push-pull voltages for cathode-ray-tube deflection. In this case, a four-tube amplifier gave a voltage gain of 14, a bandwidth greater than 40 megacycles and a peak-to-peak output of 100 volts with all lines correctly terminated at both ends. The third was a band-pass distributed amplifier stage, using three tubes and yielding a gain of approximately 10 decibels over the frequency range from 87 to 237 megacycles. In general, gain-bandwidth performance in these circuits was about twice as good as could be expected from 6AK5 tubes, which are cited as a comparison.*

Introduction

With the demands made by modern society for the distribution of ever-increasing quantities of information, and the requirements of workers in the physical sciences for progressively better time resolution in the study of the events with which they are concerned, a corresponding increase becomes necessary in the bandwidth of the electronic equipment which must be provided to fill these and related needs. The circuit designer who is called upon to meet such requirements has at his disposal many useful methods for obtaining the wide-band amplification which is fundamental to the operation of the equipment aforementioned.[1,2] However, unless some new principle emerges, his ability to meet gain–bandwidth specifica-

---

* Decimal Classification: R363.4.

† Research Department, RCA Laboratories Division, Princeton, N. J.

‡ Formerly, Research Department, RCA Laboratories Division, Princeton, N. J. Now with the Defense Research Laboratories, University of Texas, Austin, Texas.

[1] E. L. Ginzton, W. R. Hewlett, J. H. Jasberg, and J. D. Noe, "Distributed Amplification," *Proc. I. R. E.*, Vol. 36, p. 956, August 1948.

[2] A. B. Thomas, "Stagger-Tuned Intermediate-Frequency Amplifier Design," *Jour. Inst. of Engineers*, Australia, Vol. 22, June 1950.

tions is ultimately limited by the performance of the amplifying tubes available to him.

It is thus not surprising that tubes for wide-band circuit applications are chosen from a very limited number of tube types. While many types may offer only slightly lower gain–bandwidth performance than that of the favored few, the necessity for obtaining the utmost in such performance restricts the choice almost as effectively as would complete absence of competitive types. Under these circumstances it is evident that a new tube having perhaps twice the gain–bandwidth figure of existing wide-band tubes, and presenting no unusual problems in the techniques of its use, would be a most welcome addition to the circuit designer's resources. Such a tube, applying secondary-emission principles, has in fact been developed, and it is the purpose of this paper to describe a number of successful applications of this tube in a representative variety of wide-band amplifier circuits.

Description of the Tube

The construction of the tube is described in a paper by C. W. Mueller.[3] It uses the same grid or input structure as the standard 6AG5 type. Further details of its construction, as well as its characteristic curves, may also be seen in the Mueller paper. The tubes used in the applications to be described here were essentially similar in structure and characteristics to that shown in Figure 7 of Reference (3), but as the result of further development were placed in a 9-pin miniature envelope. This modification allowed the internal shields to be brought out independently, each to its own pin — a desirable configuration for high-frequency work.

Salient characteristics of the experimental secondary-emission tube are given in the following table, together with the same data for the type 6AK5 for comparison purposes.

Tube Type	Transconductance micromhos	C_{input}, $\mu\mu f$	C_{output}, $\mu\mu f$	Gain–Bandwidth Figure of Merit $G_m/2\pi C_t$	Sum of Anode and Screen Currents milliamperes
Exp.	15,000	6.3	4.8	215	15.7
6AK5	5,100	4.0	2.8	120	10.1

[3] C. W. Mueller, "Receiving Tubes Employing Secondary Electron Emitting Surfaces, Exposed to the Evaporation from Oxide Cathodes," *Proc. I.R.E.*, Vol. 38, p. 159, February 1950.

It is seen that the secondary-emission tube has a gain–bandwidth figure nearly twice that of the 6AK5. In a physical circuit, the greater input and output capacitances are less of a disadvantage than might at first appear, since a given amount of stray and wiring capacitance would affect the realizable gain–bandwidth performance proportionately less.

The practical examples which follow will give an indication of the experimental tube's capabilities.

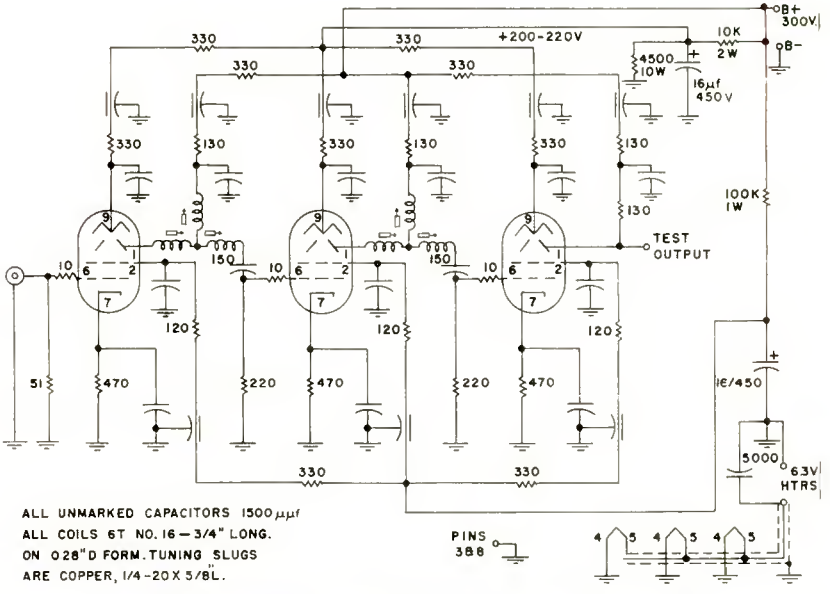

Fig. 1—Schematic diagram of double-tuned amplifier.

Radio-Frequency or Intermediate-Frequency Amplifier

A band-pass amplifier suitable for amplification at frequencies up to 250 megacycles is shown schematically in Figure 1. A double-tuned, one-side-loaded coupling configuration was chosen as offering a maximum of gain–bandwidth performance with relatively simple circuitry. A desirable by-product of this design is the low resistance in the grid return path, which allows rapid recovery of the amplifier after an overloading signal which causes grid current to flow. For simplicity and flexibility in the research model, an inductive T-section was used for the coupling network; values were readily derived from data available in Vol. 18 of the Radiation Laboratory Series.[4]

[4] G. E. Valley, Jr. and H. Wallman, *Vacuum Tube Amplifiers*, McGraw-Hill Book Co., Inc., New York, 1948, pp. 216-221.

The performance of one stage of this design is shown in Figure 2. Bandwidth to the 3-decibel points was 55 megacycles, centered on 103 megacycles, with a voltage gain of 6.4. It will be noted that the gain of this stage is constant within ± 0.25 decibel over a bandwidth of 42 megacycles, which is just the width of the spectrum occupied by the entire upper portion of the very-high-frequency television band (channels 7 to 13 inclusive), or more than twice the width of the frequency-modulation broadcasting band.

These figures show a realized gain–bandwidth performance of ap-

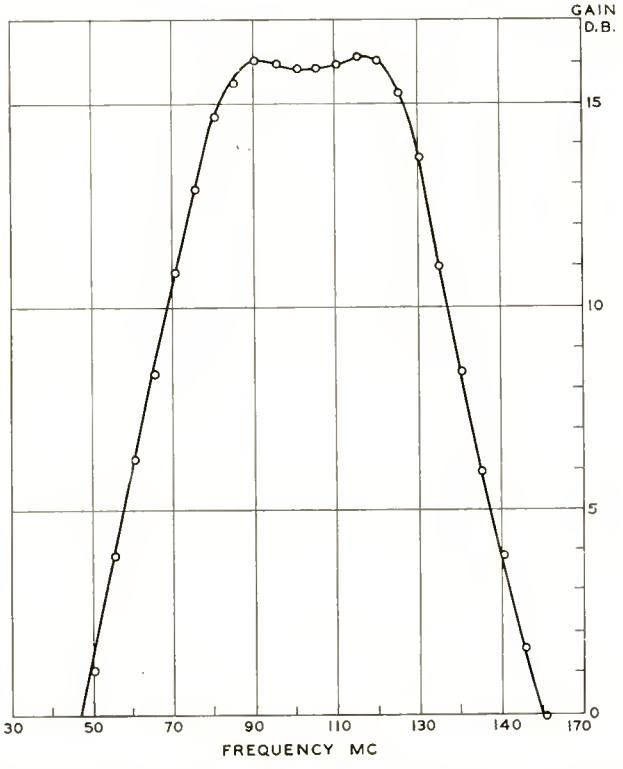

Fig. 2—Frequency response, one stage of double-tuned amplifier.

proximately 350. The fact that this value so greatly exceeds the tube's rated figure of merit, 215, is due to the properties of the double-tuned, one-side-loaded coupling configuration, which affords a factor-of-two improvement in gain–bandwidth figure over that given by $G_m/2\pi C_t$. In the complete absence of stray circuit capacitances, the gain–bandwidth product of the stage could have been 430. However, the realized product of 350 is about twice as large as one could expect to obtain

with a 6AK5 tube, which would suffer more than the secondary-emission tube from the effects of circuit capacitance because its internal capacitances are smaller.

Photographs of the amplifier are shown in Figure 3.

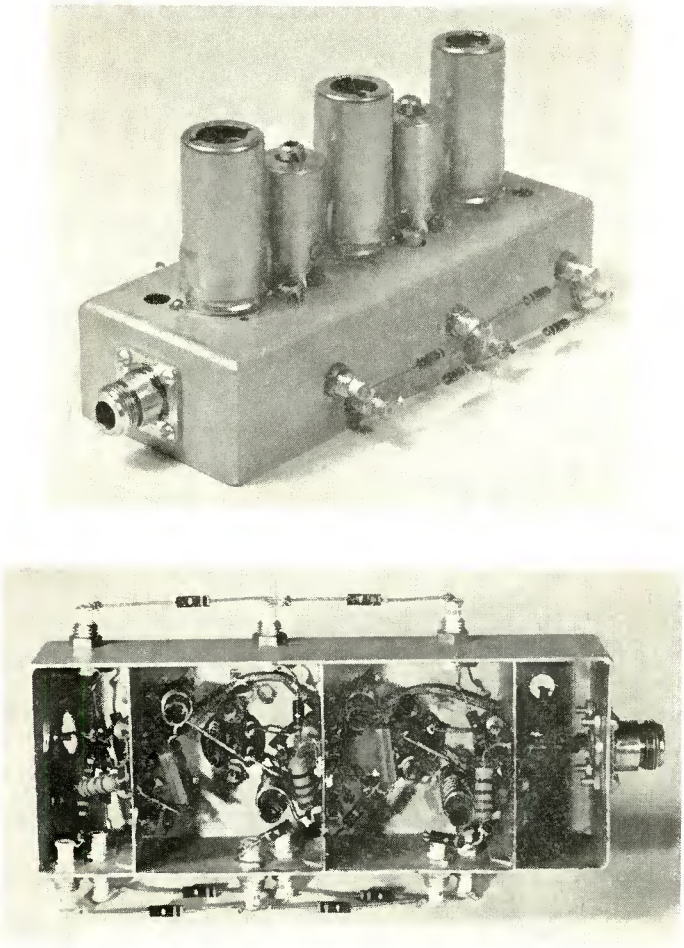

Fig. 3—Photographs of double-tuned amplifier.

Video Deflection Amplifier

This amplifier takes advantage of the fact that the net plate and dynode currents are of opposite polarity. Since this is the case, the tube can be used to provide push-pull outputs from a single-ended input, and will yield approximately twice as much peak-to-peak output

voltage swing as would be given by the same tube in a single-ended stage. Push-pull output is particularly desirable for electrostatic deflection in a cathode-ray tube, the application for which this amplifier was designed.

The configuration used was a "distributed" amplifier employing lumped low-pass lines. Such amplifiers have been described[1, 5, 6] and constitute an important area in the field of wide-band techniques.

The schematic diagram of the deflection amplifier is given in Figure 4. Constant-K low-pass filter sections were used to form the

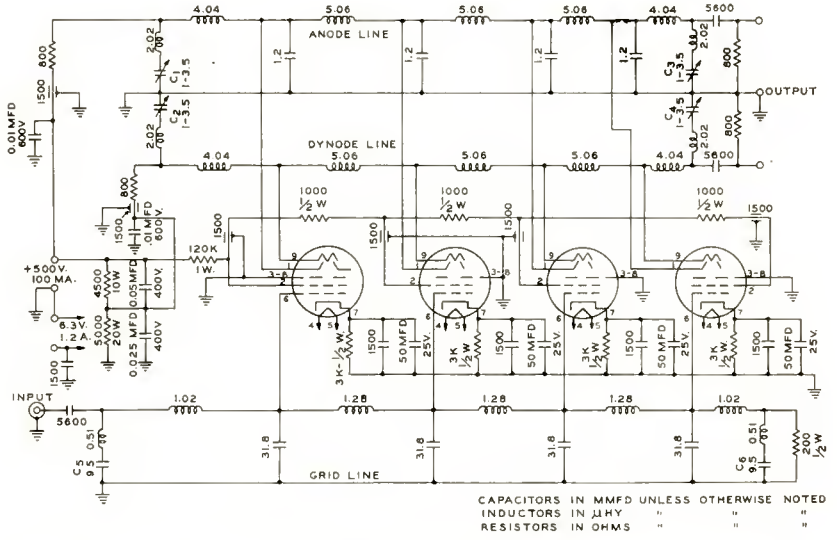

Fig. 4—Schematic diagram of 40-megacycle video deflection amplifier.

grid, plate and dynode lines. The same design cutoff frequency, 50 megacycles, was used in all three lines in order to maintain identical phase characteristics. The grid line characteristic impedance was made 200 ohms in order to match available driving amplifiers and to use cable of substantially this impedance which is an item of commercial manufacture. The dynode line impedance was 800 ohms, the maximum possible with the tube and circuit nodal capacitance present, which was 8 micromicrofarads.

---

[5] W. H. Horton, J. H. Jasberg, and J. D. Nee, "Distributed Amplifiers: Practical Considerations and Experimental Results," *Proc. I.R.E.*, Vol. 38, p. 748, July 1950.

[6] N. F. Moody and G. J. R. McLusky, "Secondary Emission Tubes in Wideband Amplifiers", *Wireless Engineer*, Vol. 26, p. 410, December 1949.

If equal outputs are to be obtained from plate and dynode lines, the ratio of the line impedances should be the reciprocal of the ratio of the respective plate and dynode transconductances. If the secondary-emission ratio of the dynode is δ, then the ratio of dynode to anode transconductance is $(\delta - 1)/\delta$ since for δ electrons reaching the anode a *net* of $\delta - 1$ electrons leave the dynode. Making use of this ratio, however, results in an impedance unbalance which, for this amplifier, was considered to be more detrimental than an output-voltage unbalance. Accordingly, the plate line was made 800 ohms to match the dynode line. Padding capacitors of 1.2 micromicrofarads each were added at the nodal points of the plate line to bring the total capacitance to the same value as that of the dynodes.

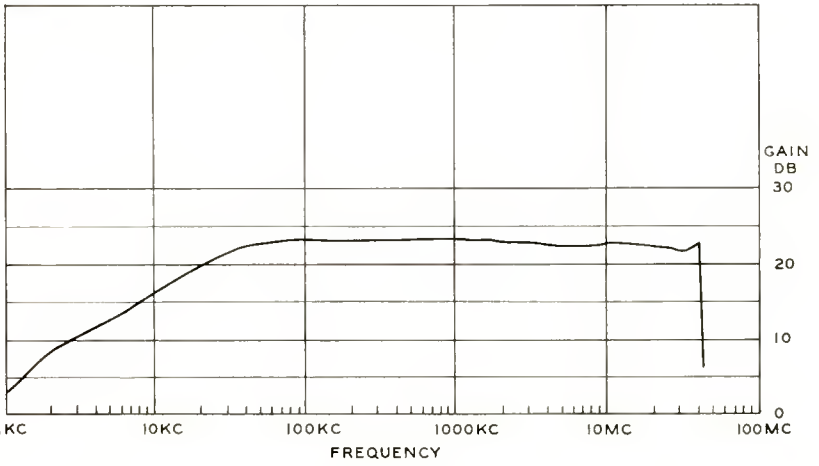

Fig. 5—Frequency response of 40-megacycle video deflection amplifier.

Using four of the secondary-emission tubes, this amplifier provided a voltage gain of 14 and an output swing of over 100 volts peak-to-peak with all lines correctly terminated at both ends. The frequency response, shown in Figure 5, was flat with a total variation of 3 decibels from 10 kilocycles to 41 megacycles. The output might, of course, be increased by removing the terminating resistances from the output ends of the plate and dynode lines, but some deterioration in the smoothness of the frequency response would result.

As shown by the photographs of Figure 6, the plate and dynode lines were placed in the same compartment of the chassis. A more uniform response would have been obtained had they been shielded from each other.

It is estimated that twice as many 6AK5 tubes would be required to give the same gain and output over the frequency range obtained.

Band-Pass Distributed Amplifier

The use of band-pass lines in a distributed amplifier is suggested

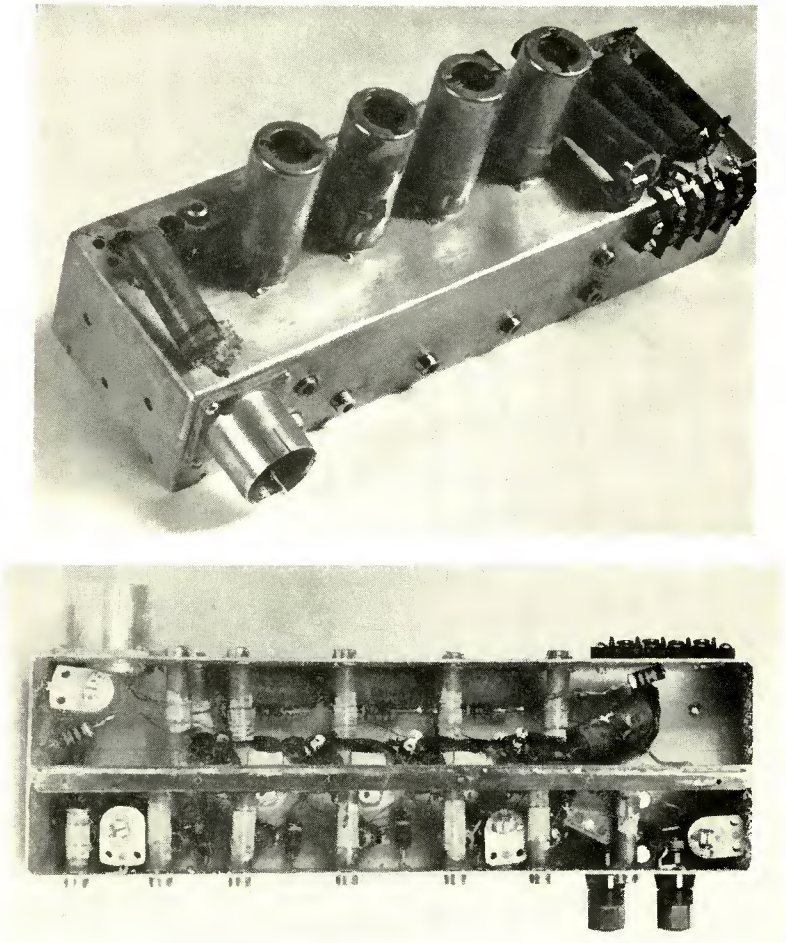

Fig. 6—Photographs of 40-megacyle video deflection amplifier.

in Section III of the Ginzton paper;[1] but to the best of the writers' knowledge, this conception has not heretofore been put into practice. For applications in which a lower range of frequencies is not required, the band-pass configuration has the advantage of confining the avail-

able gain and bandwidth to the frequency region where they are needed, without sacrificing performance by providing gain at frequencies below those of interest.

The circuit is shown schematically in Figure 7. Constant-K band-pass filter sections were used for the lines as these sections offered the highest impedance obtainable with a simple circuit for a given value of shunt capacitance. Reverse terminations were provided with m-derived half sections ($m = 0.6$). The impedance of both grid and

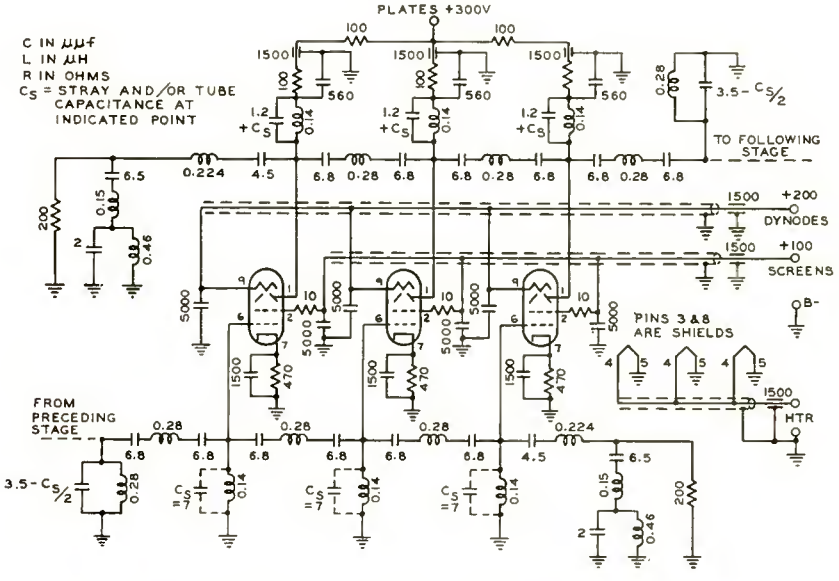

Fig. 7—Schematic diagram of band-pass distributed amplifier.

anode lines was 200 ohms. Since this stage was envisioned as one block in an amplifier of several cascaded stages, push-pull output was not required. The dynodes were therefore simply bypassed to ground. Photographs of this amplifier stage are shown in Figure 8.

The performance of the band-pass distributed stage is not readily shown by the usual graphical means. Due to the number of adjustments possible, the number of greatly differing gain–frequency response curves is very large. Since no frequency-swept signal generator capable of sweeping through the pass band of this amplifier is known to exist, adjustments could not be made by the convenient visual method of the "wobbulator–oscilloscope" combination. It is possible to summarize some results, however, by stating that in one case, a gain

of 9.5 decibels and a 3-decibel bandwidth of 143 megacycles, from 84 to 227 megacycles, was obtained with gain variations of ± 1.25 decibels. In another case, a gain of 9.4 ± 1.5 decibels was observed over a bandwidth of 150 megacycles, the 3-decibel points occurring at 87 and 237 megacycles. This response is shown in Figure 9.

Discussion

The wiring techniques necessary at the frequencies used in the

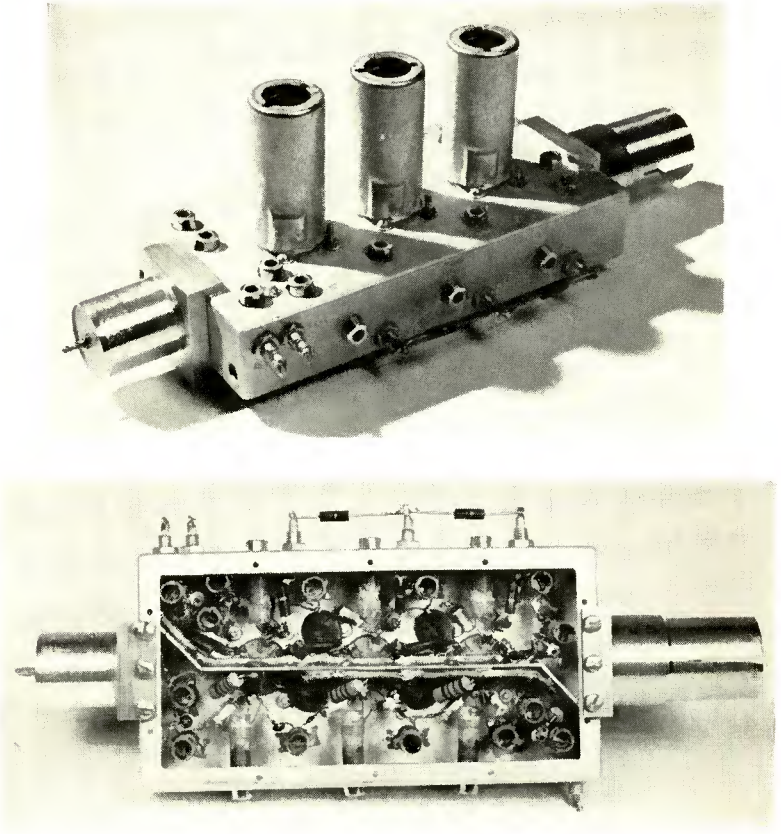

Fig. 8—Photographs of band-pass distributed amplifier.

amplifiers described above, e.g., short leads and a narrow chassis, are well known and do not require elaboration here. Reasonable measures were applied in the way of shielding and de-coupling, as the schematic diagrams and photographs show. Since this work was completed, improved compact bypass capacitors providing extremely short effective

ground paths have become commercially available. Such components would have facilitated this work and are certain to be of great benefit to further developments of a similar kind.

The adjustment of tuned-circuit components was usually made before their incorporation into the circuit. For this purpose a grid-dip or "megacycle" meter was practically indispensable. In some cases resonance frequencies could be varied or checked by this means after the components were in place, a desirable condition. As previously noted, the bandwidths involved were entirely too great for commercial swept-frequency oscillators to be of any value. Over-all adjustments had to be made on the basis of laborious point-by-point plots. The problems of instrumentation were, in fact, of a magnitude comparable to those of design or construction.

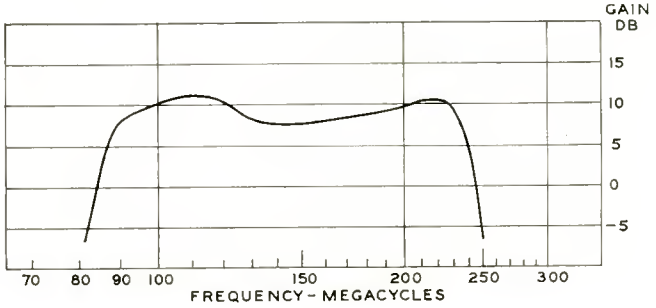

Fig. 9—Frequency response of band-pass distributed amplifier.

One characteristic of the secondary-emission tubes which is not found in conventional types is the requirement that the dynode potential be supplied from a source having relatively low impedance, not over 10,000 ohms in the case of one tube. By the same token, a common dynode supply for N tubes should have a source impedance of 10,000/N ohms. The present work used the simplest, but least economical, expedient of providing a voltage divider from plate supply to ground, such that the parallel combination of the resistors in the upper and lower arms came to less than 10,000/N ohms. Greater efficiency could be obtained by the use of a nonlinear material (e.g., "Thyrite") in the divider. Alternatively, an independent dynode supply may be used, and regulated in any convenient manner.

As noted above, reasonable but not elaborate precautions were taken against undesired couplings or feedback in the amplifiers constructed. It is gratifying to report that no difficulties were experienced with instability; the secondary-emission tubes appeared to be perfectly "clean" in this important respect.

Conclusions

It is evident that the secondary-emission amplifier tube whose applications have been described offers a significant improvement in gain–bandwidth performance over conventional tubes currently in use. It is hoped that the present work has shown to the circuit designer the advantages of this secondary-emission tube.

Acknowledgment

It is a pleasure to acknowledge the encouragement and many helpful suggestions received from D. G. C. Luck, as well as the assistance of D. S. Bond in connection with some of the problems of instrumentation.

A LEVEL-SETTING SYNC AND AUTOMATIC-GAIN-CONTROL SYSTEM FOR TELEVISION RECEIVERS*

By

E. O. KEIZER† AND M. G. KROGER‡

Summary—*A television receiver sync separator and automatic-gain-control system which provides good impulse noise immunity at low cost has been developed. Voltage obtained from the gain-controlled intermediate-frequency amplifier stages is used to automatically bias a direct-coupled sync separator to the correct operating point for good sync separation and noise clipping. The automatic-gain-control voltage source is protected from strong noise impulses by clipping in the sync separator stage. This paper describes the system, and gives an example of its application to a television receiver.*

INTRODUCTION

WHEN a modern television receiver is properly tuned to a good signal, the adjustment of the vertical and horizontal "hold" controls to obtain a steady picture is usually not very critical. However, if strong interference is received along with the signal, the picture may jitter or roll unless a more careful adjustment of the controls is made. In cases of severe interference, it may be impossible to synchronize the picture. Automobile ignition systems and sparking electric motor brushes are typical sources of strong interference. These generate noise pulses or bursts which are particularly troublesome to television receiver synchronizing circuits. The interference is most troublesome when the desired signal is weak, and is a serious problem in some areas. In many cases the video signal is such that the picture would still be usable, even in the presence of the interference, if it were steady.

The failure to synchronize in the presence of impulse type noise is usually the result of charging up of the sync separator and automatic-gain-control circuits by such noises, resulting in suppression of the useful sync information. It is the purpose of this paper to describe a sync separator and automatic-gain-control system which has little tendency to charge up on impulse noise, thereby giving steadier pictures.

---

* Decimal Classification: R583.15.

† Research Department, RCA Laboratories Division, Princeton, N. J.

‡ Formerly, Research Department, RCA Laboratories Division, Princeton, N. J. Now with Motorola, Inc., Chicago, Ill.

Conventional System

Figure 1 is a block diagram of a conventional sync separator and automatic-gain-control system for a television receiver. The diagram has been simplified by lumping all automatic-gain-controlled amplifier stages into one block, and all other signal stages into another.

A portion of the video output is applied to the sync separator. In most receivers the sync separator is self-biasing, the bias being developed from the peaks of the composite video signal. Conduction normally occurs during the sync peaks, but not during the picture portion of the signal. However, if there are large interference pulses, the self-bias voltage will increase so that conduction on sync peaks will be reduced or lost. As a result, the sync separator output will

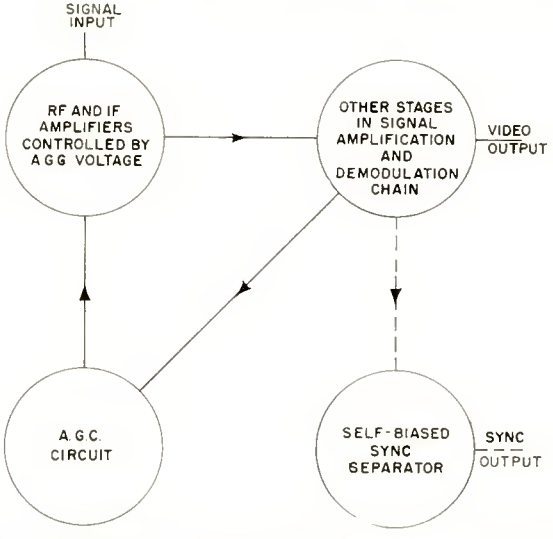

Fig. 1—Conventional sync and automatic-gain-control system.

contain noise pulses, but sync pulses will be missing.

The automatic-gain-control voltage may be derived from the video output, or from an earlier point in the receiver. In either case, it, also, may be susceptible to the same long or numerous noise pulses that affected the sync separator. As a result, too much gain control bias may be developed, causing a reduction in the amount of desired signal present at the input to the sync separator. Where the noise is especially bad, the desired signal may be almost completely suppressed.

If either the sync separator circuit or the automatic-gain-control circuit charges up on noise energy, poor synchronization is likely to result. Therefore, for good operation where there is strong impulse noise, both circuits must be noise immune.

Fixed-Bias Sync Separator System

Since the sync separator self-biasing circuit charges up on noise pulses as well as on sync peaks, it would be helpful to eliminate the self-biasing feature entirely and replace it by an external bias source. One way to accomplish this would be to provide a very-high-gain receiver with a very flat automatic-gain-control characteristic so that the level of the sync peaks in the video output would be constant for all usable signal levels. Since the sync peaks would then be uniformly maintained at a fixed d-c level in the video output, a sync separator could be direct-coupled to the video output, and externally biased to operate in the sync region. In such a receiver, sync output would not fail in the presence of impulse noise so long as the signal level was maintained. Actually, the performance of such a system would depend upon the accuracy and reliability to which the sync peak level could be maintained compared to the bias voltage under conditions of varying signal level and interference.

Three practical difficulties are usually encountered in such a receiver. First, the gain or speed of response of the automatic-gain-control loop may be inadequate to keep the sync portion of the video amplifier output within the operating range of the sync separator. This results in loss of sync or in picture information being present in the sync output. Second, the automatic-gain-control voltage may be affected by interference, resulting in failure to maintain the proper signal level and in loss of sync. Third, the signal may be so weak that the maximum gain of the receiver is insufficient to maintain full video output. Then sync peaks do not reach the sync separator operating level, again resulting in loss of sync output.

Bias Level-Setting Sync and Automatic-Gain-Control System

The system to be described uses a direct-coupled externally-biased sync separator, but overcomes the three difficulties just mentioned. This results in good over-all sync and automatic-gain-control performance with improved immunity to impulse noise.

A simplified block diagram outlining the system is shown in Figure 2. The self-biasing sync separator of the first figure has been replaced by an externally-biased d-c coupled sync separator which also provides automatic-gain-control loop amplification. The automatic-gain-control voltage itself is derived from the sync separator output by another circuit.

The sync separator stage has a definite noise-limiting level. The automatic-gain-control stage which follows is biased so the sync peaks

are automatically held close to, but not actually at, that level. Because the automatic-gain-control stage then operates on a signal from which the noise peaks have been clipped close to sync peaks, its noise immunity is considerably improved.

The external bias voltage applied to the sync separator is not fixed, but decreases on weak signals. It is obtained from the low-voltage terminal of a resistor connected in the plate circuit of the gain-controlled intermediate-frequency (i-f) amplifier stages. At this point the voltage drops when a weak signal is being received, due to the increased current in the amplifiers at low automatic-gain-control voltages. This connection is indicated in the block diagram, as a cross

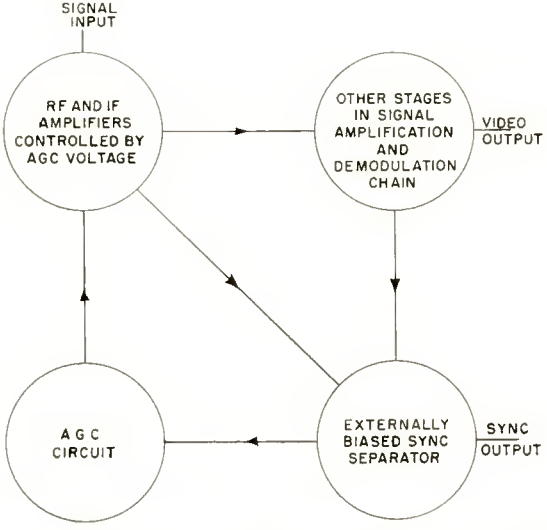

Fig. 2—Level-setting sync separator and automatic-gain-control system.

connection between the gain controlled amplifiers and the sync separator.

Effects of the Variable External Bias

Using the i-f amplifiers to bias the sync separator stage adds a d-c amplifier stage to the control loop. This stage is most effective for weak signals where the normal automatic-gain-control voltage control is least effective. With this d-c amplification added, the total control circuit loop gain is kept high at all signal levels, insuring close tracking between the level of sync peaks and the noise clipping bias.

The gain control loop regulates the video output to a level deter-

mined by the gain-controlled i-f amplifier plate voltage rather than by a fixed delay voltage. As a result, the output voltage versus radio-frequency input characteristic of the receiver is not as flat as it would be with a conventional high-gain delayed automatic-gain-control circuit. Figure 3 shows two output-versus-input curves illustrating this effect. Data for Curve I was taken on a relatively low-gain receiver converted to the new system. For comparison, Curve II is shown. It is a composite curve. Its sloping portion is the output-versus-input characteristic of the same receiver with the automatic-gain-control voltage shorted to zero. Its level portion shows the constant output that would result if the system were perfectly flat.

In operation, the new system must always develop some control bias. It is fortunate for its performance, therefore, that at very low biases

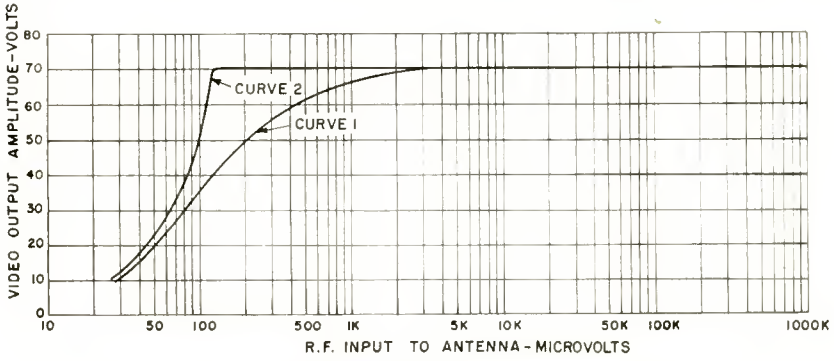

Fig. 3—Video output versus signal input of receiver under controlled conditions.

the percentage gain of the controlled i-f amplifiers does not change rapidly with bias. Thus, the maximum gain of the receiver is not greatly affected. However, voltage delay of the application of automatic-gain-control to the tuner is probably more important for best noise factor for this system than for systems developing no automatic-gain-control voltage on weak signals.

Since the sync separator bias tracks the signal level, the noise-clipping level of the sync separator remains close to the top of the sync peaks for weak as well as for strong signals. As a result, good noise immunity is maintained for signal levels that would be below the automatic-gain-control threshold in a conventional system.

Also, since the sync peak level of the video output is held close to the external bias level of the sync separator, that bias level is useful in maintaining background in the presence of rapid or large signal strength changes, for example, when airplanes pass nearby.

Circuit Details for a Particular Receiver

There are a number of circuit arrangements which are suitable, provided that the video amplifier is d-c coupled to the second detector, and the output of the video amplifier is d-c coupled to a combination sync separator and automatic-gain-control amplifier whose bias is controlled by the automatic-gain-control voltage.

Figure 4 shows the details of one version of this circuit applicable to a particular receiver. This cathode-input type first sync separator version of the circuit is particularly applicable to receivers having horizontal control circuits of the balanced phase detector type, where some rounding of the horizontal sync waveform is permissible. The three-tube sync and automatic-gain-control circuitry is shown in the upper portion of the drawing, while the video amplifier and kinescope input circuitry is shown in the lower portion. V_1 is the combination sync separator and automatic-gain-control amplifier tube, V_2 the sync amplifier tube, and V_3 the automatic-gain-control rectifier tube. The cathode of V_1 is designated point "A" for convenience. The voltage at the grid of V_1 (and the plate return voltage of the gain-controlled i-f stages) is designated E_1.

Operation of Cathode Input Version of the Circuit

As shown in Figure 4, the video amplifier is conventional except for the video load resistance which has been split into two branches, one connected to the cathode of the sync separator (point "A") instead of directly to the supply voltage. Using this connection, the video amplifier operates with normal gain and load impedance during the video portion of the signal, since the grid and cathode of V_1 act as a diode clamp to prevent point "A" from becoming more than slightly negative with respect to E_1. However, during the sync portion of the signal, V_1 approaches cutoff, making the impedance seen by the video amplifier at point "A" large compared to its value during the video portion of the signal, and large compared to the video load resistance; thus the sync portion of the signal is amplified more at point "A" than it would be by conventional video amplifier circuits. In other words, the video amplifier sees point "A" as a high impedance during the sync portion and as a low impedance during the video portion of the signal, resulting in amplified sync and compressed video signal at that point.

The solid line (a) in Figure 5 represents the signal at point "A" with reference to the voltage E_1 and to V_1 cutoff voltage. The dotted curve (b) represents the video portion of the voltage at point "A" that would appear if the clamping action of tube V_1 were not functioning.

Output Voltage Waveform

The voltage appearing at the plate of V_1 is an amplified version of the signal at point "A", except that the tops of the sync are somewhat compressed. Because the input to V_1 is to the cathode, the output has

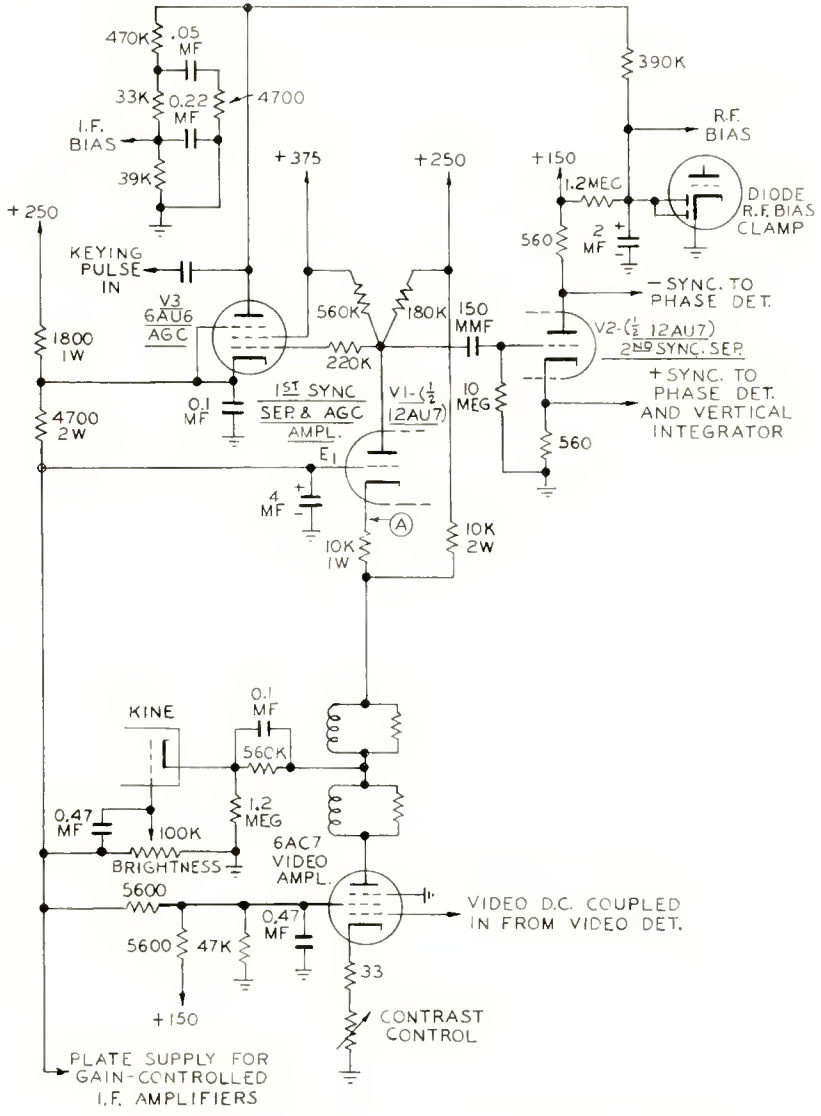

Fig. 4—Video amplifier, sync, and automatic-gain-control of modified receiver.

the same phase as the input, i.e., there is not the usual phase reversal in the amplifier stage.

As V_1 approaches cutoff its gain decreases, and for this reason the tips of sync are compressed in the plate circuit as compared to the cathode circuit. This compression is desirable because it clips the noise impulses and results in more nearly constant-amplitude sync pulses.

The output of V_1 is applied to the grid of a keyed automatic-gain-control tube, V_3. Because of the clipping of the noise pulses close to sync tips by V_1, the noise immunity of this automatic-gain-control circuit is better than that of conventional keyed circuits.

The output of V_1 is also applied to a second sync separator, V_2. It is permissible for the second sync separator to be self-biasing, since the noises have been clipped by V_1. Positive sync appears at the cathode of the sync separator and negative sync appears at the plate. The amplitude of sync is of the order of 5 to 10 volts for this particular circuit.

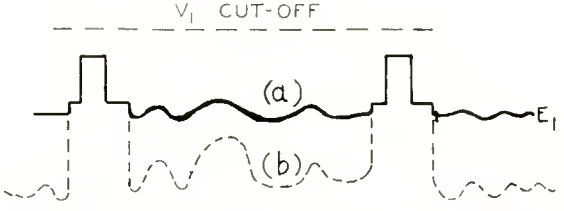

Fig. 5—Voltage form appearing at point "A" of Figure 4.

Contrast Control

A cathode circuit contrast control is shown in the video amplifier. Another means for contrast control is the use of a 50,000-ohm variable resistance in series in the screen supply circuit. The cathode contrast control not only varies the video amplifier gain but also changes the automatic-gain-control operating point so that the output at the second detector will vary with contrast control setting.

Brightness Control

The brightness control potentiometer is supplied from the voltage E_1. Since the sync region of the signal follows E_1, this connection results in improved background setting. By-passing the brightness control to E_1 rather than a fixed voltage also results in improved background stability in the presence of rapid signal fluctuations, such as those due to airplanes.

Video Amplifier Screen Supply

While the video amplifier screen voltage may be supplied directly from a fixed voltage, it has been found helpful to supply it from a tap on a voltage divider between a fixed voltage and E_1, as an aid in weak-signal compensation. A large series screen resistor supplied from a relatively high supply voltage would also help weak-signal compensation, but would have the disadvantage that the average video output affects sync height and automatic-gain-control level. Use of a high-value series screen resistor can also lead to poor synchronization of an all-black signal.

Weak-Signal Compensation

The value of the resistance in series with the plate returns of the gain-controlled i-f stages is chosen to give a voltage drop across it such that when there is no signal, an i-f bias of approximately one volt is developed. The voltage E_1 should then be well above the "knee" of the I_p-versus-E_p characteristic of the i-f tubes for those operating conditions. Altering the relative value of the two resistances in the video amplifier affects the amount of compensation needed. The screen supply circuit for the gain-controlled i-f stages also affects the compensation. In the particular receiver from which Figure 4 was derived, the screens were connected through small decoupling resistors to the +150-volt supply point. Where it is desired to make the over-all circuit performance tolerate several-fold changes in transconductance of the gain-controlled i-f tubes, the screens of these tubes should be supplied through series resistors from a higher supply voltage, and the weak-signal compensation should be readjusted to result in somewhat more than 1 volt of i-f bias on no signal. Since there will always be some bias, the operating screen voltages on zero signal may be higher than normal without exceeding the screen dissipation rating of the tube; that is, screen resistors somewhat smaller than normal may be used.

Keying Pulse

The positive horizontal keying pulse may be supplied from a point in the horizontal supply where the peak-to-peak magnitude of the pulse is in the order of 700 volts.

Cathode Potential

The cathodes of the sync and automatic-gain-control tubes operate above ground potential by an amount which makes necessary the use

of a separate heater winding which is elevated in potential to about 100 to 150 volts above ground. The heater of the kinescope may well be supplied from the same heater winding.

Automatic-Gain-Control Tap

The location of the tap of the automatic-gain-control rectifier cathode in the gain-controlled i-f plate supply circuit is not critical, but in a new design should be near the middle of the operating range.

Pentode versus Triode Automatic-Gain-Control

The use of a pentode for the automatic-gain-control rectifier has the advantages of reduced pulse feedback to the sync output, and reduced susceptibility to variations in keying pulse height. The use of a pentode is therefore preferred, but in some cases where considerable care is taken in the design, it is possible to use a high-mu triode for the same function.

A KEYED MINIMUM-SIGNAL DETECTOR FOR TELEVISION RECEIVER IMPULSE-NOISE IMMUNITY*

By

Albert Macovski

Industry Service Laboratory, RCA Laboratories Division,
New York, N. Y.

Summary—*This paper describes automatic-gain-control and sync-separator circuitry which is virtually immune to impulse noise. The reference voltages are obtained by detecting the minimum instead of the maximum of a sync-positive video signal. Since impulse noise is predominantly in the black direction of the television signal, the maximum value of the signal is increased, but its minimum value is relatively unaffected by noise pulses. This contrasts with conventionally used sync and automatic-gain-control circuitry which references on the maximum of the signal. In its simplest form the circuit requires the addition of a double diode to obtain the noise immunity. A high performance automatic-gain-control system can be realized by changing one of the diodes to a triode and adding an additional triode.*

Principles of Operation

Figure 1 shows a conventional method of sync separation using a peak detector. As with any sync separator, a biasing arrangement is required which will line up the synchronizing information at a given potential to allow for separation. The diode shown is usually the grid-cathode space of the sync separator tube.

In order to detect the minimum of the signal, the diode is reversed as shown in Figure 2, so as to conduct in the opposite direction. If the plate of the diode were connected to some positive direct-current voltage, the condenser C_1 would charge to the minimum of the signal, which would correspond to the peak white information in the signal. In order to make the clamping action work on the sync region only and not conduct during video information, the plate is keyed with pulses from the horizontal deflection system. The minimum video signal during the time of the flyback pulse will be the signal black level. Thus during the keying pulse, condenser C_1 charges to the difference between the peak of the keying pulse E_1 and the black level of the signal, thereby holding the black levels of all signals at potential E_1. The synchronizing information of the signal is then lined up for sync separation independent of signal strength, video modulation, or noise peaks. The voltage E can be utilized for automatic gain control if referenced to ground in a suitable manner.

* Decimal Classification: R583.5.

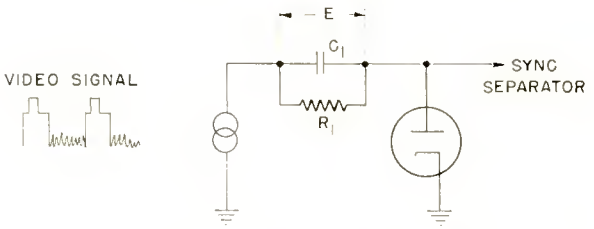

Fig. 1—Conventional peak detector.

Keying Pulse Requirements

The peak potential of the keying pulse must at all times be greater than the peak potential of the signal, to keep the diode in conduction. To keep the peak of the keying pulse fixed, an additional diode is used to limit the pulse at a fixed potential. A convenient potential to use is B+ on the video amplifier plate supply, a voltage which is always greater than the sync tips. In the circuits shown, the keying pulse driving source is grounded. If a minimum of peak-to-peak amplitude of the pulse is desired, the keying pulse driving source can be raised above ground with d-c voltage such that the total keying waveform will be d-c, plus a pulse. The only limitation on this arrangement is that the peak-to-peak pulse amplitude must always be greater than the peak-to-peak amplitude of the video signal.

The keying pulse must overlap the sync pulse in order to reference on the black level. This will insure that over the range of the horizontal hold control the minimum of the signal for the duration of the pulse will always correspond to the black level. In general, the flyback time of most horizontal deflection systems is greater than the sync width. If widening is required, the pulse can be integrated slightly before it is limited.

The requirements on the timing of the keying pulse are the same

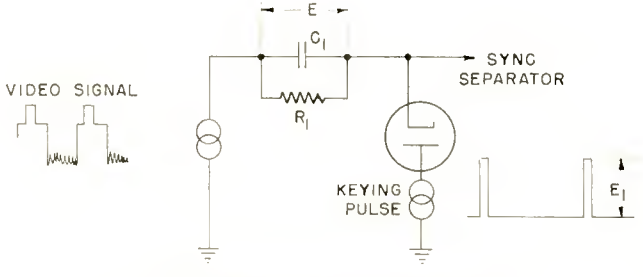

Fig. 2—Minimum-signal detector.

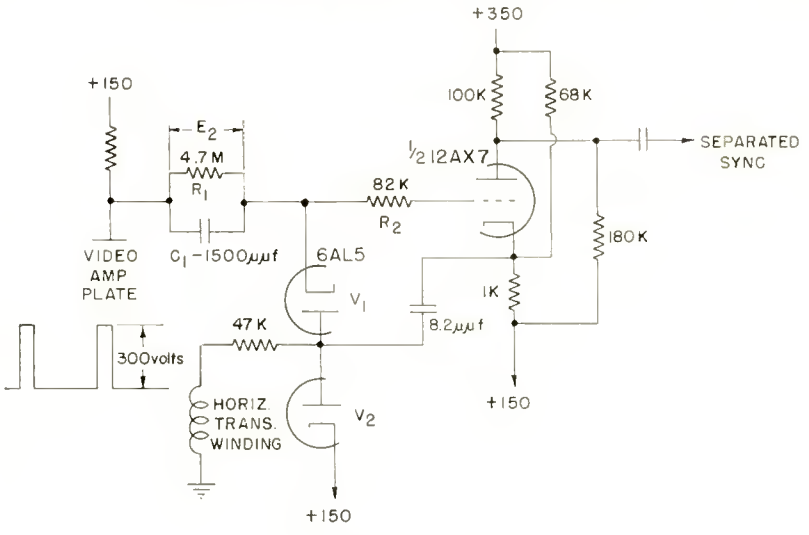

Fig. 3—Sync separator.

as those on the deflection system. The keying pulse should be kept within the limits of the blanking interval over the range of the hold control so that at no setting of the hold control will the pulse reference on the video information. Since this mistiming condition would correspond to foldover on the screen, proper design of the deflection system to prevent foldover is a requirement.

Sync Separation

A schematic diagram of the keyed minimum-signal detector used for sync separation is given in Figure 3. In this circuit V_2 acts as a limiter to keep the peak of the keying voltage at exactly +150 volts. During the keying interval the plate of V_1 is at +150 volts so that C_1 charges up to the voltage E_2 shown in Figure 4, which is the difference between +150 volts and the lowest voltage at the video plate,

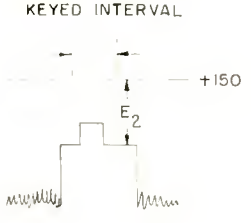

Fig. 4—Video amplifier plate waveform.

the black level. This d-c voltage E_2 is added to the video signal, placing the black level at +150 volts regardless of signal strength or contrast (see Figure 5). The cathode voltage of the sync separator is raised somewhat above +150 volts so that the blanking information falls below cutoff, and the sync tips are clipped in grid current. It will be noted that the video amplifier plate supply, the keying pulse clipping level, and the sync separator cathode are all tied to the same supply voltage, insuring noncritical operation with changing voltages.

The keying pulse is differentiated by the diode capacitance and appears across the video load resistor. To prevent it from appearing in the sync separator output, the same differentiated pulse component was put on the sync separator cathode through an 8.2-micromicrofarad condenser from the clipped keying pulse.

Automatic Gain Control

The circuit in Figure 3 for sync separation will operate satisfac-

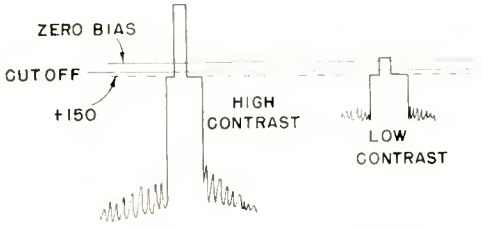

Fig. 5—Waveform at cathode of V_1.

torily whether the video detector is a-c or d-c coupled to the video amplifier. If it is a-c coupled, the voltage E_2 will vary with signal strength and with average video level to keep the pedestals lined up. If it is d-c coupled, it will vary with signal strength only, making this voltage suitable for automatic gain control (a-g-c) if properly applied.

A method of applying E_2, the noise-immune reference voltage, to a-g-c is shown in Figure 6. A triode V_3 replaces the keyed diode. The clamped 150-volt pulse is applied to the grid of the tube, while the plate is connected approximately 30 volts above the 150-volt reference. The a-g-c voltage is developed across the 4.7-megohm resistor in the plate circuit of the triode. An additional keyed triode V_4, is used to take the a-g-c voltage from the plate of V_3 and reference it to ground with a low impedance output.

As shown in Figure 6 for purposes of explanation, V_3 has equal

loads in cathode and plate with the plate voltage being +30 volts with respect to the keying pulse. Thus for signals where the black level is within 30 volts of +B, equal voltages are developed in the plate and cathode loads. However, if the black level drops more than 30 volts below +B, the voltage across the plate load does not increase but the cathode network is charged by grid-cathode conduction. This is the action below a-g-c threshold.

When the a-g-c is operating, the black level will be held between +B and +B—30 volts. It may be seen then that the control voltage applied to the grid of the a-g-c tube V_4 can vary between the limits

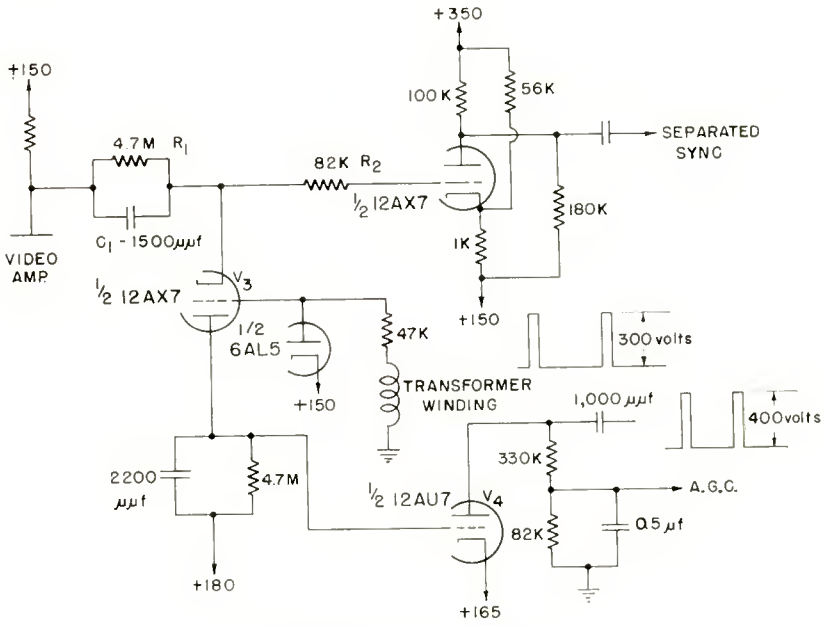

Fig. 6—Sync and a-g-c system.

of +180 and +150 volts. The voltage applied to the cathode of the a-g-c tube is chosen to set the black level at the desired point on the video amplifier characteristic. None of these values is critical, and no level-set control should be necessary.

The reduced grid-to-cathode capacitance of the triode, as compared to the plate-to-cathode capacitance of the diode used in the previous arrangement, reduces the keying pulse feedthrough problem. This circuit has been successfully used with a cathode-type contrast control having a normal range, with the sync separation effective throughout the range. As with any a-g-c system connected to the video amplifier,

the detector must be d-c coupled to the video amplifier grid. To maintain background changes, the kinescope cathode may be d-c coupled to the video amplifier plate.

Figure 7 shows a somewhat different version of this circuit applied to another receiver. This circuit was evolved to satisfy the requirement that the video amplifier operate from the highest +B in the receiver, and that negligible power be taken from the boosted +B. The clipping level of the sync separator is set by clipping the pulse at a potential below +B instead of raising the sync separator cathode above +B as previously shown. The plate voltage of the keyed triode V_3 consists of d-c voltage plus the clamped pulse, rather than d-c voltage

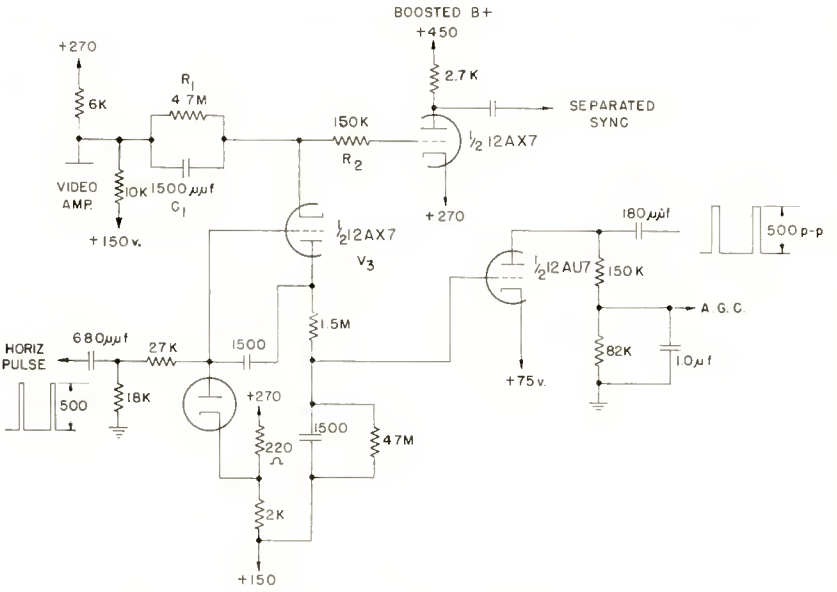

Fig. 7—Another version of sync and a-g-c system.

alone. Since the tube conducts during the keying pulse only, a pulse on the plate acts the same as d-c voltage.

Impulse-Noise Performance

V_3 and its load circuit R_1C_1 should be a highly efficient peak detector. C_1 discharges on noise through the sync separator grid and gets charged through the diode on the succeeding keying pulse. To maintain the voltage across C_1 under noise, R_1 and R_2 are made as large as possible, and C_1 is made small. Thus the amount of charge C_1 loses on noise is made small, and it is rapidly recharged on a keying

pulse. The only limitation on R_2 is integration of the horizontal sync, since the sync separator is not grid-leak biased. C_1 is made large enough to filter the vertical component.

No sign of setup of the a-g-c or sync separator circuitry can be observed under the most adverse signal-to-noise ratios. However, the a-g-c voltage may set down (decrease) slightly thus increasing the signal output. This is due to the increased charging current required when the sync referencing condenser (C_1) tends to discharge on noise. This increased plate current in the keyed triode corresponds to the reception of a weaker signal resulting in less a-g-c voltage. If, with strong impulse noise, the a-g-c set-down action is too severe, it will tend to crush the sync at the video amplifier. Inserting a resistor of approximately 50,000 ohms in series with the plate of V_3 will reduce the efficiency of the a-g-c detection only, minimizing the set-down action. White noise in the signal can also cause a-g-c set-down and

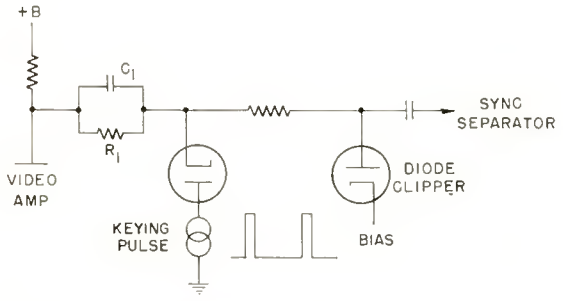

Fig. 8—Automatically regulated diode clipper.

can increase the sync separator bias voltage, causing the pedestal to appear in the separated sync output. This action contrasts with peak detectors which suffer from loss of sync and a-g-c setup when the reference voltages are disturbed by noise.

Additional Applications

Once the referencing level is established independent of noise as shown in Figure 2, methods other than d-c coupling into a sync separator can be employed. The clamped signal could be applied to a diode limiter to clip the noise before separation, as shown in Figure 8, or to a noise inverter as shown in Figure 9.

In the diode clipper circuit of Figure 8, the keying pulse amplitude, and cathode bias voltage, are chosen so as to clip the noise at the sync tips.

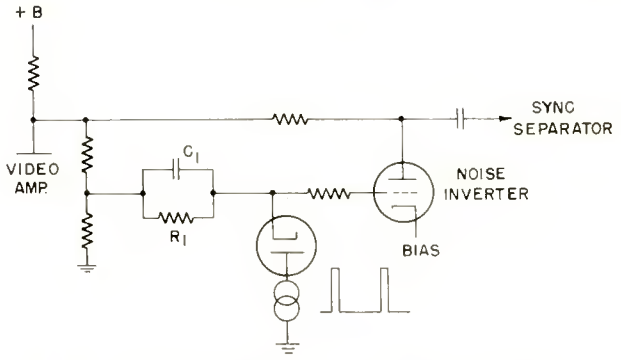

Fig. 9—Automatically regulated noise inverter.

In the noise inverter circuit of Figure 9, the keying pulse amplitude is chosen so as to keep the grid voltage of the noise inverter lower than the plate voltage, and the cathode bias is chosen so that the tube will conduct on noise pulses extending beyond the sync tips.

In either of these methods, the system is self-regulating, and will provide optimum results independent of signal strength.

DISTORTION IN PHONOGRAPH REPRODUCTION*†

By

H. E. Roys

Engineering Products Department, RCA Victor Division
Camden, N. J.

Summary—*Three distortion methods, the harmonic, the intermodulation, and the difference frequency, have been studied, mainly on a theoretical basis, as a means of analyzing distortion encountered in phonograph reproduction. The harmonic method is somewhat difficult to apply and some of the harmonics may be beyond the range of the system. The intermodulation method has been used in the past with considerable success, and appears to be a good method of analyzing tracing distortion. The difference frequency method appears to be somewhat insensitive to tracing distortion but offers theoretical advantages in that the analysis may be made right up to the cutoff frequency of the system. Practically, it is somewhat difficult to apply.*

Introduction

In order to obtain optimum results in making phonograph distortion measurements, it is quite possible that both methods and equipment should differ from those used for amplifiers and other systems of sound recording. Records are cut with the turntable revolving at a constant angular velocity or rotational speed. The linear speed of the medium past the recording stylus is not constant, therefore, but is a function of the distance of the stylus from the center of the disk as well as the turntable speed. For this reason, the wavelength of the wax impression for a given audio frequency will vary, being longest at the outside of the record, and shortest at the inside. This is a difference that exists between disk and other methods of recording such as magnetic tape and photographic film, where the linear speed of the medium is constant, and the wavelength of any frequency remains the same throughout the entire recording. This effect does not, of course, exist in amplifiers.

The recorded disk is reproduced by a pickup having a stylus of a finite size, and one which is spherical in shape in contrast to the chisel-shaped cutting stylus. It becomes apparent, then, that difficulty can be expected in having the stylus accurately follow the recorded groove, particularly at the inside of the record where the wavelengths are short and the curvature great. Distortion introduced under such conditions,

* Decimal Classification: R148.11 × R391.12.

† This paper first appeared in the *Journal of the Audio Engineering Society*, January, 1953.

due to the geometry of the groove and the reproducing stylus, is known as tracing distortion.

Hunt and Pierce[1] and somewhat later Hunt and Lewis[2] investigated this type of distortion. Corrington[3] reviewed this work and added some refinements, so that today there exists a good over-all mathematical analysis of tracing distortion. Experimental data appears to be in good accord with the theoretical work so that it is possible to use theoretical analysis to obtain a better understanding of distortion encountered in phonograph reproduction.

Pickup Distortion

A phonograph reproducing system includes amplifiers and loudspeakers in addition to pickups and records. It is not the purpose of this article to discuss methods of distortion analysis applicable for

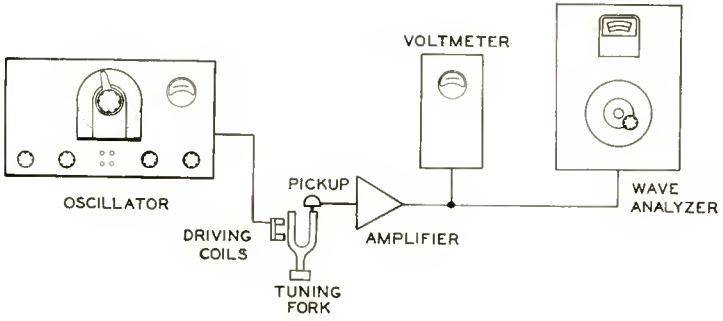

Fig. 1—Block diagram of the setup for measuring nonlinearity of a pickup.

either amplifiers or speakers but rather to stress measurements involving the pickup and, in particular, the type of distortion encountered during reproduction. It is desirable, during the development period, to learn something about the linearity of the moving system of the pickup without involving the record, and a simple but effective means of doing this is by the tuning fork method.* One tine of the fork (see Figure 1) is excited by an electromagnet connected to the output

[1] J. A. Pierce and F. V. Hunt, "On Distortion in Sound Reproduction From Phonograph Records," *Jour. Acous. Soc. Amer.*, Vol. 10, pp. 14-28, July, 1938.

[2] W. D. Lewis and F. V. Hunt, "A Theory of Tracing Distortion in Sound Reproduction from Phonograph Records," *Jour. Acous. Soc. Amer.*, Vol. 12, pp. 348-365, January, 1941.

[3] M. S. Corrington, "Tracing Distortion in Phonograph Records," *RCA Review*, Vol. 10, pp. 241-253, June, 1949.

* This method was developed by H. J. Hasbrouck, formerly of RCA Victor Division.

of an oscillator whose frequency is adjusted to sustain vibration of the fork. The other tine drives the pickup, and a small chisel dent in the end of the tine provides a groove for the stylus tip. Since the chisel dent does not remove metal, it does not affect the frequency of vibration. Different forks may be used, and the amplitude of vibration changed by adjusting the oscillator current, so that distortion measurements may be made at different frequencies and levels.

The mechanical coupling between the two tines is very low and, in addition, the second and higher modes of vibration of a tuning fork are not in simple harmonic relation with the fundamental so that any harmonics** that appear in the output voltage from the pickup are most likely due to the pickup itself and not the driving system. Care must be taken when using magnetic types of pickups to shield either the pickup or the electromagnet that drives the fork, in order to prevent coupling between them.

Measurements have been made to determine the linearity of pickups by the tuning-fork method with good results. They have not always agreed with measurements obtained while reproducing a record, however, and so the tuning-fork method cannot be recommended as being sufficient. In one particular case, a pickup that showed less than one per cent distortion by the tuning-fork method, indicating good linearity of the moving system, showed a value of over 20 per cent intermodulation (IM). Listening tests confirmed the IM measurements. Several experiences of this nature soon made it apparent that it is advisable to obtain an over-all evaluation by checking the pickup while reproducing a record.

Equipment Requirements

Generally, variations of the angular velocity of the disk are unavoidable. The resulting variations in linear speed of the medium past the recording or reproducing point, commonly known as "wow" or "flutter," impose severe restrictions upon the measurement equipment. For measuring distortion under such conditions, the equipment should be relatively insensitive to changes in frequency and phase shift. Analyzers that require critical phase and frequency adjustments, are difficult, if not impossible, to use. Harmonic analyzers of the broad-band type can be used and filter type of analyzers, such as used for intermodulation measurements, are more nearly ideal. If the passband

** Lord Rayleigh in his *Theory of Sound*, Vol. I, Macmillan & Co., 1926, page 280, reports that the second mode of a vibrating reel, clamped at one end is 2.64 times the fundamental; the third mode, 4.13; the fourth, 5.1; and the fifth, 5.83.

of the filter is great, such as might be encountered with the total harmonic meters where the fundamental is filtered out and the residue measured, noise may impose a limiting factor.

Disk recording heads and reproducers usually have a limited frequency range and a sharp cutoff. Harmonics that appear above the cutoff frequency may not be evident, and those that appear at the upper resonance frequency of the pickup may become greatly exaggerated. This becomes evident when one examines the wave shape of the output voltage from a pickup as a frequency record that has some distortion is being reproduced. At one-third the resonance frequency, third-order distortion will govern the wave shape, and at one half the peak frequency, second order distortion will predominate. As higher frequencies are reproduced, the pattern will once again become a sine wave (see Figure 2). If the pickup is damped mechanically, or electrical compensation added in the filter to compensate for the peak, the distortion assumes its normal value.

The apparatus for measuring the distortion of phonograph systems, then, should involve a record, and should be sensitive to groove and stylus contact and tracing distortion. It should also give representative results with systems of limited frequency range.

To do this, equipment is required that is relatively insensitive to phase and frequency changes due to wow and flutter, and that has a restricted passband so that the distortion, and not noise, is the quantity measured.

Methods of distortion analysis such as the difference frequency (CCIF) method, or the intermodulation (SMPE) method, where sidebands due to intermodulation of the two frequencies are produced within the frequency range of the system, may offer some advantages over the straight forward harmonic method. However, even though the harmonic method does not appear to be the best means of investigating phonograph distortion, it is advantageous to compare it with others because of its long usage and knowledge of values that are generally acceptable.

Third-Harmonic Method

Using the mathematics developed by Hunt and Lewis[2,4] the expression for the third-harmonic term is

---

[2] W. D. Lewis and F. V. Hunt, *loc. cit.*

[4] H. E. Roys, "Analysis by the Two-Frequency Intermodulation Method of Tracing Distortion Encountered in Phonograph Reproduction," *RCA Review*, Vol. 10, pp. 254-269, June, 1949.

$$\frac{\frac{3\,\pi^2\,r^2\,f^2\,u^3}{4\quad V^4}}{u-\frac{\pi^2}{4}\cdot\frac{r^2\,f^2\,u^3}{V^4}}\times 100$$

where r = radius of the stylus tip,

f = frequency of the recorded signal,

u = recorded velocity,

V = groove velocity (πdn, where n is the turntable speed and d the record diameter for the groove under consideration).

Third-harmonic distortion terms were calculated for frequencies ranging from 700 to 10,000 cycles, and for groove velocities encountered in present day recordings. Calculations were made for a recorded velocity (maximum modulation velocity) of 5.55 inches per second which is believed to be close to the maximum velocity used in present-day fine-groove recording. Other calculations were made at a recorded level 10 decibels below this value, in which case the recorded velocity is 1.75 inches per second.

It is customary, in phonograph recording, to tip up the high frequency end during recording, and roll it off in inverse manner during reproduction, in order to obtain a signal to noise improvement while still maintaining a flat over-all frequency response characteristic. However, in order to keep the problem simple, the calculations in this article were based upon a constant velocity recording characteristic for frequencies above 700 cycles and no tip-up was included.

Manner of Presentation

It is believed that the manner in which the curve data is presented is of importance. A view that encompasses the entire sheet, like looking at a picture, is apt to convey a first impression that is difficult to overcome, even after a more thorough understanding of the scales has been achieved. For example, Figure 3 shows the calculated values of third harmonic distortion obtained for frequencies from 700 to 10,000 cycles at the groove velocities indicated and for the maximum recorded velocity of 5.55 inches a second. The frequency indicated is the frequency of the fundamental, and the ordinate represents the third-order distortion value for that fundamental. The frequency of the third-order term is, of course, three times that of the fundamental. Yet,

knowing all of this, many readers who are familiar with phonographs will reject the data as being misleading, because the distortion values are so high. Compare then, Figure 3 with Figure 4, where the same

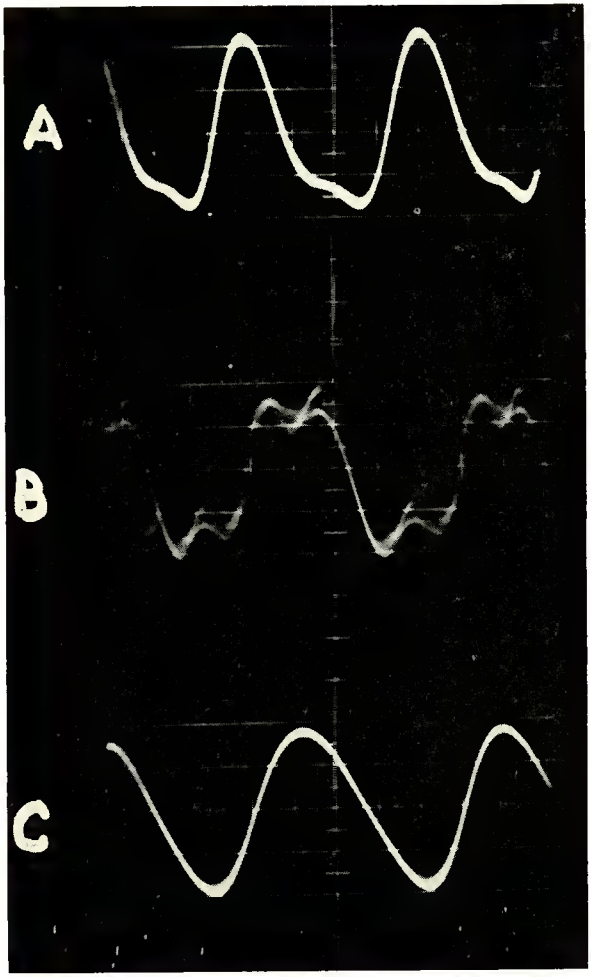

Fig. 2—Oscilloscope traces showing recorded frequency of 7500 cycles reproduced, on variable speed turntable, at 6000 cycles (A), 4000 cycles (B), and 7500 cycles (C). The pickup showed a substantial resonance at 12,000 cycles. The second-harmonic term can be seen in (A), and the third-harmonic term in (B). The distortion in (C) is very low.

data is involved, but a frequency scale that corresponds to the frequency of the third-order term, instead of the fundamental, is used for the abscissa. Figure 4 is believed to be more realistic because the third-

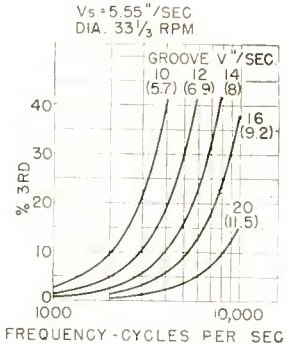

Fig. 3—Calculated values of third-harmonic distortion for a recorded velocity of 5.55 inches a second. The frequency scale is for the fundamental tone rather than the harmonic.

order terms are pictured in their rightful position in the frequency spectrum. For a limited range phonograph which extends up to 4000 or 5000 cycles, the maximum tracing distortion is indicated in Figure 4, and is of the order of 7 per cent. Distortion of this magnitude does not appear to be very serious.

For a wide-range system, the distortion will, of course, become more obvious. Figure 5 shows the results obtained for a level 10 decibels below the assumed peak recording level used for Figures 3 and 4. Here again, the frequency scale is that of the harmonic and not the fundamental. The values are low, and even for a wide-range system extending out to 15,000 cycles, they are not alarming. For the peak recording level, they would become much greater and, of course, more readily discernible.

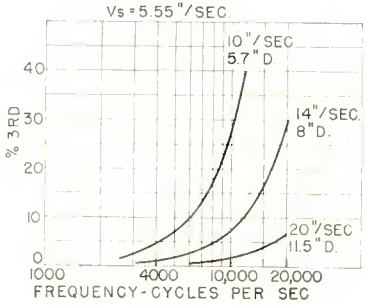

Fig. 4—Same as Figure 3 except that the frequency scale is that of the harmonic rather than the fundamental.

Playback Loss

The pressure created with the small spherical stylus tip resting on the groove side walls is considerable, and as a result, there is some yield of the record material. Within limitations, it appears that the yield primarily results in a loss of output voltage, much the same as if the recorded level were reduced. If such is the case, the reduction in level would result in a decrease in distortion. Earlier experimental work[1] indicated this to be so, and the results are shown in Table 1. The calculated third-harmonic distortion for the various frequency bands being tested did not agree with the measured values. The playback loss due to yield of material was carefully measured and the third harmonic distortion again calculated taking into account the apparent loss in level due to yield of the record. The results, as can

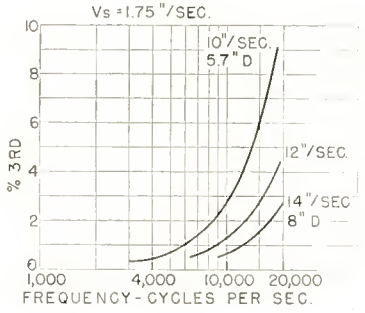

Fig. 5—Calculation for third-harmonic term at a reduced level. This level is 10 decibels below the value used for Figures 3 and 4. The frequency is that of the harmonic and not the fundamental.

be observed in Table 1, then agreed much better with the measured values. More recent measurements tend to confirm these results.

Table I—Effective Reduction in Recorded Level Due to Playback Loss Results in Reduced Distortion

	Per Cent Third-Harmonic Distortion			
		Calculated		Playback
Frequency Cycles	Measured	No Loss	With Loss	Loss, Decibels
6000	3.0	12.0	4.4	3.7
4000	2.5	7.0	3.8	2.1
2000	1.8	2.0	1.4	0.7
1000	1.5	0.6	0.6	0.0

The measurements were made in the following manner, using a

variable speed turntable.[5] Each recorded frequency was played back at a speed such that the reproduced frequency was 1000 cycles. For the 6000-cycle band, the turntable was slowed down to 1/6 of 33⅓ or 5.55 revolutions per minute; for 1000 cycles, the speed was nominal, or 33⅓ revolutions per minute. Such procedure offers several advantages. For example, the frequency range covered by the amplifier and pickup is the same for each set of measurements. Harmonics up to the 5th or 7th are well within range of the pickup response, since the 7th harmonic for 1000 cycles is 7000 cycles. If the record were revolved at its nominal speed, the third harmonic of 6000 cycles would be 18,000 cycles and so, perhaps, beyond the range of the reproducer and the harmonic analyzer. The mechanical impedance of the pickup is the same for the different sets of measurements and it is also low, since the free resonance of the moving system in air lies between 1000 and 2000 cycles. The pickup is, therefore, easiest to drive throughout

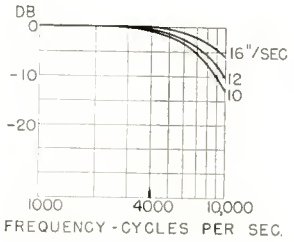

Fig. 6—Playback loss or loss in output voltage due to yield of the record material.

the range involved, and so does not impose too great a load on the record. The tracing conditions are not believed to be greatly changed by reproducing the disk at a lower speed since there is no changed wavelength, curvature, or physical dimensions involved in tracing distortion.

It appears that to the first order of magnitude, playback loss or yield of material will result in a decrease in distortion and so should be considered in the study. Measurements with a pickup representative of those obtainable today for wide range reproduction show that a playback loss, as illustrated in Figure 6, can be expected. Applying this loss as a reduction in level and recalculating for the third harmonic, the curves shown in Figure 7 are obtained. The greatest difference

[5] H. E. Haynes and H. E. Roys, "A Variable-Speed Turntable and Its Use in the Calibration of Disk Reproducing Pickups," *Proc. I.R.E.*, Vol. 38, pp. 239-243, March, 1950.

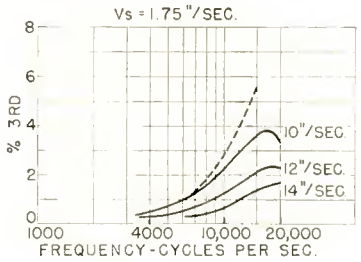

Fig. 7—Third-harmonic distortion with playback loss included. The recorded velocity before loss was the —10-decibel level, or 1.75 inches per second.

results for harmonic frequencies above 10,000 cycles, and the reduction would only be observable on a wide range system.

Intermodulation Method

In using the intermodulation method, two frequencies, 400 and 4000 cycles, were combined to form the test signal; the 4000-cycle signal being 12 decibels lower in level than the 400-cycle tone. The combined signal, as illustrated in Figure 8, is passed to the device under test, and then to the analyzer. The analyzer filters out the 400-cycle signal, and also any second and third order harmonics of 400 cycles that might be present, by means of a 1600-cycle high-pass filter. The remainder is treated as a 4000-cycle carrier that has been amplitude modulated due

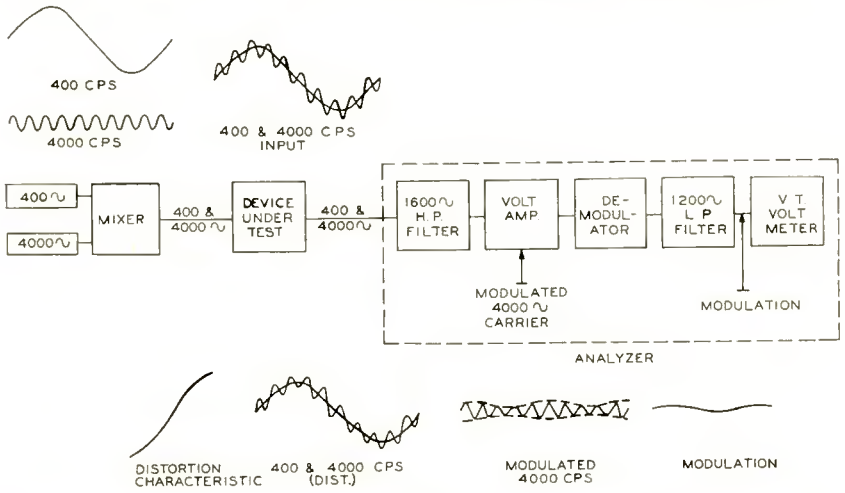

Fig. 8—Block diagram of intermodulation equipment. 400 and 4000 cycles are combined in a linear network as the test signal. In the analyzer, the 4000-cycle signal, amplitude modulated due to nonlinearity in the device, is treated as a modulated carrier.

to nonlinearity in the device undergoing test. The amplitude of modulation is measured with respect to the magnitude of the 4000-cycle carrier, and is expressed as per cent modulation.

Using the theory presented by Hunt and Lewis[2,4] the expression for the percentage intermodulation is

$$\frac{\frac{\pi^2}{4}\frac{r^2 u_1^2 u_2}{V^4}\left[(2f_1+f_2)^2+(2f_1-f_2)^2\right]}{u_2-\frac{\pi^2}{2}\frac{r^2 f_2^2}{V^4}\left(\frac{u_2^3}{2}+u_1^2 u_2\right)}\times 100$$

where $u_1 =$ 400-cycle velocity,
$u_2 =$ 4000-cycle velocity, normally 12 decibels below the 400-cycle level,
$f_1 =$ 400 cycles per second,
$f_2 =$ 4000 cycles per second,
$r =$ radius of playback stylus tip,
$V =$ groove velocity.

Calculations were made with a low frequency of 400 cycles and a high frequency ranging from 2000 to 10,000 cycles. Since lateral recording is push-pull, the even harmonic terms do not appear in the mathematics, and sidebands of the high frequency plus and minus 800 cycles are the only ones of direct concern. These calculations were made for a stylus velocity of 1.75 inches per second and a groove velocity of 10 inches per second, which corresponds to a record diameter of 5.7 inches at a turntable speed of 33⅓ revolutions per minute. The 1.75 inches per second stylus velocity is the sum of the maximum values of the 400- and 4000-cycle signals, or 1.4 inches a second for 400 cycles and 0.35 inches a second for 4000 cycles. The results are illustrated in Figure 9 along with the results obtained for the third-harmonic calculations both with and without loss. The sidebands created due to distortion or nonlinearity are displaced equally on either side of the carrier frequency, so that the mean frequency is that of the carrier. It is customary, therefore, to plot the percentage intermodulation with respect to the carrier.

As before, the third harmonic is plotted with respect to the actual third-order term and not the fundamental frequency. It is interesting to note that the intermodulation values are about four times the third-harmonic values. At 10,000 cycles, for example, the third-harmonic

term is about 2.7 and the intermodulation is 10.8 per cent. This is in keeping with the general, but somewhat erroneous, conception that the intermodulation value should approximately be four times the harmonic value. There is no need of applying playback losses to the intermodulation equation, since the loss term that appears in the denominator and subtracts from u_2 depends upon the geometry of the stylus and groove, and is small for low values of distortion. Assuming that for the values considered here it can be neglected, then the only term that appears in the denominator is the velocity term u_2. This now cancels out the u_2 term in the numerator, leaving the distortion equation independent of the high-frequency velocity. It is not independent of frequency, however, as the frequency term remains so that the distortion increases as the square of the frequency.

A low-frequency value of 400 cycles offers advantages over a lower frequency for the following reason. The cross-over frequency in disk

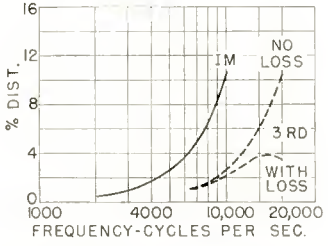

Fig. 9—Results of intermodulation calculations using a low frequency of 400 cycles and various high frequencies from 2000 to 10,000 cycles. The third-harmonic curves illustrated in Figure 8 are included for comparison.

recording, where lower frequencies are recorded on a constant amplitude basis, occurs at about 500 cycles. Velocity is a function of both amplitude and frequency, and if the amplitude is maintained constant as the frequency is decreased, the velocity will decrease in the same proportion. The low-frequency velocity term u_1 appears as a squared term. If 100 cycles were chosen instead of 400 cycles, the value would be one-fourth the 400-cycle velocity. Squaring would give one-sixteenth, so that the per cent intermodulation would be reduced by approximately 16. The test would no longer be sensitive to tracing distortion, but might be used for measuring cutter distortion. It seems reasonable, however, that cutter distortion can be evaluated just as well by using 400 cycles, since the amplitude of motion of the armature and stylus remains essentially the same for all frequencies below the cross-over frequency. Therefore, a low frequency of 400 cycles is preferred to 200 or 100 cycles for disk recording purposes, where it

is desirable to place emphasis upon a method that is sensitive to stylus and groove contact.

Difference-Frequency (CCIF)* Method

In the difference-frequency method,[6] two signals are combined to form the test signal, but they are usually varied in synchronism, so that the difference frequency is constant. The difference signal is measured and expressed percentage-wise with respect to the sum of the magnitudes of the two test frequencies. The advantage of the method lies in the fact that the range up to the cutoff frequency of the system can be readily examined.

For this analysis, the same equation as used for the intermodulation calculations was used, and the amplitude of each signal was made the same, corresponding to a velocity of one half of 1.75 inches per second.

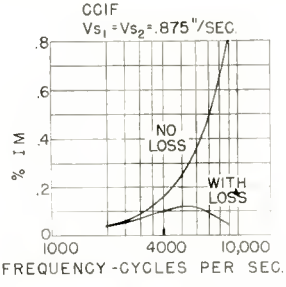

Fig. 10—Calculated curves for the difference frequency term that results due to intermodulation. The two high frequencies were maintained 1000 cycles apart.

Playback loss was also taken into account, and curves with and without loss are shown in Figure 10. These curves, as expected, show an increase in distortion with frequency. The two test frequencies were 1000 cycles apart. For this case, the $(2f_1 + f_2)$ term that appears in the equation is of no concern, since it is a sum term and, according to procedure, is not measured. This leaves $(2f_1 - f_2)$, and for the case where $f_1 = 9000$ cycles and $f_2 = 10{,}000$ cycles, the difference frequency is 8000 cycles. The abscissa value of distortion in this instance was plotted for this difference frequency.

Note that the ordinate scale is in tenths. With the distortion so low in magnitude and so close to the test signal in frequency, accurate measurements are difficult to make. Due to flutter and wow of the

---

* International Telephonic Consultative Committee.

[6] A. P. G. Petersen, "The Measurement of Nonlinear Distortion," General Radio Company Technical Publication B-3, 1949.

turntable, a band-pass filter of appreciable width is necessary. Under such conditions, leakage of the test signal into the measurement channel is apt to occur and show up on the meter as distortion. This appears to be a disadvantage of the CCIF difference-frequency method. A wider separation of test frequencies would help, but would also decrease the effectiveness of the method in being able to operate close to the cutoff frequency.

Practical Results

Measurements have been made using the third-harmonic method and also the intermodulation method with frequencies of 400 and 4000 cycles. More recently, an effort to use the difference frequency (CCIR) method was made without much success due to signal leakage into the measurement channel. The third-harmonic method requires an analyzer with a suitable passband and a turntable of low wow content. Second order terms have been found and apparently they exist even though the theory does not allow for them. Pictures of worn styli usually show more wear on one side than the other indicating unequal pressure on the groove side walls. It is quite likely that such unequal pressure accounts for some of the even order distortion. It is therefore desirable to measure both even and odd order terms. It is of interest to note that the intermodulation analyzer with its filters measures both even and odd order terms and should, therefore, give an accurate evaluation. It was also observed that the rate at which the third harmonic increased as smaller diameters were encountered and the playback loss increased, was less than the rate at which the second harmonic increased.

Apparently, the reduction in third-harmonic distortion due to yield of material is offset by the increase in second-order distortion and the over-all distortion is apt to increase rather than decrease. Results obtained a number of years ago with the intermodulation method[7] showed good correlation with calculated values. Records were cut and processed and many measurements were made with the pressings. In one particular case, the rapid increase in distortion that occurs as smaller record diameters are reached was observed with a pickup having a 2.5-mil-radius tip before the increase was obtained with a large tip radius, which is contrary to theory. Close examination showed a flat of 1.2 mils length at the stylus tip to be the cause of the increased distortion. Hence, the method appears to be sensitive to stylus wear.

[7] H. E. Roys, "Intermodulation Distortion Analysis as Applied to Disk Recording and Reproducing Equipment," *Proc. I.R.E.*, Vol. 35, pp. 1149-1152, October, 1947.

The method also appears to be useful in the study of distortion introduced during processing. In making the pressings, one master was polished excessively in order to determine the effect of such mistreatment with respect to distortion. The change in intermodulation was large and much greater than the change in 400-cycle distortion. The 400-cycle distortion was measured by a total harmonic type of distortion meter using a separate 400-cycle band that had been recorded for such purposes.

Good correlation between measurements and listening tests have been obtained, and data obtained by the intermodulation method was used advantageously in designing the "45 rpm" record system.[8]

The intermodulation method has also been used in pickup development work to determine the vertical force required at the pickup in order to obtain good tracking.[9]

Conclusions

Summing up the results of the study of the three methods of distortion analysis as applied to phonograph reproduction, it appears that:

1. Pickup linearity can be checked without reproducing a record and it may be desirable to do so, but measurements should be made with a disk in order to obtain a true evaluation of the distortion encountered in reproduction.

2. The third harmonic should be plotted with respect to third-order term instead of the fundamental, in order to present a more realistic picture. Such presentation seems to give better agreement with listening tests.

3. The third-harmonic method is difficult to apply, and some of the higher terms may be beyond the range of the pickup and even the measurement equipment.

4. The difference frequency method (CCIF) appears to offer advantages because of the possibility of analysis up to the cutoff frequency. Unfortunately, the distortion term being measured is so low in amplitude, and so close to the test signals, that difficulty is encountered with practical measuring equipment. More measurement experience is needed for a better evaluation.

5. The intermodulation method using a low frequency of 400

---

[8] B. R. Carson, A. D. Burt, and H. I. Reiskind, "A Record Changer and Record of Complementary Design," *RCA Review*, Vol. 10, pp. 173-190, June, 1949.

[9] H. E. Roys, "Determining the Tracking Capabilities of a Pickup," *Audio Eng.*, Vol. 34, pp. 11-12, 34-40, May, 1950.

cycles is sensitive to the type of distortion encountered in record reproduction, and hence well suited for phonograph distortion analysis.

6. Using the 400- and 4000-cycle intermodulation method, good correlation has been obtained among measurements, calculations, and listening tests. The test, with these two frequencies, although not encompassing a wide frequency range, yields results that are useful in the analysis of phonograph distortion.

ACKNOWLEDGMENT

The author wishes to express appreciation for the assistance of J. M. Salani in obtaining the print for Figure 2, and some practical information on the CCIF method.

PERFORMANCE EVALUATION OF "SPECIAL RED" TUBES*

By

H. J. Prager

Tube Department, RCA Victor Division,
Harrison, New Jersey

Summary—*This article reviews and analyzes life-test results accumulated on "Special Red" tubes during the past four years. Information is presented on the range of major characteristics and the changes in these characteristics during the life of the tubes. This information will be of value to both the designer and the user of electronic equipment because it will provide data on the life expectancy and the range of anticipated performance variations.*

Introduction

SINCE the introduction of "Special Red" tubes in 1948, extensive information has been obtained on the performance of these tubes, particularly with regard to life expectancy and the range of anticipated variations in electrical characteristics. This information, which is of special interest to designers and users of industrial electronics equipment, is included in this article in the form of charts and graphs based on results of tests made by the tube manufacturer.

Before discussing performance of the "Special Red" tubes, it may be well to describe them, and to consider briefly their history and their construction. The "Special Red" tubes are small receiving-type tubes designed and manufactured specifically for industrial applications where 10000-hour life, rigid construction, uniformity, and stability are required. The need for such tubes became apparent when neither radio tubes, which were built for the field of home entertainment, nor the so-called ruggedized tubes made during the war were capable of meeting the many different and exacting demands of the industrial consumer. These demands have often been summed up by the word "reliability." Reliability of general-purpose industrial tubes, however, may mean different things to different users, depending upon the tasks the tubes are required to perform. Among the particular things that reliability may mean are uniformity from tube to tube of such characteristics as transconductance and plate current, stability of characteristics throughout long life, a minimum failure rate during the early hours of life, or numerous other special requirements.

---

* Decimal classification R331 × 339.

Because the "Special Red" tubes were to be general-purpose industrial tubes, an investigation was made to select a minimum number of types having the maximum usefulness, and to determine the most important characteristics requiring improvement. As a result of this investigation, three receiving tubes then being widely used in industrial equipment were chosen as prototypes for the new industrial line. The 6SL7-GT high-mu twin triode was selected as the prototype for the "Special Red" 5691, the 6SN7-GT medium-mu twin triode for the 5692, and the 6SJ7 sharp cutoff pentode for the 5693. Structures of the receiving-tube prototypes were redesigned to provide the rigid construction and other special characteristics desired in the "Special Red" tubes. Figure 1 shows cutaway drawings of these three "Special Red" tubes and lists some of the special features used in their construction.

A sound basic construction, although essential, is only the first step in the development of a successful industrial tube. Experience has proved that special attention must be given to the quality of materials and processes throughout the manufacture of such tubes. The very best raw materials must be used, and the finest possible workmanship, which requires excellent tooling and working conditions. Rigid controls must be applied during manufacture, and rigid test specifications must be used on the completed tubes. Finally, carefully designed circuits and conservative operating conditions are required to attain utmost reliability.

Test Specifications

Figure 2 lists the limits for various characteristics as shown in the electrical test specifications for the 5692, and includes the limits for the 6SN7-GT for comparison. Most of the tests and limits are self-explanatory. The center column denotes whether the test is performed on every tube or on a sampling basis. This list includes only the major characteristics of the 5692, most of which are tested 100 per cent in the factory and then sample-tested by both the Quality and the Engineering Departments. Other characteristics, such as amplification factor, plate resistance, transconductance at zero bias, transconductance at reduced heater voltages, and interelectrode capacitances, require testing on a sampling basis only.

Because the "Special Red" tubes are general-purpose types, they were designed to provide reliable service in many varied industrial applications. The limits on heater current, for example, have been specified at ± 3 per cent. In addition, sampling tests are made to assure that 75 per cent of the tubes will be within limits of ± 2 per cent in order to improve stability of performance in battery-operated series

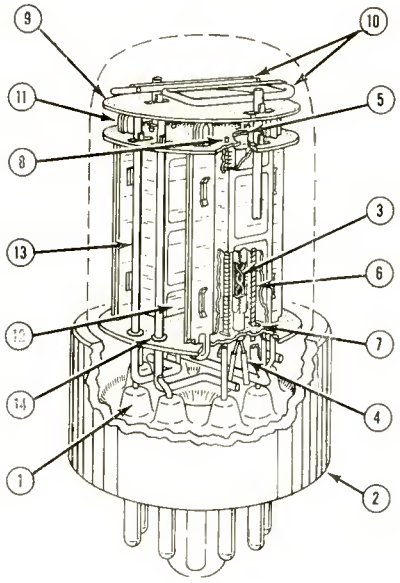

5691 and 5692

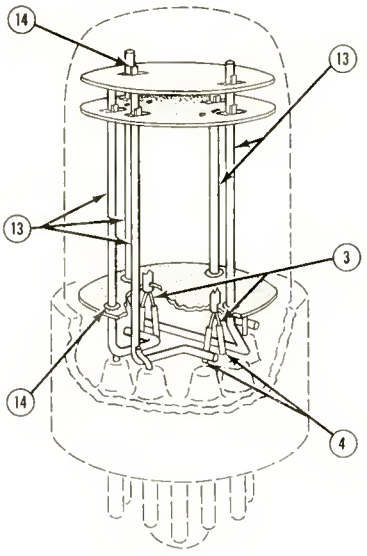

5691 and 5692

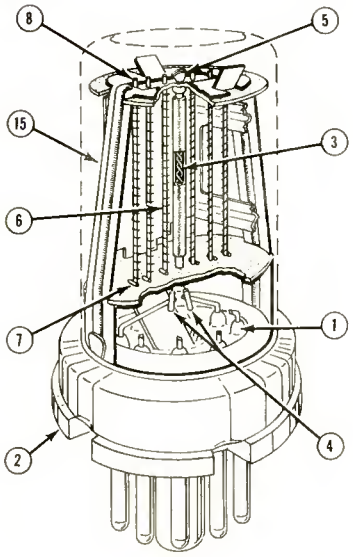

5693

1. Low leakage button stem.
2. Non-hygroscopic base.
3. Pure-tungsten heater for high mechanical strength.
4. Sleeves on heater legs insure good mechanical and electrical bond between heater and heater leads.
5. Cathode sleeves locked to mica insulator.
6. Grid plated to minimize variation in contact potential
7. "Stops" prevent vertical movement of grid rods.
8. Grid rods fit tightly into mica insulators.
9. Extra mica insulator provides getter shield.
10. Two getters for long life.
11. Plates held rigid by plate ears wedged into mica insulators.
12. Plates are designed to minimize electron coupling between units.
13. Mount secured by five supporting rods.
14. Twelve reinforcing eyelets provide a firm bond between mica insulators and five supporting rods.
15. Integral "A-Frame" for strength.

Fig. 1—Cutaway drawings of the 5691, the 5692, and the 5693, showing special features of construction.

strings in aircraft use. The 40-millivolt maximum limit on vibration also improves tube operation in airborne equipment. For use in balanced bridge circuits in automatic control equipment, a maximum limit is specified on unbalance of plate current and plate voltage. Inverse grid current is limited to 0.2 microampere to improve performance in circuits using high grid impedance, and a high-resistance short test is made to reveal the presence of loose particles which may cause intermittent shorts.

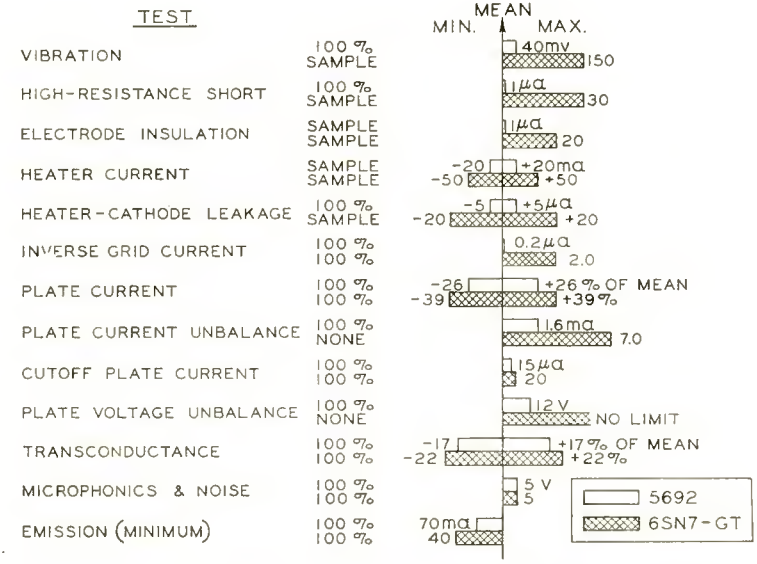

Fig. 2—Comparison of electrical test specifications for the 5692 and the 6SN7-GT.

Life Tests

The test specifications for both the 5692 and the 6SN7-GT also include sampling tests for "life". The life tests specified for "Special Red" tubes are more rigorous and complex than those specified for conventional receiving tubes, and the rest of this article will be devoted to a detailed discussion of life-test results obtained with the "Special Red" tubes. It is probably in this type of test, more than in any other, that more information is needed for premium tubes than for receiving tubes. Due to the length of time required to collect the necessary data, however, very little information has been published in this field.

Prior to all tests, the "Special Red" tubes are stabilized at life-test conditions for 48 hours. This stabilizing helps to assure uniform char-

acteristics and minimize early failures. Then, in addition to the 500-hour life test specified for receiving tubes, the "Special Red" tubes are subjected to 10000-hour life tests, cutoff-life tests, heater-cycling tests, vibration-fatigue tests, and impact shock tests.

500-Hour Life Tests

The 500-hour life test has been an industry standard for many years and is still the major life test in the premium-tube specifications. It is neither necessary nor practical to base acceptance of tubes on a 10000-hour test and wait more than a year to find out whether the product being made is commercially acceptable. The use of accelerated life tests on long-life tubes has been suggested a number of times, but no test has yet been found which uniformly accelerates all types of failures. For example, it was thought at one time that life-testing tubes at maximum plate current would provide complete protection over the entire plate-current range. A new application was then developed, however, in which the tubes were used under plate-current-cutoff conditions for unusually long periods of time; the failure rate in such service was excessively high. Subsequent tests revealed the cause of failure in this application, and it was possible to remedy the situation by changing the chemical composition of the cathode base metal. Since then, however, production-control life tests have been run not only at the maximum rated plate current, but at plate-current cutoff as well. Obviously, the same accelerated life test could not serve for both these conditions.

For the "Special Red" tubes, therefore, the 500-hour life test is modified through the use of more stringent limits to assure satisfactory long life. For conventional receiving tubes, it is standard procedure to specify a life-test end point for a major characteristic (for example, 35 to 40 per cent below the rated value for transconductance) and to require that the average life of the sample tubes, the so-called life-test rating, be at least 80 per cent of the specified 500 hours. These requirements have been tightened appreciably for the "Special Red" tubes. The 500-hour life-test end point for transconductance is only 20 per cent below the rated value, and the average-life requirement has been raised from 80 to 95 per cent. In the production of "Special Red" tubes thus far, only 1.5 per cent of the tubes submitted for life test failed to meet these tightened 500-hour limits. All of the tube failures encountered were due to low transconductance; there was not a single inoperative type of failure. On the basis of lot acceptance, of 254 lots tested 96.5 per cent passed successfully. The average-life test rating for all lots was 98.9 per cent.

Although the tightened 500-hour limits represent a big step toward assuring improved performance on life, a minimum life-test end point for transconductance may not be considered strict enough for general-purpose industrial tubes. In most applications in either industrial or military instruments, these tubes must remain very stable to assure equipment stability. When a life-test end point is specified for minimum transconductance only, however, a tube may begin life at the maximum limit of the initial specification, and then, during the 500-hour life test, slump down to the life-test end-point minimum. In the case of the "Special Red" tubes, a tube at the maximum limit initially could drop as much as 30 per cent during the 500-hour test. A suggested method of controlling the stability of the tubes is to specify a maximum limit on the amount of change in transconductance within the 500-hour life-test period.

The results of all the life tests made on "Special Red" tubes during the production year of 1951 were studied to determine whether this method would be practical. Figure 3 shows distribution curves of the observed change in transconductance in per cent for "Special Red" tubes life-tested for 500 hours at both conduction and cutoff conditions. The curves on the left show the distribution of readings on individual tubes, and those on the right of the average of the weekly sample groups. On the basis of this data, additional life-test end points have tentatively been added to the 500-hour test for "Special Red" tubes. These new limits restrict the average change in transconductance of a test sample within the 500-hour period to a maximum of 10 per cent, and the change for individual tubes to a maximum of 15 per cent on the 5691 and the 5693, and 20 per cent on the 5692.

10000-Hour Life Tests

In addition to 500-hour life tests, it is essential that the long-life performance of "Special Red" tubes be closely observed. Therefore, a portion of each 500-hour conduction and cut-off life test is continued to 10000 hours. The information accumulated from these tests represents a good-sized test sample based on all production experience since "Special Red" tubes were first manufactured.

The results of these 10000-hour life tests can be shown in several ways. Figure 4 shows curves of per-cent survival on life for the three "Special Red" tubes and their prototypes. Each of the six tube types was life-tested at its maximum rated plate voltage and plate dissipation. The life-test end points used when the per-cent survival information was computed were about 40 per cent below initial rated values for transconductance. All readings were taken under fixed-bias conditions.

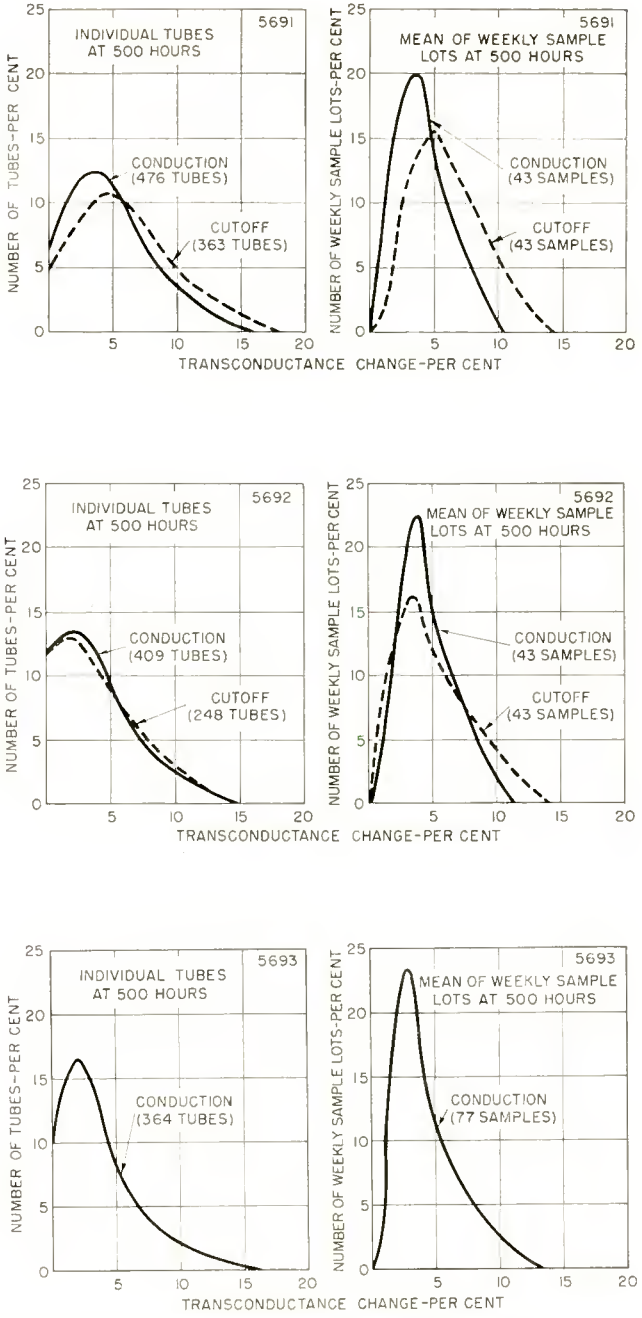

Fig. 3—Distribution curves showing change in transconductance in per cent for "Special Red" tubes within the 500-hour life-test period.

Per-cent survival figures at 10000 hours were 80 per cent, 78 per cent, and 94 per cent for the 5691, 5692, and 5693, as compared with 42 per cent, 34 per cent, and 48 per cent for their respective prototypes. A comparison of the average failures of the three "Special Red" tubes with the average of the three prototypes showed that the total number of failures at 10000 hours has been reduced from 58 to 16 per cent, the inoperative failures from 15 to 2 per cent, and the electrical failures (which are due mostly to low transconductance) from 43 to 14 per cent.

In the field of industrial gas tubes, it has long been customary to publish curves showing the operating range of the major characteristics

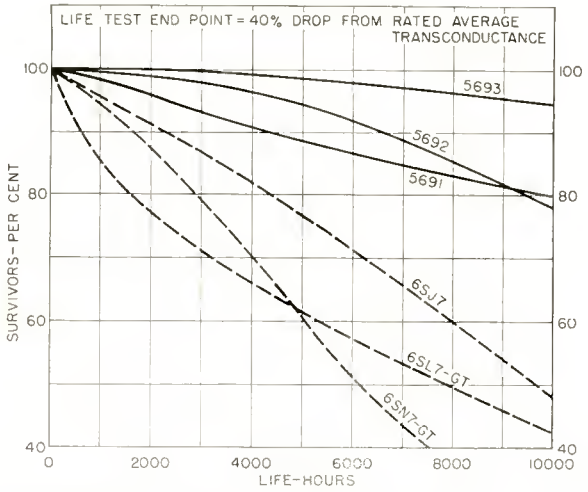

Fig. 4—Survival curves for "Special Red" tubes and their RCA prototypes during life.

throughout the life expectancy of the tubes. Figure 5 shows such curves of operating range for the transconductance and the plate current of the three "Special Red" tubes over the 10000-hour life period. The separate curves at the bottom of the range illustrate the relationship between the life-test end point and the percentage of survivors. On the 5691, for example, if a life-test end point of 1300 micromhos is used, only 50 per cent of the tubes will be satisfactory to 10000 hours. If the end point is 1100 micromhos, however, 75 per cent of the tubes will remain within the limit. For an end point of 1000 micromhos, 80 per cent will be good, and 85 per cent would remain within a limit of 900 micromhos (approximately 43 per cent drop from initial rated value). Using curves of this type, a designer may choose the best combination of life-test end point and per cent survival for a particular application.

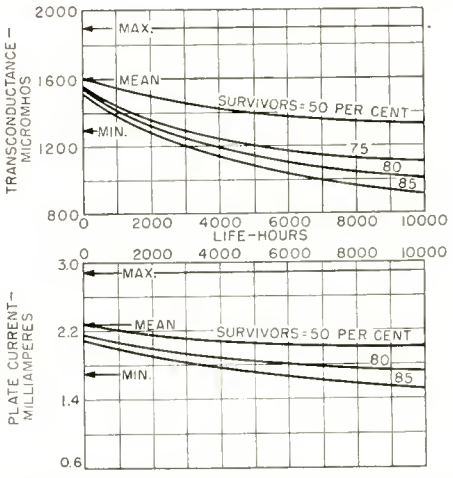

Fig. 5a—Operating range of transconductance and plate current for the RCA 5691 tube during life. Separate curves at the bottom of the range illustrate the relationship between the life-test end point and the percentage of survivors.

For applications where stability of characteristics is more important than absolute values of transconductance and plate current at any particular time of life, the operating range of these characteristics can be shown in terms of per cent change from initial values. Figure 6 shows curves of per cent survival on life for the 5691 "Special Red"

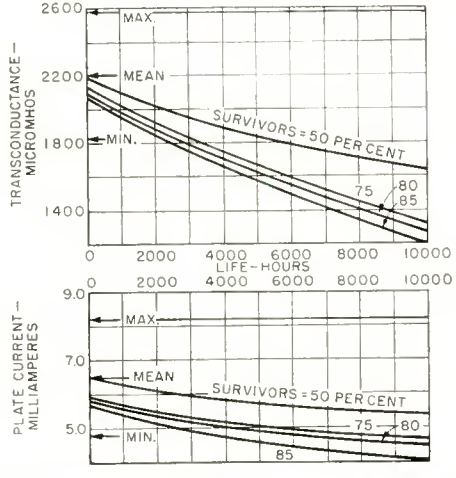

Fig. 5b—Operating range of transconductance and plate current for the 5692 tube during life. Separate curves at the bottom of the range illustrate the relationship between the life-test end point and the percentage of survivors.

tubes when various per cent changes in transconductance and plate current were used as end points. As used here, the term "change of transconductance" or "change of plate current" represents the change in transconductance or plate current from the initial readings recorded at zero hours. The values are given in absolute per cent, and may indicate either a drop or a rise.

It can be seen from these curves that the amount of variation which can be tolerated in the equipment affects the number of failures which may be expected. With the 5691, for example, if very narrow tolerances

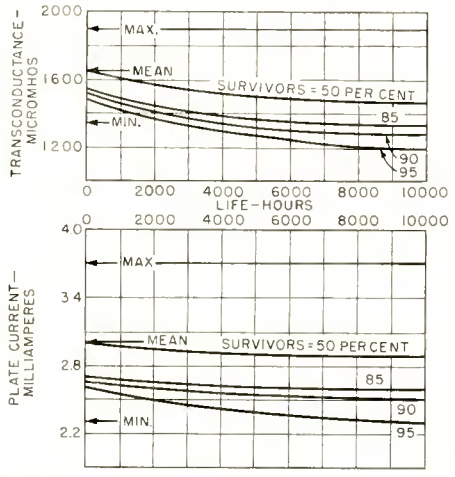

Fig. 5c—Operating range of transconductance and plate current for the 5693 tube during life. Separate curves at the bottom of the range illustrate the relationship between the life-test end point and the percentage of survivors.

of 10 per cent were required on the variation of transconductance, the 80 per cent survival point would occur at 1750 hours of life. If the permissible variation is 20 per cent, 80 per cent of the tubes will be good to 4100 hours. If a change of 40 per cent is tolerable, the 80 per cent survival point will be beyond 10000 hours. If circuits can be designed to tolerate or compensate wider variations in tube characteristics, maximum equipment reliability can be obtained.

The dotted-line curves representing the results of cutoff life tests on the 5691 indicate that this type of operation is more severe when extremely narrow limits of transconductance change are required, but less severe for normal tolerances. Contact-potential variations within the tubes are probably the cause of the higher failure rate when a ten-per-cent limit is used. The lower failure rate at normal limits indi-

cates that there is less deterioration of cathode emission at cutoff conditions than during conduction life.

Figure 7 shows similar survival curves for type 5692 for various limits of transconductance and plate current change. The lower survival percentages, as compared to the 5691, are due to the higher transconductance of the 5692, and its relatively high plate dissipation, which is

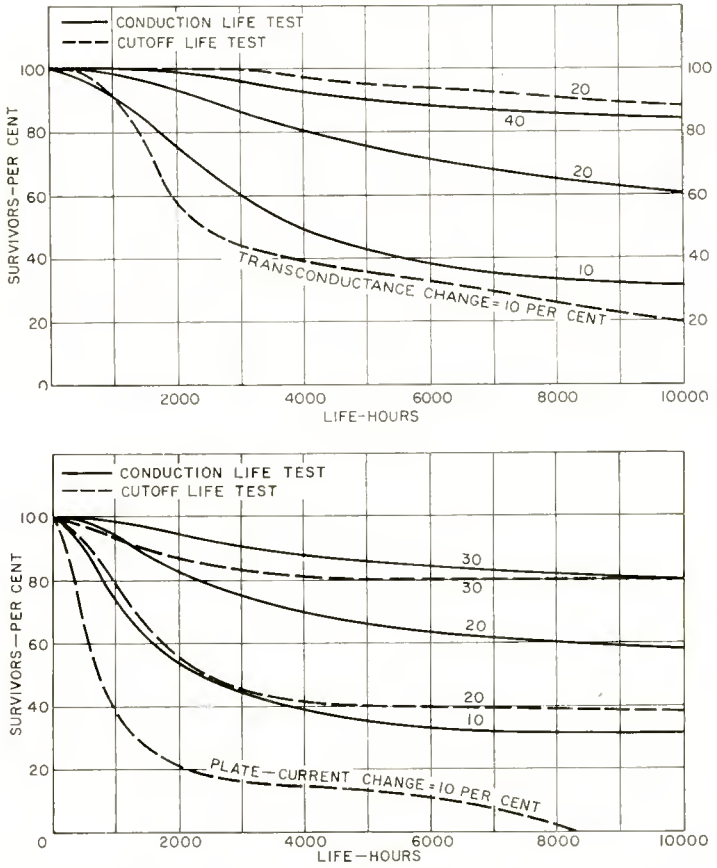

Fig. 6—Survival curves for the 5691 with various limits of transconductance and plate current used as end points.

twice that of the 5691. Life at cutoff conditions is less severe for the 5692 even when extremely narrow tolerances of transconductance change are required because the 5692 is tested at a grid bias of — 9 volts, as compared to — 2 volts for the 5691, and is less subject to effects of contact-potential variation.

Similar curves for the 5693, as shown in Figure 8, illustrate a

better survival record than that of either of the twin-triode types. There are three principal reasons for the higher survival figures: (1) as a voltage amplifier pentode, the 5693 is less subject to changes in transconductance; (2) it has a relatively low plate dissipation; (3) as a single tube, it has only half the potential failure points of the twin triodes. No cutoff-life curves are shown in Figure 8; the dotted-line

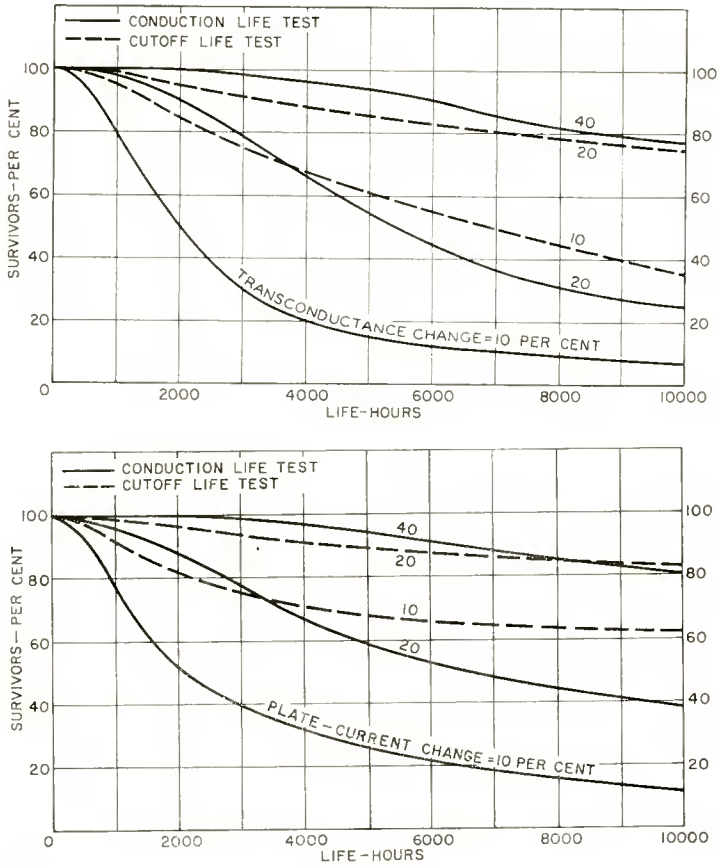

Fig. 7—Survival curves for the 5692 for various limits of transconductance and plate-current change.

curves show per cent survival on life for various percentages of change in plate current.

Mechanical Endurance Tests

An evaluation of the performance of premium tubes should also include results of special mechanical tests specified for such tubes.

Various mechanical endurance tests are made on "Special Red" tubes on a sampling basis similar to that used for life testing. These tests include heater cycling, vibration fatigue, and impact shock.

Heater-Cycling Test

The heater-cycling test is made to determine the ability of tubes to withstand repeated on–off switching during operation. The heating and cooling associated with each switching cycle produce expansions and contractions in the heater-cathode structure, setting up strains which could cause such failures as heater burnouts, open cathode con-

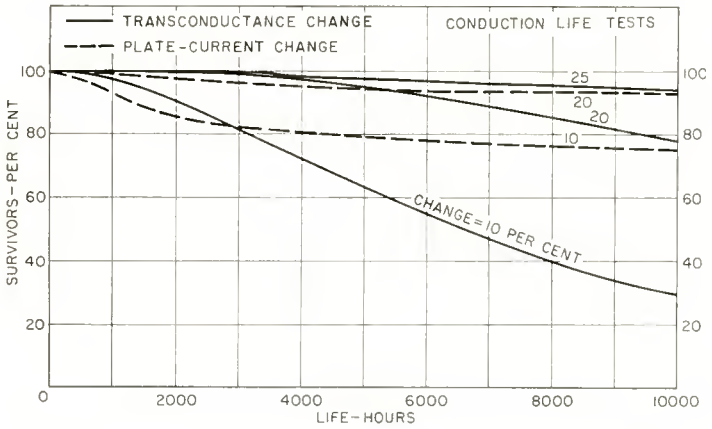

Fig. 8—Survival curves for the 5693 for various limits of tranconductance and plate-current change.

nectors, or heater-cathode shorts. In the cycling test, a heater voltage 20 per cent above the 6.3-volt rating is applied to the tubes, and the heaters are switched on and off at one-and-one-half minute intervals for a total of 2000 cycles. The 2000-cycle figure was chosen rather arbitrarily as a practical control test, and does not indicate that larger numbers of switching cycles cannot be obtained. As a matter of fact, in a special test of 5692 tubes, the entire lot completed 200,000 cycles without failure. In the production-control test, in all tubes tested thus far only one failure has been found; the calculated process average is less than 0.1 per cent. The heater construction using pure tungsten wire, special heater connectors, and extra heater insulation, has proved its effectiveness.

Vibration Fatigue Tests

The vibration fatigue test is conducted as specified in the Joint

Army-Navy Specification for ruggedized and premium tubes. The test is conducted for 96 hours at an acceleration of 2.5g, a frequency of 25 cycles per second, and an amplitude of .040 inch. These conditions, although somewhat arbitrary, are probably more rigorous than would usually be experienced in actual operation. At the conclusion of the fatigue test, the tubes must pass short and continuity tests, as well as vibration and transconductance tests. Results show that 98.7 per cent of the 5691 and 5692 tubes tested to date complied with the specified requirements, and that all of the 5693 tubes tested met the requirements. These results are considerably better than the 90-percent minimum survival limit required by the Joint Army-Navy Specification for this test.

Impact Shock Test

"Special Red" tubes are also subjected to an impact shock test of approximately 500g. The conditions and sampling procedure for this test are also in accordance with the Joint Army-Navy Specification for ruggedized and premium tubes. Five shock applications are given in each of four different position, with all rated voltages applied to the tubes. At the conclusion of the test, the tubes are examined for mechanical failures, and are then checked for shorts, continuity, and certain electrical characteristics such as transconductance, heater-to-cathode leakage, plate-current cutoff, and vibration. Test results for the 5691 and 5692 tubes combined showed only 4.8 per cent failures. For the 5693, 4.5 per cent failed. This failure rate is also well within acceptable service standards for premium tubes. The extra design precautions providing a more rugged tube structure and the careful manufacturing methods have again proved their value.

Conclusion

The importance of this performance information on "Special Red" tubes is that it represents quantitative results on actual tests; previously it had been possible only to make qualitative statements in terms of general experience. These results, however, should not be interpreted as design ratings to be applied to individual tubes, but rather as engineering information which will help equipment designers to obtain the maximum usefulness from "Special Red" tubes.

THEORETICAL RESISTIVITY AND HALL COEFFICIENT OF IMPURE GERMANIUM NEAR ROOM TEMPERATURE*

By

P. G. Herkart and J. Kurshan

Research Department, RCA Laboratories Division,
Princeton, N. J.

Summary—*The resistivity of high-quality single-crystal germanium is determined by its impurity content and, in turn, resistivity can be used as a measure of purity. The semiconductor device engineer will find it most convenient to specify germanium purity in electrical terms by its conductivity type (n or p) and its resistivity at some standard temperature such as 25°C. In this paper, the temperature variation of resistivity over the range —100°C to +140°C has been calculated and plotted for both n-type and p-type germanium with different impurity content, ranging from 0.1 ohm-centimeter to 60 ohm-centimeters at 25°C.*

When germanium is first purified and then intentionally doped with a single impurity, it is desirable to know the relationship between actual impurity content and resistivity or Hall coefficient. Ordinarily, with reasonably perfect crystals, resistivity can be used to specify impurity; on the other hand, for highly doped material or if crystal perfection is uncertain, the Hall coefficient is a more reliable index. These relationships have been calculated for 25°C and are plotted, again for both n- and p-types. The curves can be used either to predict electrical values from known impurity content, or to interpret measured electrical values in terms of germanium analysis.

A useful rule of thumb that applies between 20 ohm-centimeters and 0.1 ohm-centimeter at 25°C (the resistivity range useful for transistors) gives the inverse proportionality between impurity content and resistivity ρ in ohm-centimeters, as follows:

$$\textit{mol-fraction of impurity} = \frac{3.8 \times 10^{-8}}{\rho} \quad \textit{(for n-type germanium)}$$

$$\textit{mol-fraction of impurity} = \frac{8.1 \times 10^{-8}}{\rho} \quad \textit{(for p-type germanium).}$$

Introduction

THE heart of a germanium device is the germanium itself. The performance of the ultimate rectifier or transistor will depend greatly on the electrical characteristics of the semiconductor material. This study is concerned only with germanium, although other semiconductors can be treated in a similar manner.

The electrical behavior of bulk germanium is determined largely

* Decimal Classification: R282.12.

by two factors—crystal perfection and impurity content. Techniques are well developed for growing single crystals that exceed the perfection required in transistors. In the transistor field, the impurity content is measured as a very small fraction—of the order of one part in one hundred million. Such small impurity concentrations are incapable of detection by conventional chemical or physical analysis. However, since these small concentrations determine the important electrical behavior of the germanium, the electrical measurements of resistivity and Hall coefficient can be used to evaluate the impurity content. Indeed, it has become customary to specify the purity of germanium by its resistivity. This paper gives a computation and graphical plot to assist in the interpretation and use of measured resistivity and Hall-coefficient values as well as in predicting the electrical effects to be expected at various temperatures from a given impurity concentration.

Since the Hall coefficient is a direct and unique measure of the electrical carrier concentration (and hence the impurity content) in germanium below about 20 ohm-centimeters in resistivity, it is the most reliable measure of purity, especially when the crystal perfection is uncertain. However, in cases where a high-quality single crystal is under consideration, resistivity will furnish an adequate evaluation of the material. Being a simpler measurement to make, resistivity will normally be the criterion used by the engineer to evaluate germanium.

For the device engineer, the most important part of this study will be the information on the temperature dependence of resistivity of germanium. This provides the basis for understanding how certain important device parameters (e.g., equivalent base resistance of a transistor) vary with temperature. Another important characteristic that will be demonstrated is the fact that n-type and p-type germanium of a given resistivity at room temperature may not exhibit the same temperature variation.

For the scientist charged with purifying germanium and reconstituting its impurity content ("doping"), this paper will aid in converting room-temperature resistivity and Hall-coefficient measurements to absolute and relative impurity concentrations and vice versa. It is significant that n-type and p-type germanium of the same resistivity correspond to different impurity concentrations. Of even greater significance is the fact that with increasing purity, the curve of approach to a limiting (intrinsic) resistivity is entirely different for the two conductivity types.

The basic equations used in this study, and the necessary physical

constants of germanium, are all conveniently available in a single reference.[1] The novelty in the present work lies in: (a) solving the necessary equations simultaneously to get the quantities desired, and (b) plotting numerical values in the range of interest.

The curves given cover the temperature range of —100°C to +140°C, and the resistivity range from 0.1 ohm-centimeter at 25°C to intrinsic or pure germanium (60 ohm-centimeters at 25°C). The temperature 25°C (77°F) is emphasized as being representative of the room temperature at which measurements are often made.

Basis of Calculations

A physical picture of conduction in semiconductors may be found in Shockley's book.[1] The application of this theory is based on the following assumptions:

1. Only a single impurity type is present.
2. Each significant impurity atom contributes one energy state in the forbidden energy band.[2]

These assumptions do not seriously curtail the applicability of the results provided that: (1) The material is first purified and then doped with a single impurity as is the current practice for germanium devices; (2) The significant impurity is from column three (for p-type) or five (for n-type) of the periodic table. This is common practice in doping.

Even when the impurities arise from partial purification without redoping, these results may still be used as an approximate guide to the "net" impurity concentration—that is, the difference in the concentrations of n-type and p-type impurities. In this case, as well as in the case where doping has added more than one significant impurity, an extension of the resistivity measurements to liquid helium temperatures will furnish a better analysis.

Theory

A brief outline of the physical and mathematical bases for the computations will be given here. Further details of the calculation are given in the Appendix.

The resistivity ρ (or its reciprocal, the conductivity σ) depends only on the electronic charge q (a positive constant), and the concen-

[1] W. Shockley, *Electrons and Holes in Semiconductors*, D. van Nostrand Company, Inc., New York, N. Y., 1950.

[2] This has been proved experimentally for antimony by G. L. Pearson, J. D. Struthers, and H. C. Theurer, "Correlation of Geiger Counter and Hall Effect Measurements," *Phys. Rev.*, Vol. 77, pp. 809-813, March 15, 1950.

trations and mobilities of the electrons and holes (n, μ_n, p, μ_p, respectively) that are the electrical carriers in the conduction process. The equation is

$$\sigma = 1/\rho = q(n\mu_n + p\mu_p). \tag{1}$$

The mobilities are constants of the germanium, the electron mobility being about twice that for holes. In the range of interest, the mobilities are determined primarily by lattice scattering and are slowly varying functions of the absolute temperature, T. This dependence has generally been assumed to be proportional to $T^{-3/2}$. Although deviations from this behavior, especially for holes, have recently been reported,[3] the published evidence is not yet sufficiently complete to warrant changing this assumption. The following variation is therefore assumed here:

$$\mu_n = 3600\ (298/T)^{3/2}\ \text{cm}^2/\text{volt-sec}. \tag{2}$$

$$\mu_p = 1700\ (298/T)^{3/2}\ \text{cm}^2/\text{volt-sec}. \tag{3}$$

The electron and hole concentrations are further related by an equation expressing the electrical neutrality of the material:

$$n + n_d + N_a = p + p_a + N_d, \tag{4}$$

where N_d and N_a are concentrations of total donor and acceptor impurity atoms and n_d and p_a are concentrations of un-ionized donor and acceptor atoms.

The following approximate expressions, valid for the range of interest here, can now be written relating the various concentrations with the temperature and with universal constants. The Fermi level E_F appears implicitly in these relations, but need not be solved for, explicitly. It has been determined and plotted, however, since other questions can be answered directly by a knowledge of its behavior.

$$n = CT^{3/2} \exp\ (E_F - E_c), \tag{5}$$

$$p = CT^{3/2} \exp\ (E_v - E_F), \tag{6}$$

$$n_d = N_d \exp\ (E_F - E_d), \tag{7}$$

[3] M. B. Prince, "Temperature Variation of Drift Mobilities of Minority Carriers in Semiconductors," *Bull. Amer. Phys. Soc.*, Vol. 28, p. 10, March 26, 1953.

$$p_a = N_a \exp (E_a - E_v). \tag{8}$$

The E_x's are dimensionless; that is, energies are expressed in units of kT. Only energy differences are involved. E_c is the floor of the conduction band, E_v is the roof of the valence band, E_d is the donor level, and E_a is the acceptor level. The equations are all simplifications of Fermi distributions which hold true because the Fermi level is at least several units of kT away from any of the other energy levels in the ranges under investigation. C is a theoretical constant which should be compatible with the accepted experimental value[4] of $\rho = 60$ ohm-centimeters for pure germanium at "room temperature."

Also required for a solution are the following values which are known experimentally:

$$(E_c - E_v)\ kT = 0.72 \text{ e.v.} \tag{9}$$

$$(E_c - E_d)\ kT \approx 0.04 \text{ e.v.} \tag{10}$$

$$(E_a - E_v)\ kT \approx 0.04 \text{ e.v.} \tag{11}$$

The Hall coefficient is determined from the equation

$$R = -\frac{3\pi}{8} \frac{n\mu_n^2 - p\mu_p^2}{q\ (n\mu_n + p\mu_p)^2}. \tag{12}$$

Results

Figure 1 gives the resistivity of n-type germanium as a function of temperature. The running parameter is the resistivity at 25°C. This is a useful designation, since it corresponds to the conventional specification of purity by the equivalent resistivity. Subsequent graphs provide a transformation to absolute expressions of purity. Note that for 16 ohm-centimeters and below, the resistivity has a positive temperature coefficient at room temperature because of the mobility variation. At sufficiently high temperatures, however, a sample of any given purity will asymptotically approach the intrinsic curve which has the negative slope characteristic of an intrinsic semiconductor.

Figure 2 gives a similar family of curves for p-type germanium.

[4] The value of 47 ohm-centimeters given by E. M. Conwell, "Properties of Silicon and Germanium," *Proc. I.R.E.*, Vol. 40, pp. 1327-1337, November, 1952, was not used because direct measurements of highly purified germanium give values approaching 60.

The curves cross the intrinsic (60 ohm-centimeter) curve and approach it asymptotically from the high resistivity side. This effect is explained as follows: when p-type impurity is added to pure germanium, the concentration of holes increases and the concentration of electrons decreases. Since the holes have the lesser mobility, this

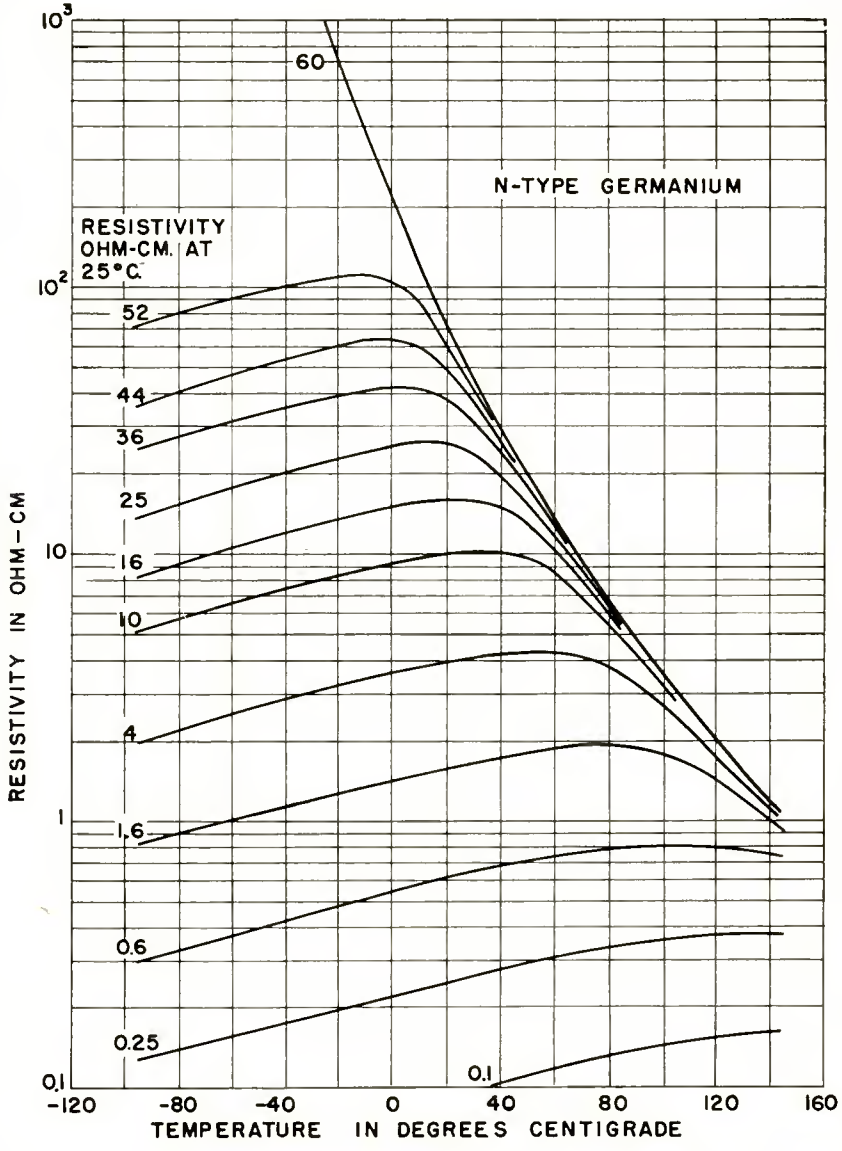

Fig. 1—Resistivity of n-type germanium as a function of temperature.

adds more to the resistivity at first than it takes away. Ultimately, the increase in hole concentration with impurity addition is the only significant effect, and the resistivity decreases as with n-type germanium. The maximum resistivity reached at room temperature is 64 ohm-centimeters. Room temperature resistivities between 60 and

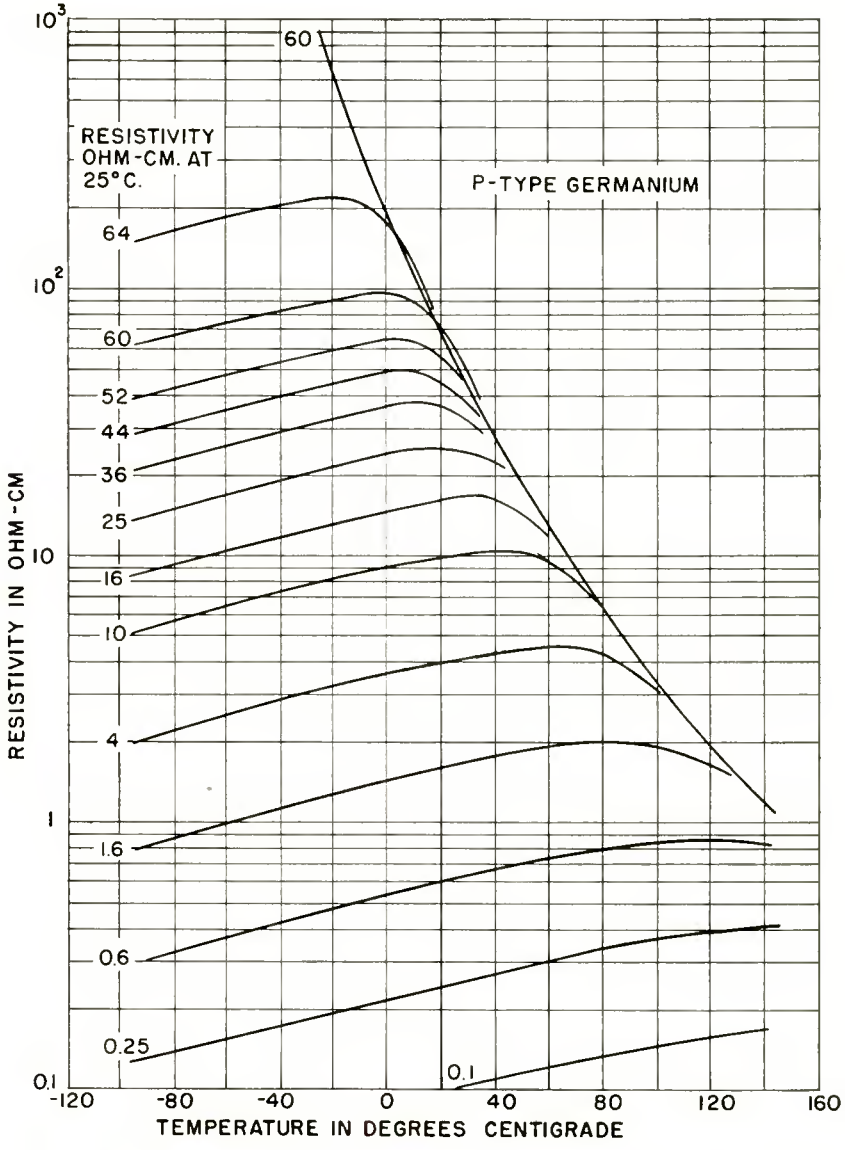

Fig. 2—Resistivity of p-type germanium as a function of temperature.

and 64 cannot be uniquely interpreted in terms of impurity content, but, practically speaking, this is a very limited region and imposes no handicap.[5]

Figure 3 is an enlarged view of curves taken from Figures 1 and 2, and shows the different temperature behavior of 52 ohm-centimeter germanium when it is either p or n-type. It emphasizes the fact that

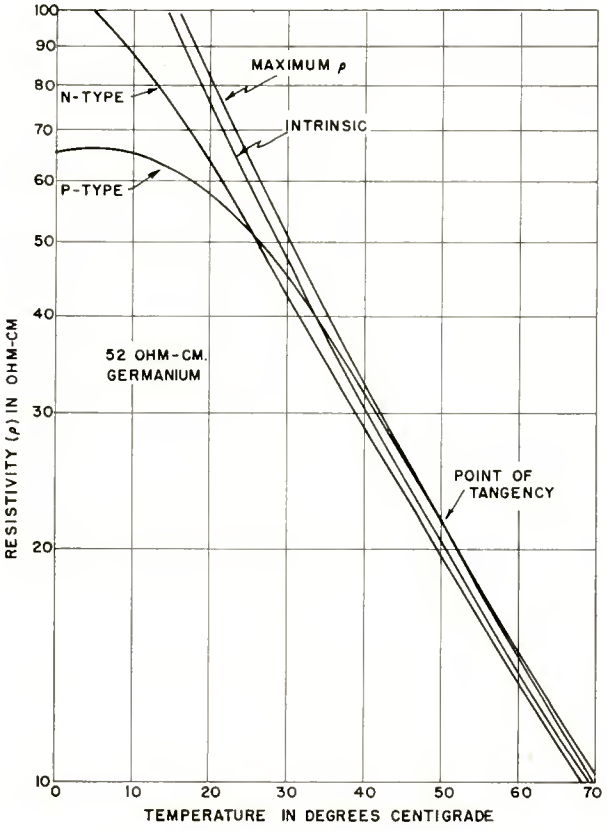

Fig. 3—Comparison of 52 ohm-centimeter germanium, both n- and p-type.

n-type material of a given resistivity is purer than p-type. It is also indicated that the p-type curves are tangent to an envelope marked "maximum ρ." This curve lies 4 ohm-centimeters above the intrinsic curve at room temperature.

Figure 4 is an enlargement of other curves from Figures 1 and 2.

[5] Assuming that the $T^{-2.3}$ drift mobility variation for holes reported by Prince (Reference (3)) holds for p-type germanium, the chief effect on Figure 2 would be to decrease the temperature coefficients of resistivity below room temperature by some 20 per cent.

It shows that for less pure material, the p and n curves coincide below room temperature. One should bear in mind, however, that using room-temperature resistivity as a parameter to designate purity is somewhat artificial, and that the ratio of impurity content in the p and n curves of Figure 4 is not the same as in the p and n curves of Figure 3.

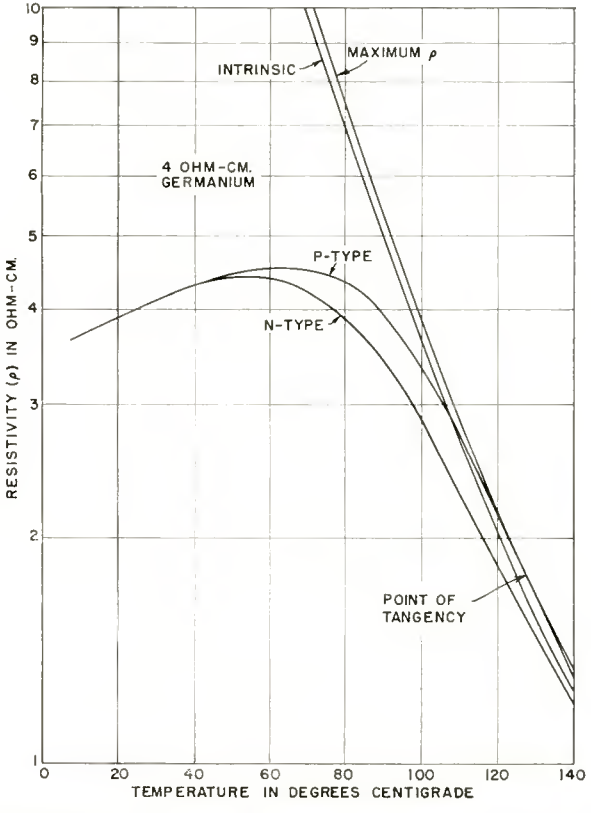

Fig. 4—Comparison of 4-ohm-centimeter germanium, both n- and p-type.

The remaining curves are all plotted for room temperature. Figure 5 relates the room temperature resistivities used above to absolute impurity concentration in atoms per cubic centimeter. As already stated, this implies that each impurity atom contributes one extra energy state near the top or bottom of the forbidden energy band. Prince[6] has determined that the mobility drops more rapidly with increasing impurity content than had previously been reported. His

[6] Private communication from M. B. Prince. Also reported at the Conference on Transistor Research held at Pennsylvania State College, July 6-8, 1953.

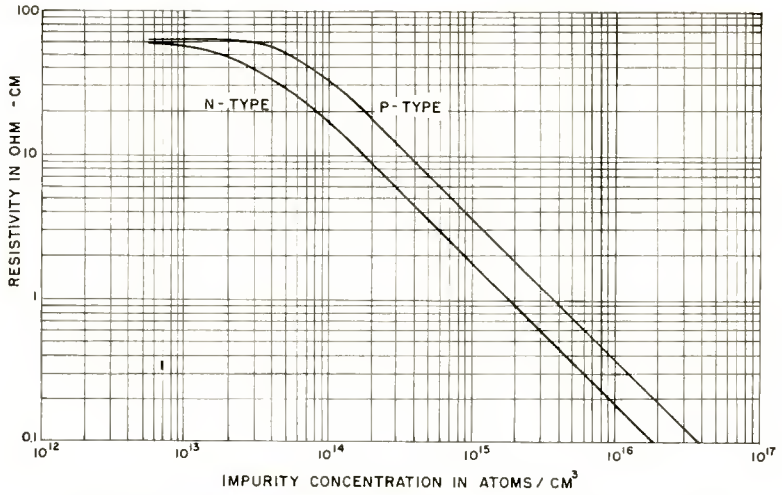

Fig. 5—Resistivity versus absolute impurity concentration for germanium at 25°C.

curves for resistivity versus impurity concentration, however, nearly coincide with those in Figure 5 (except in the intrinsic range) since the mobility change is balanced by the lower value he assumes for the intrinsic resistivity.

Figure 6 gives the same information as Figure 5 except that impurity concentration has been expressed as a mol-fraction, that is, the ratio of impurity atoms to germanium atoms. The conversion

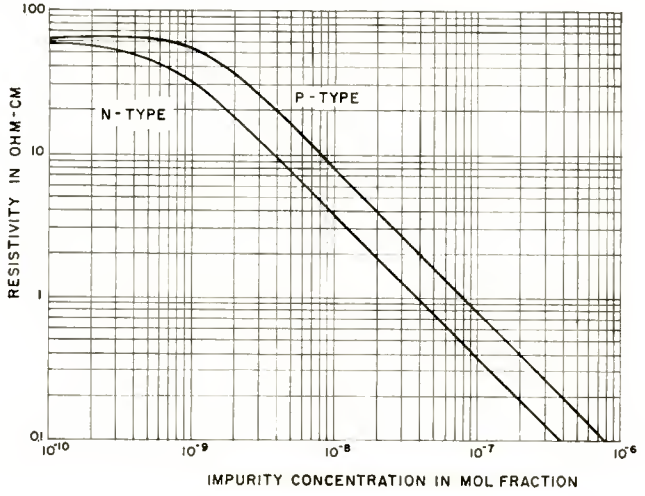

Fig. 6—Resistivity versus relative impurity concentration for germanium at 25°C.

factor is the atomic density of germanium, 4.55×10^{22} atoms per cubic centimeter. The log-log plots are linear for resistivities below about 20 ohm-centimeters. The resistivity in ohm-centimeters and the impurity concentration in mol-fraction are then related by these simple equations:

$$N_d = \frac{3.8 \times 10^{-8}}{\rho},$$

$$N_a = \frac{8.1 \times 10^{-8}}{\rho}.$$

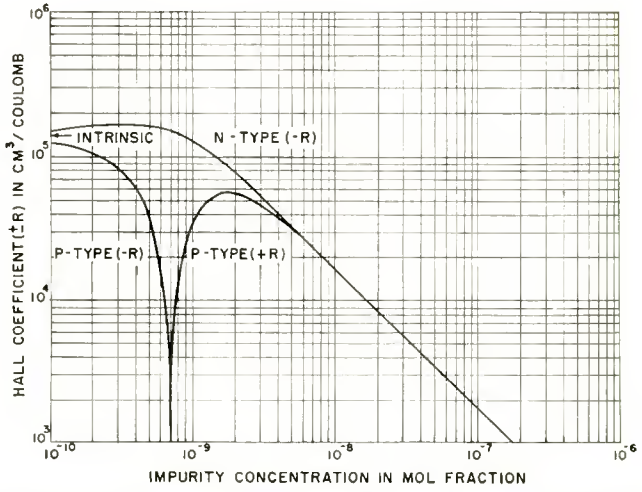

Fig. 7—Hall coefficient versus relative impurity concentration for germanium at 25°C.

These relations are not accurate below about 0.1 ohm-centimeter because impurity scattering in this region begins to affect the mobility.*

Figure 7 gives the Hall coefficient. For n-type germanium, this behaves much like the resistivity of the p-type, since the hole effect subtracts from the electron effect. As the hole contribution vanishes with increasing n-type impurity, it first causes the Hall coefficient to rise before the characteristic of a single type of carrier dominates the picture. The Hall coefficient for p-type germanium goes through zero and changes sign. The reason is that the holes predominate in impure material. With increasing purity, the concentrations of holes and electrons approach equality. Since electrons have the greater mobility, they then predominate.

* A noticeable effect of impurity scattering sets in at about 2 ohm-centimeters. See p. 1331 of Reference (4).

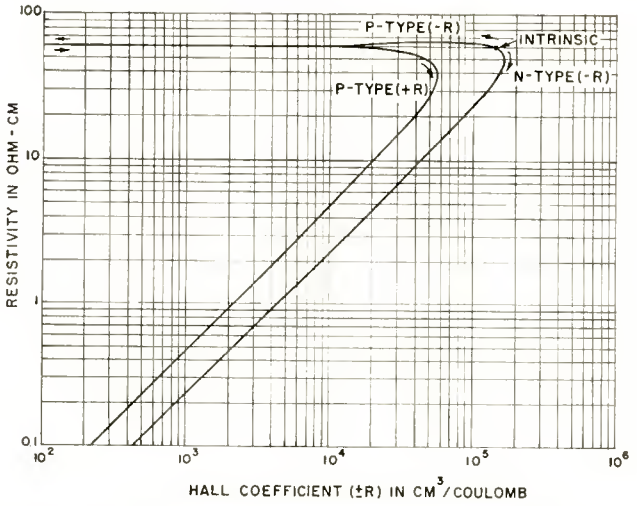

Fig. 8—Resistivity versus Hall coefficient for germanium at 25°C.

Figure 8 gives the Hall coefficient as a function of resistivity. Since these are the two values generally available after making Hall measurements, the curves are useful in determining whether the actual mobilities match those assumed in the calculation, which represent values for high-quality germanium.

Figure 9 gives the displacement of the Fermi level from the center of the forbidden band. It is actually applicable to either n-type or p-type although it is drawn for donor impurities. For n-type, energies are measured toward the conduction band; for p-type, toward the valence band.

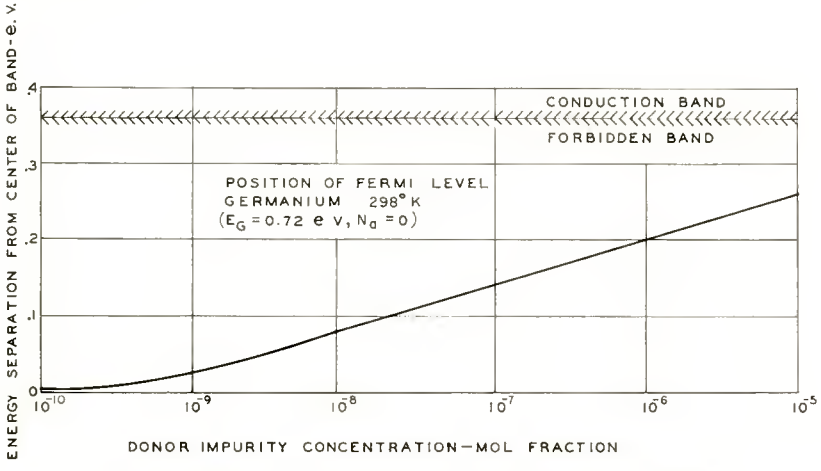

Fig. 9—Position of Fermi level for germanium at 25°C.

Appendix

For germanium in the range of interest, the equation for the conductivity can be reduced to

$$\sigma = Ae^{-E_c}\,(b\,e^{E_F} + e^{-E_F}), \tag{13}$$

where E_c and E_F are measured from the center of the forbidden band, and b is the mobility ratio:

$$b = \frac{\mu_n}{\mu_p}. \tag{14}$$

For purposes of computation, Equation (13) can be written

$$\sigma = A\,e^{-E_c}\,2\sqrt{b}\cosh\,(E_F + \ln\sqrt{b}), \tag{15}$$

or

$$\sigma = A\,e^{-E_{co}}\,2\sqrt{b}\,e^{-E_{co}[(T_o/T)-1]}\cosh\,(E_F + \ln\sqrt{b}), \tag{16}$$

where the subscript "o" stands for value at room temperature, $T_o = 298°\text{K}$ (25°C). Using the constants for germanium, this becomes

$$\sigma = 0.0156\,e^{-14.0[(298/T)-1]}\cosh\,(E_F + 0.361). \tag{17}$$

Given a value of σ at room temperature, E_{Fo} at room temperature is determined from Equation (17).

For some other absolute temperature T, $\sinh E_{FT}$ and hence E_{FT} for the same sample are given by

$$\sinh E_{FT} = (T_o/T)^{3/2}\,e^{-(E_{co}-E_{cT})}\sinh E_{Fo} \tag{18}$$

which follows from the expression for charge neutrality (Equation 4). For germanium this becomes

$$\sinh E_{FT} = (298/T)^{3/2}\,e^{-14.0\,[1-(298/T)]}\sinh E_{Fo}. \tag{19}$$

The computation of σ from Equation (14) can be facilitated by the use of the relation

$$\cosh\,(x + y) = e^{y}\sinh x + e^{-x}\cosh y. \tag{20}$$

Alternatively, values for $\sinh E_F$ can be used directly in the fol-

lowing expressions, valid in the range of interest here. Two forms of the equation are given since E_F is negative for p-type material.

For n-type,

$$\sigma = 0.0156\, e^{14.0\,[1-(298/T)]}\,(1.435 \sinh |E_F| + 1.066\, e^{-|E_F|}). \qquad (21)$$

For p-type,

$$\sigma = 0.0156\, e^{14.0\,[1-(298/T)]}\,[(\sinh |E_F|/1.435) + 1.066\, e^{-|E_F|}]. \qquad (22)$$

A knowledge of E_F also enables n and p to be calculated from Equations (5) and (6). Equation (12) then gives the Hall coefficient R, using the values for mobility given in Equations (2) and (3).

INFLUENCE OF SECONDARY ELECTRONS ON NOISE FACTOR AND STABILITY OF TRAVELING-WAVE TUBES*

By

R. W. Peter† and J. A. Ruetz‡

Summary—*It is shown that secondary electrons from a traveling wave tube collector can increase the noise factor considerably. In the experimental 3000-megacycle tubes studied, the increase was as much as 5 decibels. The effect arises in one or both of two ways. The noise current of the high-velocity secondaries will interact with the fundamental helix mode giving rise to amplified noise at the input end. Any mismatch at this end will result in a return of part of this noise power down the tube with still further amplification. When the collector is at or below helix potential, low-velocity secondaries can return through the helix and interact with higher order forward and backward wave modes. The forward wave modes give rise to an amplified noise signal at the input end of the tube. As in the first case, reflection of any portion of this signal will result in an increased noise factor. The backward wave modes give rise to noise signal amplified toward the tube output. Methods of reducing these effects are discussed.*

I. Introduction

IN the process of developing a sealed-off low-noise traveling-wave tube with characteristics similar to those obtained in experiments on the demountable vacuum system,[1] it was found that the sealed-off version of the tube had a much higher noise factor and a somewhat higher current interception on the helix. By increasing the collector potential above the helix potential in an attempt to collect secondaries, current interception and noise factor were reduced to some extent, but were still above the values obtained with the demountable tube. Therefore misalignment, defocussing, or deflection of the beam was considered to be responsible for the current interception and what was thought to be partition noise. After step-wise elimination of all constructional differences between the sealed-off and the demountable versions, a tube was finally constructed which was identical to the

---

* Decimal Classification: R339.2.

† Research Department, RCA Laboratories Division, Princeton, N. J.

‡ Formerly, Research Department, RCA Laboratories Division, Princeton, N. J. Now with the Electronics Research Laboratory, Stanford University, Stanford, California.

[1] R. W. Peter, "Low-Noise Traveling-Wave Amplifier," *RCA Review*, Vol. 13, pp. 344-368, September, 1952.

demountable tube except for having a nonmagnetic stainless steel collector instead of the magnetic kovar collector.**

A magnetic sleeve, slipped over the tube end so as to shield the collector, finally eliminated the current interception and lowered the noise factor. From this it was concluded that high-velocity (reflected) secondary electrons were the cause of the intercepted current and high noise factor. Low-velocity secondaries could not leave the collector, as long as its potential was sufficiently higher than that of the helix.

To understand this phenomenon better, experimental studies were made of the effect of secondary electrons, especially on the noise factor, in a traveling-wave tube.

II. Influence of Secondary Electrons on Noise Factor

An electron beam impinging on a collector will always liberate secondary electrons. In the traveling-wave tube, these secondary electrons may be recaptured by the collector, or may travel down the helix toward the gun, focused by the strong magnetic field. The velocity distribution of the secondaries traveling down the helix is a function of the collector potential, V_{coll}. Figure 1 shows this velocity distribution for several collector voltages. In (1a), the collector is at helix potential V_o. The secondary electrons show the well-known energy distribution.[2] If the collector voltage is lowered, (1b), the low-velocity peak of secondaries, V_{s1}, with a maximum at about 10 volts moves upward to

$$V_{s1} \doteq V_o - V_{coll} + 10 \text{ volts}. \tag{1}$$

In (1c), V_{s1} approaches the peak of reflected electrons, V_{s2}, which remains substantially constant at helix potential,

$$V_{s2} \doteq V_o, \tag{2}$$

independent of the collector potential. In (1d), the collector is made positive with respect to the helix. In this case the electrons with energies

$$V_s < V_{coll} - V_o \tag{3}$$

will be recaptured by the collector. It is seen thus from Figure 1 that the energy V_s of the secondaries reaching the helix spreads over a range

** See Figure 8 of Reference (1).

[2] See e.g., K. R. Spangenberg, *Vacuum Tubes*, McGraw-Hill Book Co., New York, N. Y., 1948.

$$(V_o - V_{coll}) \leq V_s \leq V_o. \tag{4}$$

Due to the randomness in velocity and number of emitted secondary electrons, the secondary current traveling in a direction opposite to that of the primary current is very noisy. The partial currents of different velocity classes interact with synchronous traveling-wave

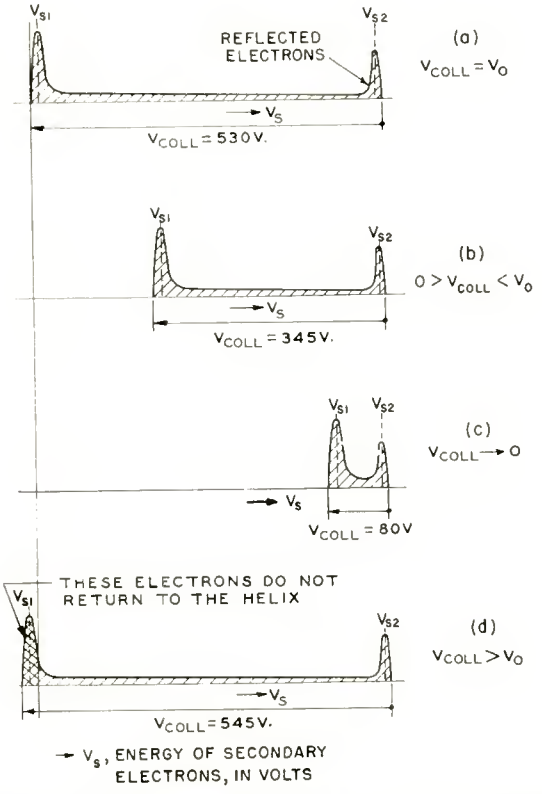

Fig. 1—Velocity distribution of the secondary electrons reaching the helix region with the collector potential as a parameter.

modes and transfer noise to the circuit.

To demonstrate these effects, an experiment was performed with a traveling-wave tube containing a filter helix.[3] One advantage of the filter tube is that it does not require added insertion loss to prevent regeneration, but relies on the dispersion of the filter helix instead.

---

[3] W. J. Dodds and R. W. Peter, "Filter-Helix Traveling-Wave Tubes," to be published in *RCA Review*.

The dispersion is chosen so that it limits the tube amplification to a band narrower than the matched band.* Another advantage of the filter helix is that it makes it possible to place the velocities of forward and backward wave modes at more convenient values. The filter helix used was of the variable-pitch type, as shown in Figure 2a. The behavior of this circuit can be well approximated by replacing the gradual change of the winding pitch p by the discontinuous change indicated in Figure 2b. This yields the equivalent circuit shown in Figure 3, which consists of a chain of line sections with alternating impedances Z_1 and Z_2.

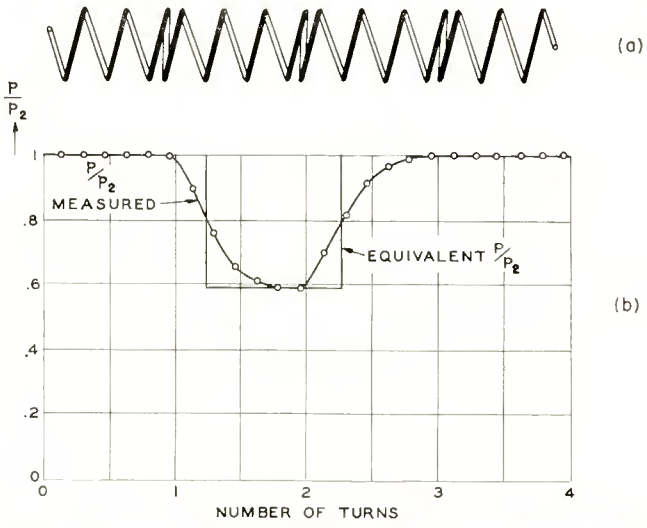

Fig. 2—Filter helix in which the impedance changes are produced by changes in the helix pitch, p.

The relative phase velocities v/c of the different modes of wave propagation for this filter helix are computed as outlined in the Appendix. The first four forward and backward modes ($n = 0, \pm1, \pm2, \pm3, \pm4$) are plotted versus frequency in Figure 3. The measured velocities for modes $n = 0$, $n = -1$ agree closely with the theoretical values. It should be noted that most higher-order modes crowd up toward very low phase velocities.

In Figure 4, the synchronous voltages $V = v^2m/2e$ for the different modes, as obtained from Figure 3, are superimposed on the secondary

* There is one ratio of beam and circuit-wave velocities under given operating conditions which yields maximum gain. At low space-charge—as in the present case—this ratio is close to unity, where unity represents synchronism of beam and unperturbed circuit wave.

electron distribution of Figure 1 for a frequency of 2675 megacycles. As the currents involved are very small, the optimum interaction will occur at synchronism between electron current and phase velocity of the particular mode.

From Figure 4 it is evident that the reflected secondaries can interact with the reverse traveling fundamental mode ($n = 0$) at all

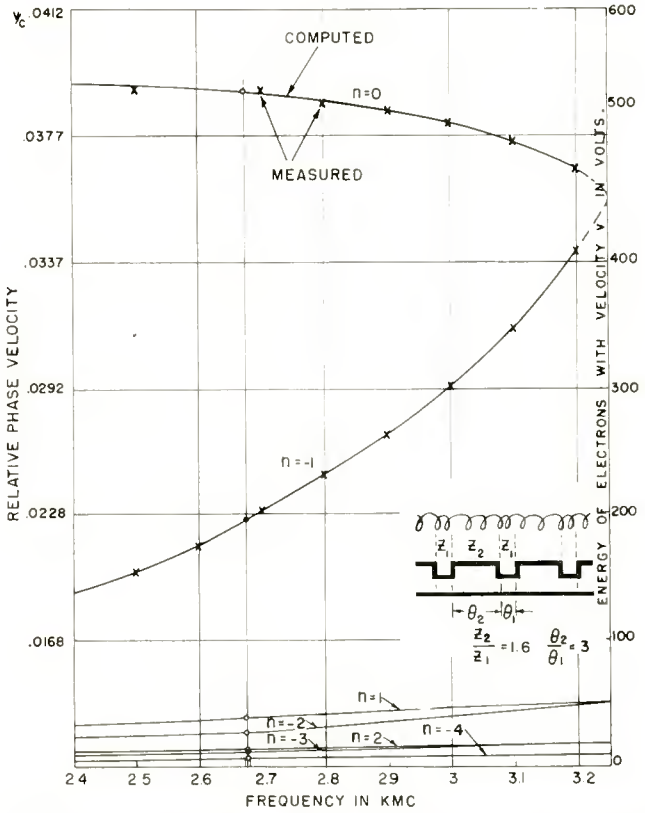

Fig. 3—The phase velocity of the various modes of the variable-pitch filter helix of Figure 2 as a function of frequency.

collector potentials. As long as the collector is at helix potential (primary-beam potential) or even somewhat higher, a large number of the returning slow secondaries can interact with higher forward and backward modes ($|n| > 2$) traveling in the reverse direction, i.e., toward the gun. As the collector voltage is lowered, the peak of low-velocity secondaries with voltage V_{s1} (given by Equation (1)) moves through all the higher order modes and approaches the fundamental

($n = 0$) through the region of the second backward ($n = -2$), the first forward ($n = 1$), and the first backward ($n = -1$) modes, as seen in Figure 4.

The backward modes interacting with synchronous electrons contribute directly to the noise output, as their energy velocity is directed toward the output. Therefore, whenever the V_s peak is synchronous

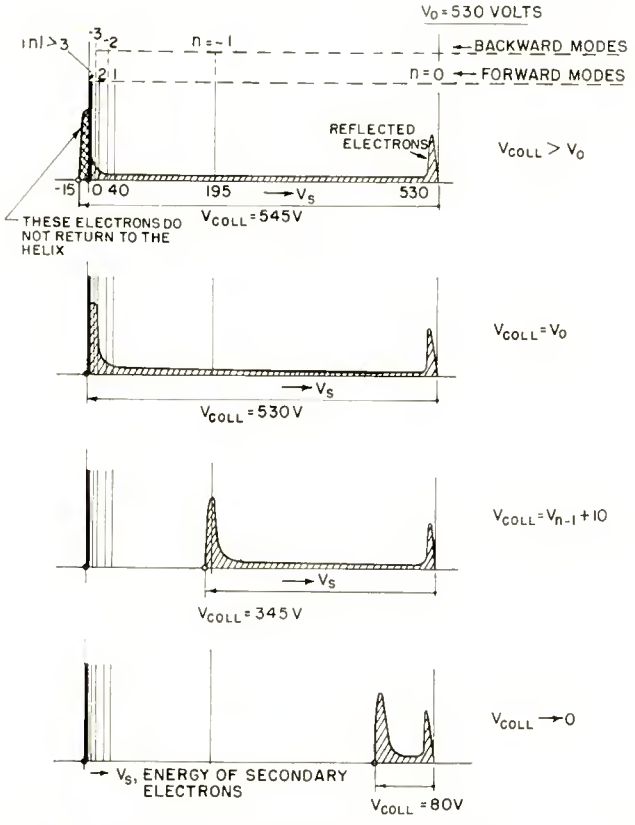

Fig. 4—Phase velocities of the different space-harmonic modes at 2625 megacycles (Figure 3) superimposed on the velocity distribution of secondaries (Figure 1). The velocities are expressed as voltage of a synchronous electron beam.

with a backward mode, one would expect a rise in the noise factor. That such is actually the case is seen from the measured data plotted in Figure 5. The measured peaks in the traveling-wave tube noise factor occur, as expected, at secondary-current voltages V_{s1} synchronous with backward waves ($-n = 1$, 2 and higher). The forward modes amplify the secondary electron noise in the direction toward the gun.

The fraction of this amplified noise power which is reflected from an imperfect input match, adds to the general noise input of the tube and is amplified together with the input signal. The secondary-electron noise current which is amplified by the negative fundamental mode ($n = 0$) accounts for the main contribution.

The dependence of the noise factor upon the amount of secondary current is demonstrated in Figure 6. The number of secondaries escaping from the collector is changed by moving a magnetic shield outside of the tube over the nonmagnetic collector (see Figure 6a). Noise factor, gain, and lost current are plotted against the position of

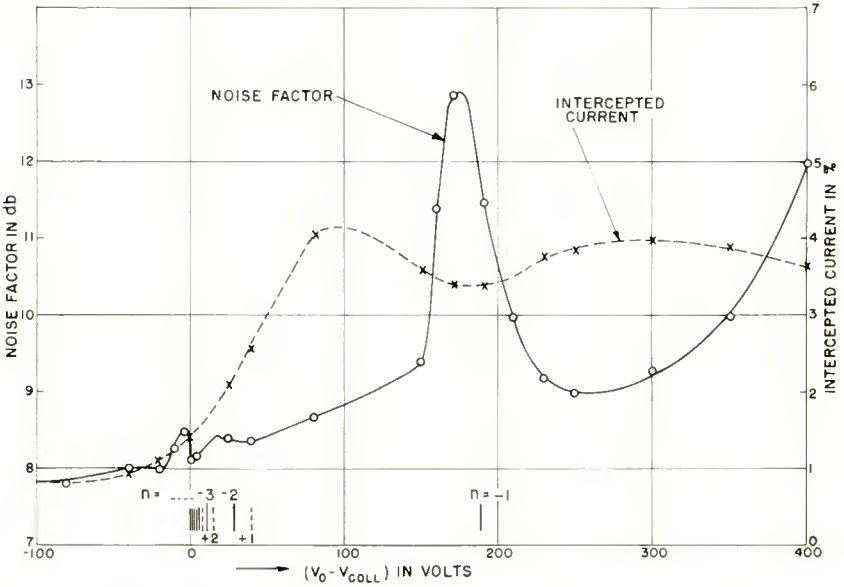

Fig. 5—Noise factor and percentage of lost current as a function of the potential difference between helix and collector.

the shield with respect to the open end of the collector. The secondary current leaving the collector represents almost all of the lost current, and therefore the noise factor increases with increasing secondary current. In the case of Figure 6b, for example, a total intercepted secondary-electron current of 8 per cent of the primary-beam current caused the noise factor to rise 5 decibels, and left the gain practically unchanged. These measurements were taken at $V_{coll} = V_{helix}$, where both the reflected and the low-velocity secondaries contribute to the noise output. At positive values of X, i.e., when the shield protrudes over the collector into the region of the helix antenna, the gain falls off due to mismatch,

and the noise factor rises slightly, as might be expected (due to loss of gain). For this particular magnetic field (385 Gauss) the best conditions occurred when the shield was flush with the collector (X = 0).

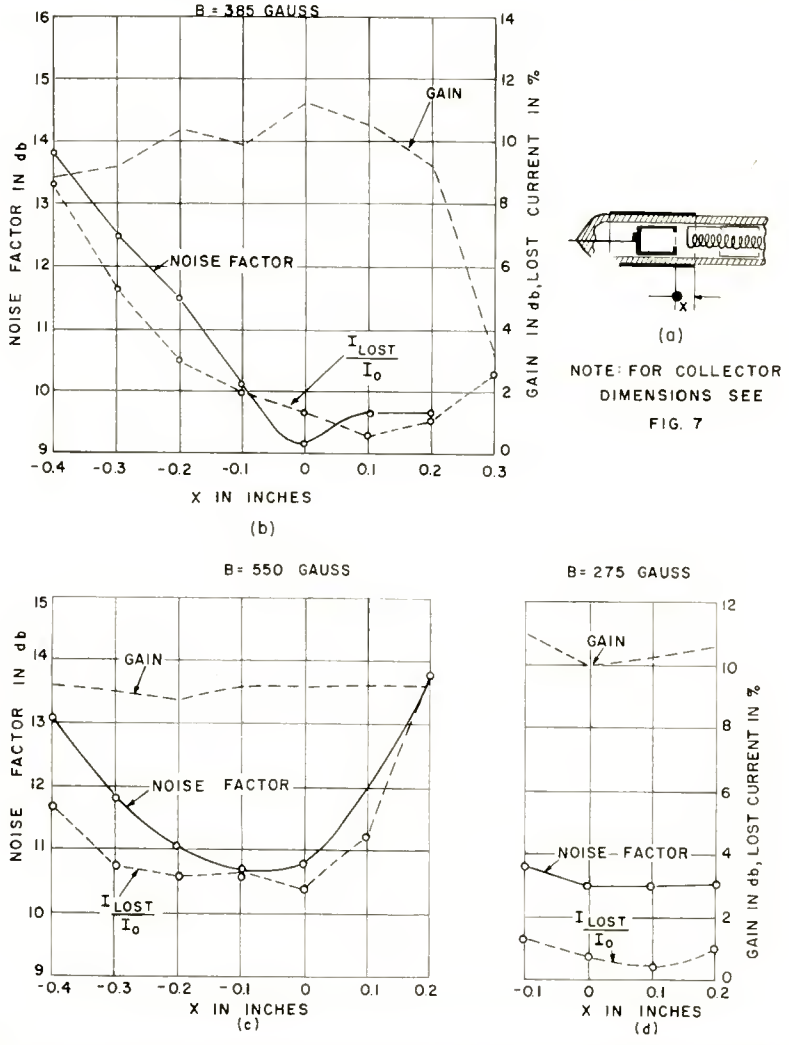

Fig. 6—Noise factor, gain, and percentage of lost or secondary current as a function of the position of an external magnetic shield.

With the magnetic sleeve surrounding the collector, the magnetic field has strong radial components which deflect the emitted secondaries back into the collector. Figure 7 shows a plot of the magnetic field around a sleeve which is assumed to have infinite permeability. This

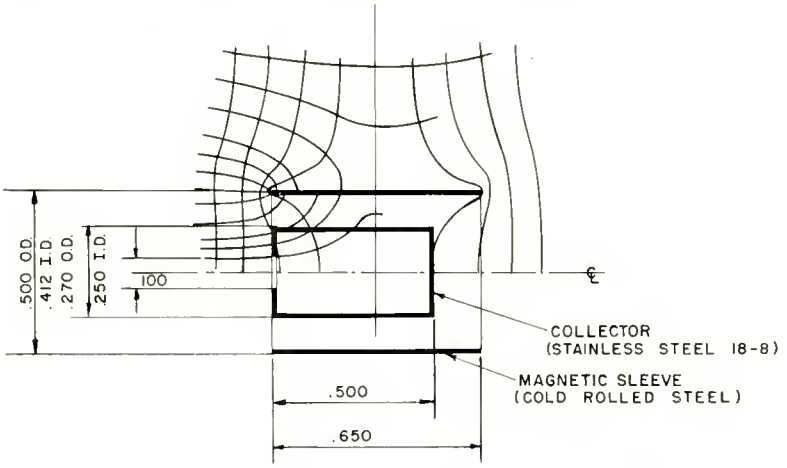

Fig. 7—Spreading magnetic field inside the collector due to surrounding magnetic shield.

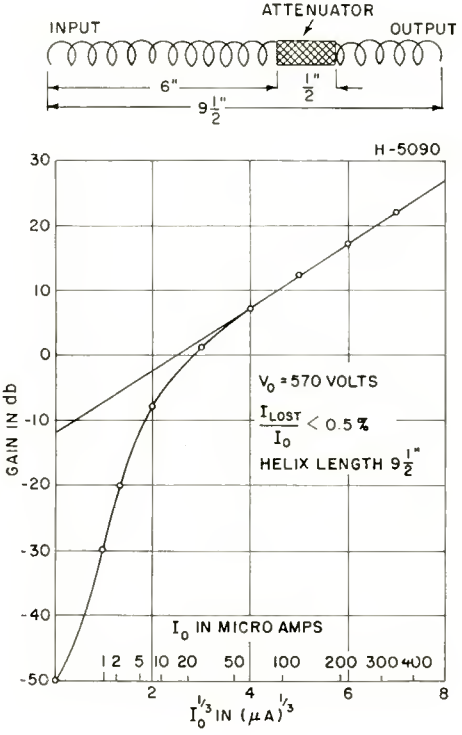

Fig. 8—A typical gain versus (current)$^{1/3}$ curve of a low-noise helix traveling-wave tube with a center attenuator.

field was measured on an electrolytic tank model.

The effect of the strength of the magnetic field is shown in Figures 6b, c, and d. In (6b) the magnetic-field condition is an optimum. At higher magnetic field strengths, (6c), the saturation of the magnetic sleeve causes the ratio of transverse to longitudinal field components to decrease. As a result, the probability of capturing secondaries by the collector is reduced. In (6d), the magnetic field is too low to focus the primary beam properly. Therefore the intercepted current and the noise-factor increase.

In addition to the magnetically shielded collector used in these experiments, there exist other collector arrangements which will prevent reflected secondaries from reaching the helix. None of them, however, seems to be as simple in construction as magnetic shielding of the collector.

Influence of Secondary Electrons on Stability

The requirement of preventing secondary electrons from entering the interaction region holds not only for low-noise traveling-wave tubes, where small amounts of secondaries can ruin the noise factor, but also in high-gain power traveling-wave tubes, where stability is the primary requirement. A few per cent of reflected secondaries may reduce the cold backward insertion loss, introduced by a center attenuator, to almost nothing. If such feedback through the secondary electron beam is large enough, the amplifier will begin to oscillate. In a uniform-pitch-helix traveling-wave tube with a gain characteristic of Figure 8. a reflected current of 2.5 microamperes (0.85 per cent of the beam current) reduces the cold insertion loss from 50 decibels to 20 decibels, which means instability at a net tube gain of 20 decibels. This is true where there is total power reflection at both ends of the helix at some frequency within the gain region of the tube. In actual wide-band tubes, this condition is almost invariably present.

Appendix—Phase Velocity of Filter Helix and Characteristic Data

We follow Reference (3) to compute the phase velocity v/c of the different modes of wave propagation along the filter helix of Figure 2. One can express v/c as

$$\frac{v}{c} = \frac{v}{v_0} \frac{v_0}{v_1} \frac{v_1}{c}. \tag{5}$$

Here v/v_0 is the relative phase velocity of the equivalent circuit

of the filter helix as shown in Figure 3:

$$\frac{v}{v_o} = \frac{\theta_1 + \theta_2}{\theta' + 2\pi n} \tag{6}$$

$$n = \ldots -2, -1, 0, 1, 2 \ldots .$$

$$\cos \theta' = \frac{\zeta + 1}{2} \cos (\theta_1 + \theta_2) - \frac{\zeta - 1}{2} \cos (\theta_1 - \theta_2) \tag{7}$$

$$\zeta = \frac{1}{2} (Z_1/Z_2 + Z_2/Z_1). \tag{8}$$

θ_1 and θ_2 represent the electrical lengths (in degrees) of the two individual line sections (Figure 3). v/v_o is plotted in Reference (3) for various parameter values for the fundamental mode, $n = 0$. For higher space-harmonic modes, v/v_o can readily be found from Equation (6).

The ratio v_o/v_1 takes into account the fact that in the actual filter helix the phase velocities, v_1 and v_2, in the two sections with lengths l_1 and l_2 may be different. From

$$\frac{l_1 + l_2}{v_o} = \frac{l_1}{v_1} + \frac{l_2}{v_2}$$

one obtains

$$\frac{v_o}{v_1} = \frac{1 + \dfrac{l_2}{l_1}}{1 + \dfrac{v_1}{v_2}\dfrac{l_2}{l_1}} \tag{9}$$

which, for a filter helix with changing pitch, p_1 and p_2, is approximately

$$\frac{v_o}{v_1} \doteq \frac{1 + \dfrac{l_2}{l_1}}{1 + \dfrac{p_1}{p_2}\dfrac{l_2}{l_1}}. \tag{10}$$

The relative phase velocity of the uniform helix, v_1/c, can be found in the literature.[4]

The dimensions of the filter helix of Figure 2 are as follows:

Pitch	$p_1 = .0208$ inch,	$p_2 = .0123$ inch,
Average Diameter	$= .103$ inch,	
Wire Diameter	$= .007$ inch,	
Length	$= 5$ inches,	
Impedance Ratio	$Z_2/Z_1 = 1.58$,	$\zeta = 1.11$,
Section Length Ratio	$\theta_2/\theta_1 = 1/3$,	
Lowest Cutoff Frequency	$f_{c1} = 3250$ megacycles.	

[4] See, e.g., J. R. Pierce, *Traveling-Wave Tubes*, D. Van Nostrand Co., New York, N. Y., 1950, Figure 3.3.

RCA TECHNICAL PAPERS†

Second Quarter, 1953

Any request for copies of papers listed herein should be addressed to the publication to which credited.*

"The Application of Transistors to an Industrial Television Synchronizing Generator," W. S. Pike, *RCA Industry Service Laboratory Bulletin LB-909* (April 17) 1953

"An Auxiliary Mixer for TV Studios," G. A. Singer, *Audio Eng.* (April) 1953

"A Bandpass Transmitter-Exciter Using an RCA 6146—Part I," Richard G. Talpey, *Ham Tips* (June-July) 1953

"Circuits for Reception of NTSC (Feb. 2, 1953) Color Television Signals," *RCA Industry Service Laboratory Bulletin LB-910* (April 24) 1953

"Color Television Signal Receiver Demodulators," D. H. Pritchard and R. N. Rhodes, *RCA Review* (June) 1953

"Colorimetric Analysis of RCA Color Television System," D. W. Epstein, *RCA Review* (June) 1953

"Designing Trouble-Free Series Tube Heater Strings," M. B. Knight, *Tele-Tech* (April) 1953

"Electronic Transitions in the Luminescence of Zinc Sulfide Phosphors," R. H. Bube, *Phys. Rev.* (April) 1953

"Equipments for Measuring Junction Transistor Admittance Parameters for a Wide Range of Frequencies," L. J. Giacoletto, *RCA Review* (June) 1953

"How to Design Bistable Multivibrators," R. Pressman, *Electronics* (April) 1953

"Intensification in Zinc Selenide Phosphors," S. Larach, *Jour Chem. Phys.* (April) (Letter to the Editor) 1953

"Light and Electron Microscopic Studies of Escherichia Colicoliphage Interactions, III. Persistence of Mitochondria and Reductase Activity During Infection of Escherichia Coli B with T2 Phage," P. E. Hartman, S. Mudd, J. Hillier, and E. H. Beutner, *Jour. Bacteriology* (June) 1953

"New Professional Television Projector," W. E. Stewart, *Jour. S.M.P.T.E.* (April) 1953

"On the Variation of Junction Transistor Current-Amplification Factor with Emitter Current," W. M. Webster, *RCA Industry Service Laboratory Bulletin LB-917* (June 23) 1953

"Optimum Utilization of the Radio Frequency Channel for Color Television," R. D. Kell and A. C. Schroeder, *RCA Review* (June) 1953

"A P-N-P Triode Alloy Junction Transistor for Radio-Frequency Amplification," J. I. Pankove and C. W. Mueller, *RCA Industry Service Laboratory Bulletin LB-915* (June 18) 1953

"Principles and Development of Color Television Systems," G. H. Brown and D. G. C. Luck, *RCA Review* (June) 1953

"Quantum Theory of Spectral Line Broadening," S. Bloom and H. Margenau, *Phys. Rev.* (June) 1953

† Report all corrections or additions to RCA Review, Radio Corporation of America, RCA Laboratories Division, Princeton, N. J.

* *RCA Industry Service Laboratory Bulletins* are not published and are issued only as a service to licensees of the Radio Corporation of America.

"The Response of a Tuned Circuit to a Ramp Function," M. S. Corrington, *Proc. I.R.E.* (May) 1953
"Review of Work on Dichroic Mirrors and Their Light-Dividing Characteristics," M. E. Widdop, *Jour. S.M.P.T.E.* (April) ... 1953
"Spiral-Beam Tube Modulates 1 KW at UHF," C. L. Cuccia, *Electronics* (April) 1953
"A Symmetrical Transistor Phase Detector for Horizontal Synchronization," B. Harris and A. Macovski, *RCA Industry Service Laboratory Bulletin LB-194* (June 11) 1953
"Television Coverage of the Presidential Inauguration," E. C. Wilbur and H. L. Grelck, *RCA Review* (June) 1953
"Thermal Conductivity of Some Metals and Alloys," L. Silverman, *Journal of Metals* (May) 1953
"The TP-6A . . . A New 16MM Professional TV Projector," H. G. Wright, *Broadcast News* (May-June) 1953
"The TTU-1B, 1-KW UHF TV Transmitter," T. M. Gluyas and E. H. Potter, *Broadcast News* (May-June) 1953
"Two Non-Elementary Definite Integrals," M. S. Corrington, *Mathematical Tables and Other Aids to Computation* (April) 1953
"A UHF Balun," A. T. Brennan, *RCA Industry Service Laboratory Bulletin LB-911* (May 5) 1953
"Use of UHF Miniature Tube Sockets for UHF Television Applications," *RCA Application Note AN-158*, RCA Tube Department, Harrison, N. J. (June) 1953
"Use of Statistical Tolerances to Obtain Wider Limits on Tube Component Dimensions," E. V. Space, *Convention Record of the I.R.E. 1953 National Convention* 1953
"The Variation of Current Gain with Junction Shade and Surface Recombination in Alloy Transistors," J. I. Pankove and A. Moore, *RCA Industry Service Laboratory Bulletin LB-916* (June 18) 1953
"Video Inset System," J. L. Hathaway and F. L. Hatke, *Electronics* (April) 1953
"A Vidicon Camera Adaptor for Television Receivers," G. W. Grey, W. S. Pike, and L. E. Flory, *RCA Industry Service Laboratory Bulletin LB-913* (May 28) 1953

AUTHORS

IRVING F. BYRNES joined the General Electric Test Department in 1918, transferring to their Radio Engineering Department in 1921. He completed extension courses in Electrical Engineering at Union College in 1926. In 1930 he joined the RCA Manufacturing Company Transmitter Division and later transferred to Radiomarine Corporation of America. Since 1946 Mr. Byrnes has been Vice President in Charge of Engineering of Radiomarine Corporation of America. He received a "Modern Pioneer" award in 1940 for inventions of maritime safety and communication equipment, and in 1947 he was awarded a U. S. Navy "Certificate of Commendation". Mr. Byrnes is a Member of the American Institute of Electrical Engineers and a Senior Member of the Institute of Radio Engineers.

CHARLES H. CHANDLER received the B.A. degree in Physics and Mathematics from the College of Wooster in 1940, and the M. Sc. degree in Electrical Physics from Ohio State University in 1946. From 1941 to 1946 he served as radar officer and communications frequency-monitoring officer in the Signal Corps, U. S. Army. Since 1946 he has been a member of the technical staff of the RCA Laboratories Division, Princeton, N.J., where his fields of research have included rapid-scanning radar antennas, radar displays, propagation in dielectric materials, and circuit development. Mr. Chandler is a member of Sigma Xi, Sigma Pi Sigma, the American Association for the Advancement of Science, and a Senior Member of the Institute of Radio Engineers.

GORDON L. FREDENDALL received the Ph.D. degree from the University of Wisconsin. From 1931 to 1936 he taught electrical engineering and mathematics, and engaged in research work in mercury-arc phenomena at the University of Wisconsin. Since 1936 he has been with Radio Corporation of America, working on television research. He is at present located in Princeton N. J., at RCA Laboratories Division. Dr. Fredendall is a Senior Member of the Institute of Radio Engineers.

P. G. HERKART received the B.S. and the M.S. degrees in Electrical Engineering in 1935 from the Massachusetts Institute of Technology. From 1935 until 1943 he was engaged in power tube manufacturing at the RCA Victor Division in Harrison, N.J. Since 1943 he has been with the RCA Laboratories Division in Princeton, N.J. Mr. Herkart is a Member of Sigma Xi, and of the Institute of Radio Engineers.

E. O. KEIZER received the B.S. degree in Electrical Engineering from Iowa State College, Ames, Iowa in 1940. He then joined the RCA Victor Division, Camden, N.J. In 1942 he was transferred to the RCA Laboratories Division, Princeton, N.J. where he is now working as a member of the receiver and circuits section. Since 1942 he has been engaged in work on receiver circuits, television receiver circuits and on related problems. Mr. Keizer is a Senior Member of the I.R.E. and a Member of Tau Beta Pi, Phi Kappa Phi, Eta Kappa Nu, and Sigma Xi.

MARLIN G. KROGER received the B.Sc. degree in Electrical Engineering from the University of Nebraska in 1949. He worked as a Research Engineer for RCA Laboratories Division in Princeton, N.J., until 1952. He is now with Motorola, Inc., Chicago, Illinois, working as a Senior Engineer on the development of television receiver circuits. Mr. Kroger is a member of Sigma Xi, Sigma Tau, Eta Kappa Nu, Pi Mu Epsilon and the Institute of Radio Engineers.

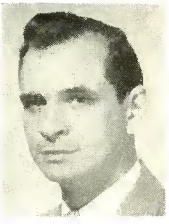

JEROME KURSHAN received the B.A. degree with honors in Mathematics and Physics from Columbia University in 1939 and was an assistant in Physics there during that year. From 1939 to 1943 he was an assistant in Physics at Cornell University where he received the Ph.D. degree in 1943. Since then he has been with the RCA Laboratories Division at Princeton, working on FM magnetrons, special receiving tube problems and, more recently, on transistors and semiconductor physics. Dr. Kurshan is a member of Phi Beta Kappa, Sigma Xi, the American Physical Society and the Institute of Radio Engineers.

GERHARD D. LINZ received the degree of Bachelor of Electrical Engineering in 1948 and the M.S. degree in Electrical Engineering in 1949 from the Georgia Institute of Technology. Prior to graduation he served with the Army Signal Corps. In 1949 he joined the RCA Laboratories Division in Princeton, N.J. He is now with the Defense Research Laboratories of the University of Texas. Mr. Linz is a member of Tau Beta Pi, Phi Kappa Phi and Eta Kappa Nu.

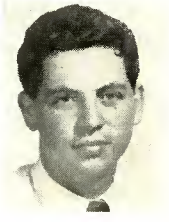

ALBERT MACOVSKI received the B.E.E. degree from the College of the City of New York in 1950, and the M.E.E. degree from the Polytechnic Institute of Brooklyn in 1953. Since 1950 he has been engaged in television engineering at the Industry Service Laboratory of RCA Laboratories Division in New York, N.Y. Mr. Macovski received an RCA Merit Award in 1952 for outstanding work on research in the field of television synchronization.

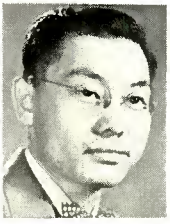

T. MURAKAMI received the B.S. degree in E.E. from Swarthmore College in 1944, and the M.S. degree from the Moore School of Electrical Engineering, University of Pennsylvania in 1947. From 1944 to 1946 he was an assistant and research associate in the Department of Electrical Engineering at Swarthmore College. Since 1946 he has been with the Advanced Development Section of the Home Instrument Department, RCA Victor Division, Camden, N. J., working on radio frequency circuit development. Mr. Murakami is an Associate Member of the Institute of Radio Engineers and Sigma Xi.

ROLF W. PETER received the M.S. degree in Electrical Engineering in 1944, and the Ph.D. degree in Radio Engineering in 1948 from the Swiss Federal Institute of Technology in Zurich, Switzerland. From 1946 to 1948 he was Assistant Professor of Radio Engineering at the Swiss Federal Institute of Technology. In 1948 he joined the RCA Laboratories Division in Princeton, N. J., where he has been engaged in research on traveling-wave tube amplifiers. Dr. Peter is a Member of Sigma Xi and a Senior Member of the Institute of Radio Engineers.

H. JOHN PRAGER received the B.S. degree in Electrical Engineering from the University of Vienna in 1938, and the M.S. degree in Electrical Engineering from the University of Michigan in 1940. From 1940 to 1942 he was associated with the Research Laboratory of the Detroit Edison Company in Michigan. In 1943 he joined the Tube Department of the Radio Corporation of America in Harrison, N.J. as a production engineer engaged in the manufacture of receiving-type tubes. He is presently a design engineer in the Receiving Tube Development Group. He has been engaged primarily in the development of the "Special Red" tubes, gas tubes, and allied special purpose tubes.

JOHN A. RUETZ received the B. S. and M. S. degrees in Electrical Engineering from the University of Michigan in 1949 and 1950, respectively. From 1944-1946 he served as an electronic technician in the U. S. Navy. In 1950, he joined the RCA Laboratories Division, Princeton, N.J., where he engaged in work on microwave amplifiers. He is now with the Electronics Research Laboratory at Stanford University. Mr. Ruetz is a Member of the Institute of Radio Engineers.

H. E. ROYS received the B.S. degree in electrical engineering from the University of Colorado in 1925. From 1925 to 1930 he was with the General Electric Company in Schenectady on radio transmitter test and later on receiver engineering. He was transferred to the RCA Manufacturing Company at Camden, N.J. in 1930 and in 1931 became associated with the Phonograph Section. In 1937 he became a member of the Advanced Development Group of the Photophone Section, which later became part of the Engineering Products Department. From 1941 to 1946 he was located with this group in Indianapolis, working mainly on disk recording and reproducing problems. At present he is located in Camden and is still associated with the same group. Mr. Roys is a member of Tau Beta Pi, Eta Kappa Nu, the Audio Engineering Society and the Acoustical Society of America. He is a Senior Member of the Institute of Radio Engineers.